U-Pb geochronology and global context of the Charnwood Supergroup, UK: Constraints on the age of key Ediacaran fossil assemblages.

Stephen R. Noble[1]*, Daniel J. Condon[1], John N. Carney[2], Philip R. Wilby[2], Timothy C. Pharaoh[2], and Trevor D. Ford[3].

[1] Natural Environment Research Council Isotope Geosciences Laboratory, British Geological Survey, Keyworth, Nottinghamshire, NG12 5GG, UK

[2] British Geological Survey, Keyworth, Nottinghamshire, NG12 5GG, UK

[3] Department of Geology, University of Leicester, Leicester, LE1 7RH, UK

ABSTRACT

U-Pb (zircon) ages on key stratigraphic volcanic horizons within the ca. 3200 m thick Ediacaran-age Charnian Supergroup provide an improved age model for the included Avalonian assemblage macrofossils, and hence, temporal constraints essential for intercomparisons of the Charnian fossils with other Ediacaran fossil assemblages globally. The Ives Head Formation (Blackbrook Group), the oldest exposed part of the volcaniclastic Charnian Supergroup of the late Neoproterozoic Avalonian volcanic arc system of southern Britain, contains a bedding plane with an impoverished assemblage of ivesheadiomorphs that is constrained to between ca. 611 Ma and 569.1 ± 0.9 Ma (total uncertainty). Higher diversity biotas, including the holotypes of *Charnia*, *Charniodiscus* and *Bradgatia*, occupy the upper part of the volcaniclastic succession (Maplewell Group) and are dated at 561.9 ± 0.9 Ma (total uncertainty) and younger by zircons interpreted as coeval with eruption and deposition of the Park Breccia, Bradgate Formation. An ashy volcanic-pebble conglomerate in the Hanging Rocks Formation at the very top of the supergroup yielded two U-Pb zircon populations: an older detrital one at ca. 604 Ma, and a younger population at ca. 557 Ma that is interpreted as the approximate depositional age. The temporal association of the fossiliferous Charnwood Supergroup with comparable fossiliferous deepwater successions in Newfoundland, and the probable temporal overlap of the youngest Charnwood macrofossils with those from different paleoenvironmental settings such as the Ediacaran White Sea macrofossils, indicates a primary role for ecological sensitivity in determining the composition of these late Neoproterozoic communities.

Keywords: Ediacaran, Charnwood, geochronology, Avalonia, Neoproterozoic, CA-TIMS

INTRODUCTION

The appearance of diverse macroscopic organisms in the late Neoproterozoic Ediacaran Period was a seminal time in the evolution of benthic marine life (Narbonne, 2005). The multicellular macroscopic biota from this time records a major expansion in morphological complexity (Shen et al., 2008; Xiao and Laflamme, 2009; Erwin et al., 2011) and a phase of pronounced ecological innovation that includes development of epibenthic tiering (Clapham and Narbonne, 2002; Laflamme et al., 2012), motility (Jensen et al., 2005; Liu et al., 2010), biomineralization (Hofmann and Mountjoy, 2001) and predation (Hua et al., 2003). The timing of key biological events, however, is poorly constrained and their relationship (causal vs. consequential vs. incidental) to coeval changes in the physical and chemical environment (e.g. Halverson et al., 2005; Canfield et al., 2007) remain speculative (Hoffman et al., 1998; Runnegar, 2000; Narbonne, 2010). Uncertainty also exists regarding the nature and tempo of the initial diversification of the biota (Narbonne and Gehling, 2003) as well as its demise at or around the base of the Cambrian (Laflamme et al., 2013).

Much of this uncertainty reflects the absence of a robust temporal framework. There is a dearth of precisely dated fossiliferous successions and biostratigraphic schemes for the Ediacaran macro-biota have yet to be widely developed. The latter may be hampered by purportedly high levels of endemism (e.g. Clapham et al., 2004) and long taxonomic ranges (*cf* Liu et al. 2012). The Ediacara macro-biota is typically subdivided into three major assemblages (Waggoner, 2003): Avalon, White Sea and Nama. Each assemblage is reported to have a distinctive taxonomic composition and accompanying ecological complexity (Laflamme et al., 2013), but there is debate regarding the extent to which they genuinely reflect evolutionary change (Erwin et al., 2011; Narbonne et al., 2012), rather than biogeographic provinciality (Waggoner, 2003; Meert and Lieberman, 2008), environmental sensitivity (Grazhdankin, 2004; Gehling and Droser, 2013) or taphonomic variation (Narbonne, 2005).

In this study, we contribute new high-precision geochronological constraints using CA-ID-TIMS (chemical abrasion isotope dilution thermal ionization mass spectrometry) U-Pb zircon dating for the fossiliferous Charnian Supergroup of Charnwood Forest, Leicestershire, central England. These supersede two first-order SHRIMP (Sensitive High Resolution Ion Microprobe) U-Pb dates (Compston et al., 2002). The Charnian succession forms part of the classic Avalon Assemblage, which occupied deepwater niches on the peri-Gondwanan Avalonian island arc and includes one of the oldest known macroscopic biotas (Narbonne, 2005), with only the Lantian assemblage (Yuan et al., 2011) and pre-Marinoan Trezona Formation possible sponge-grade organisms (Maloof et al., 2010) being potentially older. Current understanding of the temporal range of the assemblage is largely based on biotas preserved in Newfoundland that have been constrained to between ca. 578 and ca. 565 Ma and younger (Benus, 1988; Bowring in Schmitz, 2012). The lower age constraint was obtained from only ca. 150 m above the stratigraphically lowest fossiliferous surface, within ca. 3 Myrs of the termination of the mid-Ediacaran Gaskiers Glaciation, dated at 582.4 ± 0.5 Ma (Bowring in Schmitz, 2012; note ages and uncertainties used in the GTS 2012 are ± 2σ and exclude decay constant errors). It therefore provides good control on the local first appearance of the assemblage, which has been linked to a rise in oxygen in the deep ocean following deglaciation (Canfield et al., 2007). In contrast, the upper age provides little constraint on the assemblage's range, because the youngest known representatives lie ca. 1700 m stratigraphically above the highest dated surface. Our new data: 1) provide additional absolute constraint on the range of the classic Avalon Assemblage, 2) allow correlation of the Charnian and Newfoundland lithostratigraphic sections, 3) enhance the chronological framework for nascent biostratigraphic schemes (e.g. Liu et al., 2012) and proposed phylogenies (e.g. Brasier and Antcliffe, 2009), and 4) inform debate regarding the extent to which the composition of Ediacaran macro-biota communities record palaeoenvironmental setting rather than evolutionary change.

GEOLOGICAL SETTING

Stratigraphy and genesis of the Charnian Supergroup

The late Neoproterozoic strata of Charnwood Forest are exposed in a series of outcrops that occur over an approximately 7 km x 7 km area and that form inliers protruding through a cover of Triassic deposits (Watts, 1903). These Neoproterozoic strata occupy the core of a faulted anticline (Fig. 1) and have an estimated total exposed thickness of ca. 3200 meters. They collectively comprise the Charnian Supergroup and are subdivided into two groups: the Blackbrook Group and overlying Maplewell Group (Fig. 2). The succeeding Brand Group has previously been included within the Charnian Supergroup (Moseley and Ford, 1985), but it is now excluded based on the likely presence of an intervening unconformity (McIlroy et al., 1998). Much (if not all) of the Brand Group may be of Lower

Cambrian age, given the presence of *Teichichnus* burrows in the Swithland Formation near its base (Bland and Goldring, 1995).

The Charnian Supergroup is dominated by well-stratified volcaniclastic rocks and is generally considered to have been deposited in a deepwater setting, principally by gravity flow processes (Carney 1999). Field mapping and geochemical data (Pharaoh et al., 1987) suggest that much of the succession was sourced from contemporaneous volcanic centers, examples of which occupy the north-west of the inlier (see below). The Blackbrook Group is at least 1400 m thick and mainly consists of meter-scale beds of medium- to fine-grained, normally graded volcaniclastic sandstones (Fig. DR 1a-b), and parallel-laminated siltstones and mudstones. It is subdivided into the Ives Head Formation and the overlying Blackbrook Reservoir Formation, with their boundary taken as the top of the distinctive South Quarry Breccia Member, a slump breccia up to 35 m in thickness consisting of large contorted rafts of laminated mudstone set within a medium-grained sandstone matrix (Carney 2000a). Borehole core from Morley Quarry indicates that the stratigraphically lowermost exposed part of the Blackbrook Group is underlain by a further ca. 500 m of Charnian Supergroup volcaniclastic sedimentary rocks and ca. 300 m of porphyritic dacite lavas (Pharaoh and Evans, 1987). Basement to the Charnian Supergroup is not known from either surface exposures or boreholes.

The overlying Maplewell Group is ca. 1800 m thick. The base of the group is defined by the Benscliffe Breccia Member (Moseley and Ford, 1985), comprising up to 100 m of crudely stratified lithic lapilli tuffs and andesitic breccias composed of angular to subrounded blocks set within a coarse-grained, crystal-lithic matrix (Fig. DR 1c). It is interpreted as a long run-out, subaqueous, pyroclastic block flow (Carney 1999). The Beacon Hill and Bradgate formations dominate the Maplewell Group in the south and east of the inlier (Moseley and Ford, 1989), and mainly consist of decimeter-scale tabular beds of planarlaminated mudstone and siltstone, and subordinate normally graded, fine-grained sandstone. Coarser-grained lithologies are largely restricted to specific horizons within the Bradgate Formation, where they include massive, meter-scale beds of very coarse-grained sandstone. Tuffaceous beds, including probable primary water-lain ash-falls, are notably more abundant in the Beacon Hill Formation, where they form distinctive pale-weathering, siliceous horizons. The boundary between the Beacon Hill Formation and the succeeding Bradgate Formation is traditionally taken at the base of the Sliding Stone Slump Breccia Member (Moseley and Ford, 1985; 1989), which consists of 5.5 m or more of very coarse-grained, volcaniclastic sandstone containing large clasts and contorted rafts of mudstone and siltstone. However, in the stratigraphy presented here (Fig. 2), the boundary is lowered a few tens of meters to encompass a larger package of similar lithologies, including the Park Breccia (Worssam and Old, 1988), which record an interval of repeated major subaqueous debris-flow events (Sutherland et al., 1994).

In the north-west of the inlier, the Beacon Hill Formation merges with (and is replaced by) the Charnwood Lodge Volcanic Formation (Fig. 1). This unit consists of ca. 1000 m of bouldery volcanic breccias and lithic lapilli tuffs, and is interpreted as the product of repeated subaqueous pyroclastic block flows derived from dome-collapse events (Carney, 1999; 2000b). It forms an apron around the Bardon Hill and Whitwick volcanic complexes (Fig. 1), which comprise suites of massive and brecciated, fine-grained, dacitic and andesitic rocks. These likely include both high level intrusions and extrusive volcanic rocks (Moseley and Ford, 1985; Worssam and Old, 1988; Le Bas, 1996).

The Bradgate Formation is succeeded by the Hanging Rocks Formation, which constitutes the uppermost division of the Charnian Supergroup. It consists of ca. 20 m of matrix-supported, fine- to medium-grained conglomerates and interbedded medium-grained sandstones and subordinate tuffaceous siltstones, overlain by ca. 30 m of red-purple, tuffaceous pelites and greywacke sandstones (McIlroy et al., 1998). The conglomerates record a significant change in sedimentary regime, and include exotic pebbles that are petrographically distinct from the rest of the Charnian sequence (see Carney, 2000c), such as single or aggregated crystals of quartz and K-feldspar. The lower and upper boundaries of the Hanging Rocks Formation are not well exposed, prompting debate about which represents the local Precambrian/Cambrian boundary (e.g. Moseley and Ford, 1985; McIlroy et al., 1998; Boynton and Moseley, 1999).

The Charnian Supergroup is intruded by two suites of diorites that record the terminal phase of Charnian magmatism. The North Charnwood Diorites are medium- to coarse-grained and form sub-vertical sheets up to 60 m thick within the Blackbrook Reservoir and Beacon Hill formations. The South Charnwood Diorites are coarser-grained, have a granophyric texture, and form much more substantial, broadly concordant bodies. These intrusions are less sheared than the North Charnwood Diorites (Worssam and Old, 1988) and truncate flexures within the hosting Bradgate Formation (Carney and Pharaoh, 2000b), implying that they represent the youngest magmatic phase in the inlier.

The degree to which the rocks are comprised of two or more of pyroclastic, epiclastic or holoclastic components is critically important to the interpretation of the ages of the zircons for the Charnian Supergroup. Establishing with confidence an epiclastic versus pyroclastic origin for the volcaniclastic zircons from a particular sedimentary horizon will result in the associated U-Pb isotope data being interpreted as maximum versus depositional or near-depositional ages for both that horizon and its associated fossils. For the stratiform rocks of the Blackbrook and Maplewell groups sampled here (excepting the Hanging Rocks Formation), it is noteworthy that the overwhelmingly dominant granular components (Figures DR 1, a-d) are angular to subrounded lithic grains of microcrystalline andesite and dacite, together with euhedral to fragmented and sharply angular crystals of quartz and plagioclase.

This textural evidence, although not definitive, supports a volcanic pyroclastic ± epiclastic origin. Furthermore, in some Charnwood finer-grained tuffaceous rocks there are relicts of volcanic glass shards preserved, despite the overprinting Phanerozoic low-grade metamorphism affecting the rocks.

Within the Maplewell group, particularly for the Charnwood Lodge and Beacon Hill Formations, there is a spatial association of andesitic to dacitic breccias through to fine-grained water-lain tuffs, the latter commonly containing devitrified glass shards now composed of microcrystalline aggregates preserving the original shard morphology (Fig 3 a-b). Based on the presence of these glass shards and their unabraded condition, a pyroclastic origin is suggested for at least some of the grains in the tuffaceous units. Additionally, although the lithic volcanic grains mostly lack vesicular or shardic textures, this does not rule out their ultimate pyroclastic origin since ‘dense’ lithic material is a typical product of dome-collapse events (Stix, 1991), a style of volcanism inferred for the NW Charnwood Forest volcanic complexes (Carney, 2000a). Following the argument that at least some of the volcaniclastic components of the Maplewell group rocks can be assigned a pyroclastic origin, the zircons present also potentially reflect pyroclastic and epiclastic contributions. The presence of zircons that are pyroclastic in origin would be supported by observing an upwardly younging chronostratigraphy as defined by the youngest zircons dated at each sampled location. In this instance the age defined by these zircons would be, or would closely approximate, the age of the fossils at those stratigraphic levels.

The Hanging Rocks Formation is distinct from the underlying Maplewell Group rocks in that it contains a clearly holoclastic detrital component, in addition to volcanic epiclastic and pyroclastic constituents, in the form of rounded pebbles of composition distinct (e.g. quartz + K-feldspar) from any other exposed Charnwood rocks (Carney, 2000c; see also DR Fig. 4). Evidence for a pyroclastic component is provided by the occurrence of glass shards, similar to those noted in the underlying Beacon Hill tuffaceous rocks, in tuffaceous interbeds in the upper part of the Hanging Rocks Formation exposures (Worssam and Old, 1988; McIlroy et al., 1998). The presence of these potentially pyroclastic grains accompanied by abundant microcrystalline andesitic grains, and being overlain by the Cambrian Brand Formation, is consistent with the notion that the Hanging Rocks Formation is related to the waning stages of Precambrian volcanism at Charnwood. Zircons recovered from the Hanging Rocks Formation would thus be expected to represent contributions from a variety of proximal and distal sources based on the observed range of detrital material, with the youngest zircon grains possibly being pyroclastic and derived from the same volcanic centers as the other underlying Maplewell Group rocks.

The identification of a pyroclastic component in the rocks of the Blackbrook Group is more problematic than with the Maplewell Group rocks. Only the Ives Head Formation was investigated here, with the overlying Blackbrook Reservoir Formation remaining to be investigated, and so only an incomplete assessment can be made. As the Ives Head Formation turbiditic volcaniclastic sandstones through to siltstones are comprised of monomict microcrystalline andesitic to dacitic grains, they are similar to many Maplewell Group volcaniclastic rocks. In contrast to the Maplewell Group rocks, however, a link to a volcanic center based on the exposed geology cannot be made as clearly for the Ives Head Formation. In addition, tuffaceous strata have not thus far been found that might supply evidence of primary pyroclastic grains, and neither are there proximal facies coarse-grained volcanic fragmental rocks present.

This monomict nature is consistent with the criteria of Stix (1991) for primary 'mass flows of pyroclastic debris'. There are slight variations in degree of crystallinity and angularity between grains and these differences, together with the observed stacking of some turbidites into sequences of a few to several meters thickness, rather than in single very thick units, may suggest a secondary origin (Cas and Wright, 1991; Schneider et al., 2001; Stix, 1991). Such secondary turbidites need not be necessarily synchronous with an explosive eruption but could result from slumping of previously accumulated pyroclastic material (Stix, 1991) akin to recently described deep-water deposits surrounding Montserrat (Trofimovs et al., 2006).

Although a close link to pyroclastic activity is possible given the monomict character of the grains, a clear differentiation of epiclastic and pyroclastic origin based on petrography is not possible. The only diagnostic criterion available to this study is limited to observations of the degree of angularity of the andesite-dacite fragments, and so because of this limitation, it could be argued as effectively that these rocks are epiclastic volcaniclastic rocks. The unaltered and in some cases highly angular state of the grains is consistent with derivation by erosion of a volcanic arc with little or no chemical weathering and short transport distances from volcanic hinterland to basin. There is an indeterminate lag time between volcanism and sedimentary deposition in this case. The above are consistent with some microcrystalline andesite-dacite grains exhibiting a degree of rounding and that the Ives Head Formation turbidites are observed in isolation from other types of volcaniclastic rocks. Therefore, due to the uncertainty in ascribing pyroclastic versus epiclastic origins to any of the volcaniclastic materials in the Blackbrook Group, the interpretation here of the zircon ages is that the youngest zircon grain dated is representative of a maximum age estimate of these sedimentary units.

Pharaoh et al. (1987) report geochemical data for intrusive and volcaniclastic rocks in the succession and propose a general geological setting for the supergroup as a whole. They interpret major element and selected trace element compositions of andesites and dacites from the Whitwick and Bardon Hill volcanic complexes (Fig. 1) as indicative of calc-alkaline, volcanic arc-type magmatism along a convergent plate boundary. Integration of additional geochemical and field data led Carney (2000b) and Carney and Pharaoh (2000a) to further suggest that these volcanic complexes represent the roots of subvolcanic intrusions and domes whose composition is close to that of the Charnian parental magmas. Of note are the low concentrations of high field strength elements (HFSE) of these rocks (e.g. Zr ~45-80 ppm; see DR section 4), a feature shared by Maplewell Group volcaniclastic strata below the Hanging Rocks Formation. In contrast, the few available analyses for the Blackbrook Group indicate, on average, significantly higher Zr (~100-200 ppm; Pharaoh and Evans, 1987). Overall, Pharaoh et al. (1987) suggest derivation of the Charnian Supergroup from primitive, relatively unfractionated magmas generated within a volcanic arc that was located on oceanic crust or highly attenuated, immature continental crust. The spatially related South Charnwood Diorite intrusions were emplaced into the Maplewell Group and have similarly low Zr contents (~60-110 ppm), but belong to the high-K calc-alkaline series. Their composition suggests that the volcanic arc, to which the Charnwood Supergroup is related, had achieved greater maturity in its later stages and was floored by thickened crust (Noble et al., 1993).

Paleontology of the Charnian Supergroup

Precambrian fossils from Charnwood Forest were first documented as early as 1848, and played a key role in demonstrating the Precambrian age of the Australian Ediacara biota and other Neoproterozoic macro-biotas worldwide (see Howe et al., 2012, and references therein). More than a dozen fossiliferous bedding planes are known in Charnwood, ranging from the middle part of the Ives Head Formation through to the upper part of the Bradgate Formation. Their stratigraphic distribution is conspicuously uneven: there are particular concentrations around the level of the Sliding Stone Slump Breccia and the upper part of the Bradgate Formation (Fig. 2). The degree to which this distribution records a primary paleoenvironmental signal or some secondary effect(s) (e.g. taphonomic, structural, outcrop area) is currently uncertain.

The Charnian biotas (Fig. 4) have been divided into two informal assemblages (Wilby et al., 2011). The so-called Lubcloud Assemblage is restricted to a single bedding plane surface in the Ives Head Formation, close to the base of the exposed succession. It hosts a collection of at least 16 moderately high epirelief impressions, each with a broadly circular or oval outline and a relatively simple, irregular or lobate, internal architecture. These fossils were originally assigned to 3 new genera (*Blackbrookia*, *Ivesheadia*, *Shepshedia*, Boynton and Ford, 1995), but most workers now consider them to be preservational variants (i.e. taphomorphs) of other taxa (though see Laflamme et al., 2011), and collectively refer to them as ivesheadiomorphs (Liu et al., 2011; Wilby et al., 2011). Their affinities remain unclear and, consequently, distinction of the Lubcloud Assemblage may be taphonomic.

The Mercian Assemblage encompasses fossiliferous horizons within the Beacon Hill and Bradgate formations (Fig. 2). In most cases, these are dominated by rangeomorphs, a high-order clade of uncertain affinity that is characterized by fronds with a pseudofractal architecture (Narbonne, 2004; Brasier et al., 2012). Fronds of *Charniodiscus*, considered by Xiao and Laflamme (2009) and Erwin et al. (2011) to be a member of the equally enigmatic Arboreomorpha, or the “Frondomorpha” of Grazhdankin et al. (2011), also form an important contingent on several surfaces, and the discoidal holdfasts (*Aspidella*) of both groups of fronds are ubiquitous. In all cases, the fossils are preserved as low epirelief impressions and retain sub-millimetric detail. Currently, the oldest-known representative of the Mercian Assemblage is a single *Aspidella* disc in the middle of the Beacon Hill Formation, ca. 2000 m stratigraphically above the Lubcloud Assemblage.

The Mercian Assemblage has yielded the type specimens of several important Ediacaran taxa, most notably *Charnia masoni*, *Charniodiscus concentricus* and *Bradgatia* *linfordensis* (Ford, 1958; Boynton and Ford, 1995). Recent work has shown that these form part of high diversity and high density communities, preserved *en masse* and *in situ* beneath event beds (Wilby et al., 2011). The composition of the communities most closely resembles those of the Avalonian assemblages in Newfoundland (e.g. see Hofmann et al., 2008; Liu et al., 2012), which are broadly coeval and occupied comparable deepwater settings (Wood et al., 2003). A number of taxa are shared in common (e.g. *Charnia*, *Charniodiscus*, *Bradgatia, Primocandelabrum*), but both regions also host a substantial number of apparently endemic forms. Notable is the contrast in abundance of prostrate/reclining taxa (e.g. *Fractofusus*, *Hapsidophyllas*, *Pectinifrons*), which are abundant in the Newfoundland biotas but seemingly absent in the Charnian ones, implying that the communities had profoundly different structures (Wilby et al., 2011).

Regional setting and previous geochronology

Together with other late Neoproterozoic sequences in southern Britain (e.g. Tucker and Pharaoh, 1991), the Charnian Supergroup represents the local products of the eastern sector of the ‘Avalonian’ volcanic arc (Gibbons and Horak, 1996; O'Brien et al., 1996; Nance et al., 2008). In southern Britain, these East Avalonian rocks and recently recognized Meguma Terrane rocks in N Wales (Waldron et al., 2011) form a collage of tectonically bounded ‘terranes’ (Fig. 1, inset), each with a distinct tectonostratigraphic succession. Charnwood Forest forms part of the Charnwood Terrane, bounded to the east by the entirely concealed Fenland Terrane (Noble et al., 1993; Pharaoh and Carney, 2000), and to the west by the Wrekin Terrane of the Welsh Borders; the Cymru and Monian Terranes lie farther to the west beneath Wales.

Three periods of magmatism can be distinguished. The earliest period, dated at ca. 710-675 Ma, is recorded by rocks of the Wrekin Terrane, which encompass the Stanner

Hanter and Malvern complexes (Strachan et al., 2007; Schofield et al., 2010). This was followed by a moderately high-grade metamorphic episode at ca. 665-650 Ma, affecting both the Wrekin Terrane and Monian Terrane of Anglesey, and broadly coeval with the 'Avalonian-Cadomian' orogenesis (Strachan et al., 1996; Strachan et al., 2007). The next significant magmatic pulse occurred ca. 620-600 Ma and is principally recorded in the Monian and Cymru terranes (Tucker and Pharaoh, 1991; Compston et al., 2002; Schofield et al., 2008), though felsic tuffs in the Oxendon, Orton and Glinton boreholes to the southeast of Charnwood Forest (Fig. 1 inset) suggest contemporary magmatic activity in the Fenland Terrane (Noble et al., 1993). Granophyric diorites of the Caldecote Volcanic Formation at Nuneaton, part of the Charnwood Terrane, are dated at 603 ± 2 Ma (Tucker and Pharaoh, 1991).

The youngest episode of East Avalonian magmatism, between ca. 572 and 556 Ma, is recorded in the Cymru and Wrekin terranes. It is constrained in the Cymru Terrane by tuffs in the Arfon Group (Compston et al., 2002), and in the Wrekin Terrane by Uriconian volcanic rocks (rhyolite lavas) and the Ercall granophyre (Tucker and Pharaoh, 1991), bentonites and tuffs in the Longmyndian Supergroup (Compston et al., 2002), and rhyolitic tuffs of the Warren House Formation (Tucker and Pharaoh, 1991; Brasier, 2009).

SHRIMP zircon U-Pb dates for two stratigraphic levels within the Maplewell Group indicate that magmatism in the Charnwood Supergroup was coincident with this youngest Avalonian episode (Compston et al., 2002). The interpretation of the SHRIMP U-Pb data is reliant upon assumptions in converting relatively imprecise U-Pb data points (typical $^{206}Pb/^{238}U$ 2 sigma age uncertainties of ≥2%) into a more precise interpreted date (see review by Condon and Bowring, 2011). Notwithstanding these caveats, age probability density plots for the Park Breccia Member (Fig. 5), a unit at the base of the Bradgate Formation, reveal a prominent ca. 540-580 Ma peak, a subordinate ca. 600-640 Ma peak, and minor amounts of older material. In detail, the 540-580 Ma peak has three maxima corresponding to mixture-modeled ages of 548.7 ± 1.7 Ma, 559.3 ± 1.9 Ma, and 573.2 ± 1.0 Ma. The 559.3 ± 1.9 Ma date was interpreted as the true depositional age, on the basis of it being broadly within the then understood age range for other localities containing frondose Ediacaran macro-fossils. Compston et al. (2002) also investigated a 'tuff' from Bardon Hill Quarry, which gave a prominent asymmetric peak at 590.5 ± 1.6 Ma, with a small subsidiary peak at 566.1 ± 3.1 Ma, the latter interpreted as dating the time of volcanic eruption. These SHRIMP data provide some useful first-order age constraints for the Charnian Supergroup, but a more precise geochronology provided by CA-ID-TIMS analysis is needed in order to more accurately understand the global context of the biotas.

Final magmatic cessation was diachronous across Avalonia from ca. 600 Ma to 540 Ma (Nance et al., 2008), with magmatism in the part of East Avalonia now represented in southern Britain ending at ca. 560-555 Ma (Pharaoh and Carney, 2000). During or soon after that time, the arc associated with the Charnian Supergroup was tectonically juxtaposed with other volcanic arcs, marginal basins and intra-arc basins, thus forming the Avalonian Superterrane (Gibbons, 1990). Erosion and/or subsidence of the consolidated Avalonian landmass was followed by a significant Cambrian transgression of the Iapetus Ocean (Brasier, 1980). Provenance studies on the Lower Cambrian Wrekin Quartzite (Murphy et al., 2004) show that the U-Pb ages of detrital zircon grains fall into three groupings that broadly reflect the main phases of local Avalonian magmatism outlined above, these being at: 672 ± 9 to 651 ± 10 Ma, 628 ± 7 to 598 ± 6 Ma, and 564 ± 5 to 534 ± 8 Ma. Single zircon grains at 715 Ma and in the ranges 1036-1539 Ma, together with one Palaeoproterozoic (1.7 Ga) and one Archaean (ca. 3 Ga) zircon, were also recorded.

U-Pb GEOCHRONOLOGY

Seventeen horizons within the Charnian Supergroup were sampled, and 8 sample sites yielded zircon grains suitable for geochronology (Fig. 1). These span the full stratigraphic succession and include the key lithostratigraphic boundaries and principal fossil occurrences (Fig. 2). The South Charnwood Diorite intrusions were also sampled in order to constrain the youngest possible depositional age for the bulk of the succession, but no suitable zircons were recovered.

Analytical Methods

Full details of the analytical techniques employed are given in the online supplemental material[1]. In brief, annealed zircons were mounted in epoxy (Mattinson, 2005), CL imaged, and analysed by laser ablation multicollector inductively coupled mass spectrometer (LA-MC-ICP-MS) (Horstwood et al., 2003). Chemically abraded zircons (12 hr at 180° C) were analysed by ID-TIMS. This process serves to eliminate Pb-loss as well as to remove potentially high common Pb domains within the crystals, such as the large melt inclusions that occupy the central portions of many grains analysed in this study. The accuracy of the ID-TIMS $^{238}U/^{206}Pb$ dates presented herein is controlled by the gravimetric calibration of the EARTHTIME U-Pb tracer (ET535), the determination of the ^{238}U decay constant, and the present day $^{238}U/^{235}U$ (Jaffey et al., 1971; Condon et al., 2007, Hiess et al., 2012). Age uncertainties are presented as ± (X,Y,Z), where X is the uncertainty arising solely from internal or analytical uncertainty, Y includes X and the tracer calibration uncertainty, and Z includes Y and the ^{238}U decay constant uncertainty.

Results

Summary sample details and their geological contexts are provided in Table 1. Detailed field and petrographic descriptions, SEM catholdoluminescence images of typical zircon grains (Fig. DR 2), calculation of LA-ICP-MS ages, concordia plots (Figs. DR 3 and 4) and tables of U-Pb data (Tables DR 1 and 2) are given in the online Data Repository. The most salient aspects of the geology and results of the LA-ICP-MS and CA-ID-TIMS dating are summarized below and are illustrated in figures 5 and 6.

Ives Head Formation (Blackbrook Group): Samples JNC 916, 836, 917

Samples JNC 916 and JNC 836 were collected from rocks occupying stratigraphic positions within ca. 500 m of the lowest exposed part of the Charnian Supergroup and comprise normally graded volcaniclastic sandstones. Sample JNC 916 was collected at Morley Quarry just above the exposed base of the Ives Head Formation from a several meters-thick succession of volcaniclastic sandstones, siltstones and mudstones. JNC 836 was taken from 1.5 m below the bedding plane containing the Lubcloud Assemblage at the eponymous Ives Head locality (Boynton and Ford, 1995). JNC 917 is from the type locality of the South Quarry Breccia Member (Moseley and Ford, 1985; Carney, 2000a), which defines the top of the Ives Head Formation, and is representative of the coarser-grained breccia facies.

Zircons from all three samples have a virtually identical morphology. The vast majority (~99%) are sharply facetted elongate crystals with pristine surfaces, suggesting minimal sedimentary abrasion. They have well-developed oscillatory zoning and typically contain melt inclusions (Fig. DR 2a-f). Colorless mineral inclusions are also present in many grains, as are inherited cores in some grains. Petrographic examination of the host samples shows that these zircons occur in the volcaniclastic matrix and, at least in JNC 836 (Fig. DR 1a), also within volcanic lithic fragments. A trace proportion of zircons, distinct from the dominant population, are slightly- to well-rounded, suggesting sedimentary abrasion or magmatic resorption (Fig. DR 2h).

LA-ICPMS U-Pb data obtained for JNC 836 and 917 show that the majority of zircons with <5% discordance define single ca. 600 Ma populations with indistinguishable ^{206}Pb/^{238}U ages of 611 +2/-4 Ma and 611 ± 2 Ma (as calculated using TuffZirc; Ludwig, 2003; Ludwig and Mundil, 2002), respectively (Fig. 6). JNC 836 zircons additionally record older dates of 630 ± 12 Ma, 703 ± 14 Ma, 1045 ± 18 Ma, 1228 ± 20 Ma and 1484 ± 29 Ma. These dates constrain the ages of inherited cores based on textures in ablated grains (Fig. DR 2g), or possibly where mixtures of core and rim zircon material may have been accidentally ablated, although the latter was unlikely given the consistency of isotope ratios observed throughout the ablation periods for all analysed grains.

CA-ID-TIMS data corroborate and refine the LA-ICPMS results, with concordant data sets for JNC 916, 836 and 917 revealing an age range within samples from ca. 620 to ca. 611 Ma. Separate from this main group are two slightly older zircons with ^{206}U/^{238}U ages of ca. 622 Ma. The youngest grains from each of the 3 samples overlap within error between 611.3 ± (0.6, 0.8, 1.1) Ma and 612.3 ± (0.7, 0.9, 1.1) Ma. A maximum age for these rocks of 611 Ma is assigned on the basis of these youngest zircons due to the lack of definitive evidence that these grains are true pyroclastic zircons.

Beacon Hill Formation (Maplewell Group): Samples JNC 918, 907, 911

Three locations in the Beacon Hill Formation provided zircon-bearing samples whose results are presented here. The lowermost sample (JNC 918) is from the type locality (at "Pillar rock", see Moseley and Ford, 1985) of the Benscliffe Breccia Member at the base of the Beacon Hill Formation, and consists of an andesite breccia with a coarse crystal-lithic matrix (Carney, 1999). Zircons from sample JNC 918 are mostly stubby, colorless and sharply faceted, and they typically contain prominent melt inclusions. LA-ICPMS data show that the zircon population from this horizon differs significantly from the underlying Blackbrook Group due to the presence of a <600 Ma zircon component. Population unmixing calculations for <10% discordant data yields two main age components at 600 ± 2 Ma and 569 ± 7 Ma. CA-ID-TIMS analysis of the youngest grains identified by LA-ICPMS, together with additional grains prepared solely for CA-ID-TIMS, confirm <600 Ma ages (Fig. 6); 2 out of 12 analyses are concordant and give a $^{206}U/^{238}U$ age of 569.1 ± (0.5, 0.7, 0.9) Ma. The rest of the CA-ID-TIMS ages range from 618-611 Ma, which overlaps within error that of the samples from the underlying Blackbrook Group.

Sample JNC 907 was collected from Bardon Hill Quarry from the same general locality as the 'tuff' sample CH8 of Compston et al. (2002), ostensibly from the Bardon Hill Volcanic Complex, but from 'bedded volcanic rocks'. Close re-examination of the field relationships during this study indicate these 'bedded volcanics' are well-stratified volcaniclastic strata faulted against the Bardon Hill Volcanic Complex *sensu stricto*. Carney and Pharaoh (2000a) originally considered these strata to be part of the Bradgate Formation; however, the 566.1 ± 3.1 Ma age of Compston et al's (2002) CH8 sample is significantly older than their age for the Park Breccia (CH2, 559.3 ± 2.0 Ma) at the base of the Bradgate Formation, suggesting contemporaneity with a level in the underlying Beacon Hill Formation instead.

JNC 907 comprises normally graded volcaniclastic sandstones and siltstones. Petrographic examination of the coarser material shows angular quartz and plagioclase crystal fragments typical of other Charnian volcaniclastic rocks, together with tightly packed, sub-rounded to highly angular lithic fragments of varied lithology, including glassy, oxidised and locally shardic andesite, and andesite with textures ranging between aphanitic, microgranular and fluxional/intergranular. Most of the recovered zircons have morphologies and internal features similar to those in JNC 918. A minor proportion of the total amount of zircon recovered are grains with abraded, rounded surfaces. CA-ID-TIMS data were obtained for 5 euhedral and apparently unabraded grains, one of which has a $^{206}Pb/^{238}U$ age of 614.5 ± 0.6 Ma, while the other four had $^{206}Pb/^{238}U$ ages of ca. 567-565 Ma. The age of JNC 907 is interpreted here to be 565.2 ± (0.3, 0.7, 0.9) Ma, based on the $^{206}Pb/^{238}U$ ages of two overlapping and concordant analyses; this confirms and refines the Compston et al. (2002) age of 566.1 ± 3.1 Ma.

Sample JNC 911 is from the summit of Beacon Hill, where *Aspidella* has been found (Fig. 4f), lying approximately in the middle of the Beacon Hill Formation. It is a vitric tuff (Carney, 2000d) that contains abundant zircons that are morphologically similar to those recovered from JNC 918. Given their lack of surface abrasion, the grains are interpreted to be proximally derived. Only ca. 600 Ma grains were encountered, with CA-ID-TIMS data on 4 grains giving a $^{206}Pb/^{238}U$ age range of 614.7 – 611.6 Ma.

Park Breccia, Bradgate Formation (Maplewell Group): Sample JNC 912

Sample JNC 912 is from the same location that Compston et al. (2002) collected their sample (CH2) of the Park Breccia, allowing the base of the Bradgate Formation to be dated. The Park Breccia occupies a stratigraphic position a few to several meters below one of the key fossil assemblages (Memorial Crags, Bradgate Park, Wilby et al., 2011). JNC 912 is a poorly sorted volcaniclastic sandstone containing centimeter-sized slivers of mudstone and siltstone. Its matrix is comprised of andesitic grains showing a range of textures between aphanitic, microgranular and intergranular (Fig. DR 1d). The zircons are stubby, colorless and sharply facetted and as with similar zircons from the underlying Beacon Hill Formation, they typically contain prominent melt inclusions. CA-ID-TIMS analysis reveals the presence of two zircon populations. The older population has an average $^{206}Pb/^{238}U$ age of 613.5 ± 3.4

Ma, which lies within the age range of the main zircon population in the Ives Head Formation (Fig. 6). The younger zircons, however, are concordant with a $^{206}Pb/^{238}U$ age of 561.9 ± (0.3, 0.7, 0.9) Ma (n = 7) which is interpreted here as the deposition age based on the presence of volcanic glass preserved in tuffaceous rocks exposed in other parts of the Bradgate Formation. These zircons were processed using the EARTHTIME tracer and supercede the previously reported CA-ID-TIMS data (concordia age = 563.9 ± 1.9 Ma, analytical uncertainty only; n = 4) that employed the Tom Krogh Carnegie $^{205}Pb/^{235}U$ tracer formerly used at NIGL (Carney and Noble, 2007; Wilby et al., 2011).

Hanging Rocks Formation (Maplewell Group): Sample JNC 846

Sample JNC 846, from the type locality of the Hanging Rocks Formation (Carney, 2000c) and stratigraphically at the top of the Maplewell Group, is a poorly sorted micaceous sandstone containing well-rounded granules (Fig. DR 1e) and small pebbles (e.g. Carney, 1999), as well as elongate siltstone clasts. The pebbles and granules are mainly of volcanic origin, and include microcrystalline andesite and dacite, but meta-quartzite and perthitic alkali feldspar are also present. The sample yielded a varied zircon population, including sharply facetted grains that are morphologically akin to those in the underlying units, as well as well-rounded detrital grains (DR Fig 2o-p). U-Pb ages derived from the LA-ICPMS data concentrate in the range 750-550 Ma, with older grains at 1176 ± 36 Ma, 2076 ± 55 Ma and 2597 ± 76 Ma. Within the ca. 750-550 Ma range there are probability density peaks and isolated concordant analyses at 729 ± 9 Ma (n = 3), 673 ± 19 Ma (n = 1), 608 ± 2 Ma (n = 43) and 562 ± 6 Ma (n = 5). A mean $^{206}Pb/^{238}U$ age of 556.4 ± 6.4 Ma is obtained for the <10% discordant youngest grains (n = 4), whose age is distinctly separate from the ca. 600 Ma grains; this overlaps within uncertainty with the Park Breccia age.

DISCUSSION

The age of the Charnian Supergroup

The zircon ages must be interpreted within the context of the petrogenetic and subsequent depositional history of the rocks. With respect to the Ives Head Formation, the youngest zircon analysis obtained is 611.3 ± (0.6, 0.8, 1.1) Ma (JNC 917). Similar overlapping dates were obtained for all other stratigraphic levels within the Blackbrook Group. This feature, coupled with an inability to unambiguously identify pyroclastic material based on the parts of the Blackbrook Group examined in this study, coupled with the obviously resedimented (volcaniclastic) character of the succession, means that the dates are best regarded as maximum depositional ages. The lack of constraint on the time elapsed between primary eruption of the grains and their subsequent remobilization and deposition as turbidites prevents a more definitive age assignment. Noteworthy is the apparent complete absence of any <570 Ma zircons in these rocks, which stands in stark contrast to their presence in all but one of the productive samples from the overlying Maplewell Group. Given the total number of grains examined by LA-ICPMS (n = 133) and CA-ID-TIMS (n = 32) for the Blackbrook Group, any such zircons should have been detected if they were present. At the very least, a minimum age for the Blackbrook Group of ≥ 569 Ma can be assigned based on the age of the youngest, likely syn-depositional, zircons in the Benscliffe Breccia Member at the base of the overlying Maplewell Group (JNC 918).

These new U-Pb data provide broad age constraints for the ivesheadiamorph fossils preserved at Ives Head (Lubcloud Assemblage of Wilby et al., 2011) and that this assemblage must be younger than 611 Ma and older than 569 Ma. Providing tighter depositional age constraints is not possible at this point. Although the overall petrographic character of these volcaniclastic rocks is consistent with them being a primary mass flow of pyroclastic debris further evidence is needed to link such strata directly to eruptive events. Only the discovery of datable horizons within the Ives Head Formation that can be unambiguously linked to a short-lived geological event, e.g. a volcanic ash bed, will lead to improvements in this chronology. Despite intensive efforts, no suitable horizons have been identified thus far. Nevertheless, the scale of the stratigraphic interval (ca. 1000 m, compacted) separating the Lubcloud Assemblage from the Benscliffe Breccia Member suggests that the assemblage is considerably older than 569 Ma.

Interpretation of the geochronological data for the Maplewell Group is more straightforward. Pyroclastic grains in the form of unabraded volcanic glass shards are present in many of the tuffaceous horizons in both the Beacon Hill and Bradgate Formations, as noted above. Although the dated rocks are not all necessarily primary pyroclastic deposits, their sedimentology, geological relationships and the overall upward – younging trend of their zircon ages suggest that their deposition was penecontemporaneous with local volcanism. The earliest demonstrable volcanism in the group is given by the Benscliffe Breccia Member (JNC 918) at the base of the Beacon Hill Formation, dated at 569.1 ± (0.5, 0.7, 0.94) Ma on the basis of the two youngest CA-ID-TIMS analyses and the lateral association with very coarse-grained andesite volcanic breccias of the Charnwood Lodge Formation. Additional constraint on the age of this formation is given by the volcaniclastic sequence in the Bardon Hill Quarry (JNC 907), dated at 565.2 ± (0.3, 0.7, 0.9) Ma (*cf* 566.1 ± 3.1 Ma, Compston et al., 2002).

The CA-ID-TIMS age of 561.9 ± (0.3, 0.7, 0.9) Ma for the Park Breccia at the base of the Bradgate Formation (JNC 912) is within uncertainty of the 559.3 ± 1.9 Ma date of Compston et al. (2002), the latter being partly based on correlation with the dated fossiliferous horizons at Mistaken Point (Benus, 1988). The refined age provided by the CA-ID-TIMS data is consistent with the stratigraphically higher position of the Park Breccia relative to the Benscliffe Breccia Member (Fig. 2). Using the new ages of the Park Breccia and the Benscliffe Breccia Member it is possible to derive an estimate of the average rate of accumulation for the Beacon Hill Formation (compacted) and, consequently, an age estimate for included fossiliferous horizons. In the eastern part of the inlier, the formation is ca. 1440 m thick, thus giving a deposition rate of about 200 m/Myr.

Age constraints for the uppermost part of the Charnian Supergroup are provided by the LA-ICPMS data for the Hanging Rocks Formation (JNC 846) whose age and relationship to underlying and overlying units had previously been uncertain. A late Neoproterozoic depositional age for this formation is supported by overlapping <5% discordant zircons at 556.6 ± 6.4 Ma, with no zircons younger than about 550 Ma. This preliminary age is broadly supported by the apparent absence of pebbles of the distinctively granophyric South Charnwood Diorites within the unit, suggesting that these late Precambrian intrusions had yet to be erosionally unroofed, in contrast to the situation during the deposition of the overlying Lower Cambrian Brand Group (see McIlroy et al., 1998). The presence of pristine, unabraded volcanic ash shards within tuffaceous interbeds in the upper part of the Hanging Rocks Formation (Worssam and Old, 1988; McIlroy et al., 1998) demonstrates that sedimentation was coincident with volcanism. That this volcanism was probably a continuation of the Charnian arc system is borne out by the fact that the Hanging Rocks Formation and the preceding Maplewell Group rocks share the same dissected magmatic-arc petrographic signature (McIlroy et al., 1998). Hence, on balance, we consider the formation to be part of the Neoproterozoic succession and include it at the top of the Maplewell Group (Fig. 2).

The age determinations for the Charnian Supergroup place maximum age constraints on the South Charnwood Diorites that are emplaced into the upper part of the Maplewell Group (Fig. 1). A Precambrian age was strongly suggested for these intrusions by the occurrence of detrital grains of granophyric diorite in Lower Cambrian quartz arenites of the Brand Hills Formation (Brand Group) and by textural similarities with Caldecote Formation diorites at Nuneaton (Fig. 1, inset) (McIlroy et al., 1998). Petrographic similarity between the Nuneaton and Charnwood diorites were supported by similarities in major and trace element chemistry (Bridge et al., 1998) and Nd isotope signature (McIlroy et al., 1998). The new Charnian Supergroup ages establish a maximum age of ca. 561.9 ± 0.9 Ma for the South Charnwood Diorites. This is comparable to the crystallization ages of other southern British Avalonian granophyric intrusions, such as the 560 ±1 Ma Ercall Granophyre (Tucker and Pharaoh, 1991) at The Wrekin (Fig. 1 inset). If the 603 ± 2 Ma Nuneaton diorite zircon grains analysed by Tucker and Pharaoh (1991) are indeed primary magmatic grains then arguments for close geological correlation with the Charnwood diorites are invalidated.

The new U-Pb data constrain the Mercian Assemblage to a ca. 12 Myr period: from ca. 569 Ma (the youngest zircons in the Benscliffe Breccia) to ca. 557 Ma (the maximum date for the Hanging Rocks Formation). The bedding-plane that hosts the type specimens of *Bradgatia linfordensis* (Boynton and Ford, 1995), as well as examples of several other taxa (see Wilby et al., 2011), is the most precisely constrained fossil horizon, with an age of 561.9 ± (0.3, 0.7, 0.9) Ma based on the date for the Park Breccia which lies a short stratigraphic interval below (Figs. 2 and 6). No zircons amenable to dating were obtained from the stratigraphically highest recorded Mercian Assemblage fossil locality, which hosts the most diverse biota (Wilby et al., 2011). However, since the strata are only ca. 200 m stratigraphically below the Hanging Rocks Formation, their age may be as young as ca. 557 Ma.

A fundamental feature of the Charnian Supergroup U-Pb data set is the persistence of ca. 610 Ma zircons throughout the entire stratigraphic section, and the absence of zircons with ca. 600-570 Ma ages. The ca. 610 Ma zircon population is consistent and tightly age-delimited in the Blackbrook Group, whereas there is a modest spread to younger mean ages going upwards into the Maplewell Group. In the case of the Maplewell Group rocks, these older zircons could represent xenocrysts incorporated into the andesitic-dacitic magmas of the volcanic centers associated with the Charnwood primary volcaniclastic rocks and erupted along with neocrystalline zircons from those magmas. Alternatively, these older zircons may be representative of an epiclastic volcanic detritus contribution to the Maplewell volcaniclastic rocks that was persistently available throughout the entire depositional history of the group. Of note is that this older population of zircons, that is consistently present within the Charnwood rocks, is broadly coeval with arc volcanism at ca. 620-600 Ma as recorded in the Cymru and Fenland terranes (Fig. 1, inset; Tucker and Pharaoh, 1991; Compston et al., 2002; Noble et al., 2003; Schofield et al., 2008). The Fenland Terrane is a preferred candidate source for the pervasive ~600 Ma zircons in the Charnian rocks given its proximity to Charnwood. Supporting evidence is provided by geochemical data for three volcanic pebbles separated from a conglomerate of the Hanging Rocks Formation (see DR section 4 and Fig. DR 4) whose major and trace element compositions are similar to Fenland Terrane rocks (Pharaoh et al., 1991).

Global context of the Charnian Supergroup

The new data for the Charnian Supergroup augment current understanding of the wider Ediacaran macro-biota. Age constraints on the Lubcloud Assemblage of ivesheadiomorphs, and the Blackbrook Group in general (<611 Ma and >569 Ma), overlap at least the middle and upper parts of the Conception Group in Newfoundland (Fig. 7), based on zircon ages for its constituent Gaskiers and Mistaken Point formations at 582 Ma and ca. 565 Ma, respectively (Benus, 1988; Bowring in Schmitz, 2012). The oldest currently known Ediacaran macro-fossils occur towards the top of the Drook Formation in Newfoundland (Narbonne and Gehling, 2003), approximately 150 m stratigraphically below a level dated at 578.8 ± 0.5 Ma (Bowring in Schmitz, 2012). The maximum age (611 Ma) for the Lubcloud Assemblage far exceeds this date, and also that of the Gaskiers Glaciation, beneath which no rangeomorph fronds have been reported. Even so, we note the substantial size, complexity and diversity of the Drook fossils, which imply considerable antecedence (*cf.* Narbonne and Gehling, 2003; Liu et al., 2012).

Despite the potential antiquity of the Blackbrook Group there is a lack of glacigenic diamictites or related glacial lithologies at outcrop. Glacigenic strata are also absent from other Neoproterozoic successions in southern Britain (Pharaoh and Carney, 2000). This is in marked contrast to the situation elsewhere on Avalonia. For example, the Gaskiers Formation diamictite in Newfoundland is up to 300 m thick (see Eyles and Eyles, 1989). Several possibilities exist for their apparent absence in the Charnian Supergroup: (i) the Gaskiers equivalent time interval is present in the exposed succession, but glacigenic facies were not deposited/preserved; (ii) their presence is obscured by insufficient exposure and/or structural complexity; (iii) the base of the exposed succession is <582 Ma; or (iv) that there is a hiatus in deposition and/or volcanism between the Blackbrook and Maplewell groups such that material of Gaskiers age is not present. Based on the currently available data it is not possible to discriminate between these four possibilities, but the moderate level of exposure in Charnwood Forest and the scarcity of strike-parallel faults (see Fig. 1) make the second possibility unlikely.

Age constraints on the taxonomically diverse Mercian Assemblage (569 Ma to ca. 557 Ma) overlap the upper part of the Conception Group and at least the lower to middle parts of the St. John's Group in Newfoundland (Fig. 7), based on the published relatively imprecise zircon age (565 ± 3 Ma; Benus, 1988) for the tuff on top of the fossil-rich E-surface (Landing et al., 1988; Clapham et al., 2003) in the Mistaken Point Formation. Significantly, this time interval represents the acme of fossil diversity in both successions. The new Charnian data extend the known upper absolute chronostratigraphic ranges of several taxa in the classic Avalon Assemblage (e.g. *Charnia masoni*, *Charniodiscus cf. arboreus*, *Bradgatia linfordensis*, *Primocandelabrum* sp., *Aspidella*) by ca. 8 Myrs (to ca. 557 Ma). This highlights the typically long ranges (up to ca. 20 Ma) of Ediacaran taxa and the likely existence of stable, long-lived community structures within this deepwater biotope.

The new data also help to elucidate the cause of observed provincial differences in the composition of Avalon Assemblage biotas. Charnwood Forest and the Avalon and Bonavista peninsulas of Newfoundland each support seemingly endemic taxa (e.g. see Clapham et al., 2004; Hofmann et al., 2008; Wilby et al., 2011), despite paleogeographic proximity (e.g. Li et al., 2008). For example, *Fractofusus* and *Pectinifrons* are apparently absent in Charnwood Forest, whereas they are abundant through a considerable stratigraphic interval on the Avalon Peninsula (Gehling and Narbonne, 2007; Bamforth et al., 2008; see also Liu et al., 2012); *Pectinifrons* is not reported from the Bonavista Peninsula, but *Fractofusus* occurs in the Mistaken Point, Trepassey and Fermeuse formations (Hofmann et al., 2008). Equally, taxa such as *Charniodiscus concentricus*, and the informally named 'dumbbell' (Wilby et al., 2011, their Fig. 2d), are apparently unique to Charnwood Forest. Confirmation of the contemporaneity of these successions weakens the case for a temporal control on the observed differences, and supports assertions of paleoenvironmental sensitivity (Wilby et al., 2011). Significantly, taxa that are shared between the three regions (e.g. *Charnia masoni*, *Charniodiscus cf. arboreus*, *Bradgatia ?linfordensis*) also occur in younger, shallower water deposits (e.g. see Hofmann and Mountjoy, 2010; Gehling and Droser, 2013), including carbonates (see Grazhdankin, 2004), confirming their wide environmental tolerance.

Debate exists regarding the degree to which the classic Avalon, White Sea and Nama assemblages record genuine evolutionary differences, rather than paleobiogeographic or paleoenvironmental signals (e.g. see Waggoner, 2003; Grazhdankin, 2004; Narbonne, 2005; Narbonne et al., 2012; Gehling and Droser, 2013; Laflamme et al., 2013). Significantly, the youngest part of the Charnian Supergroup (562 Ma to ca. 557) may partly overlap fossiliferous strata in the Ust' Pinega Group of Russia, dated at 558 ± 1 Ma (Grazhdankin, 2004) and 555 ± 0.3 Ma (Martin et al., 2000), which are typically assigned to the White Sea Assemblage (e.g. Narbonne et al., 2012; Laflamme et al., 2013). Deposition of the Charnian succession was also contemporaneous with the turbiditic part of the Stretton Group in the Longmynd Inlier (Shropshire, UK), dated at 566.6 ± 2.9 Ma, and potentially also the overlying fossiliferous deltaic beds, parts of which predate 555.9 ± 3.5 Ma (Compston et al., 2002). The Stretton Group contains a very different fossil assemblage to the Charnian Supergroup, apparently lacking fronds and being dominated by discoidal forms such as *Intrites* and *Beltanelliformis* (see Callow et al., 2011; Liu, 2011), but nevertheless it forms part of Wrekin Terrane (see Fig 1), a component of Avalonia (see Pharaoh and Carney, 2000). All of this indicates that very different communities existed in separate settings at the same time, confirming paleoenvironment (and its likely taphonomic consequences) to have been the first-order control on biota composition (Grazhdankin, 2004; Wilby et al., 2011; Gehling and Droser, 2013).

The results of this study suggest three avenues of investigation that could be followed to further advance our understanding of this important Ediacaran fossil locality. First, the conservative interpretation of the youngest zircons discovered thus far in the Blackbrook Group as being indicative of a maximum age for the ivesheadiamorphs in Charnwood Forest needs further research. Field work for this study only investigated the Ives Head Formation turbiditic rocks. What is now needed is a careful search for, and dating of, strata that contain identifiably primary pyroclastic constituents, for example ash beds, in both the Ives Head Formation and upwards into the Blackbrook Reservoir Formation. Secondly, new fossil horizon discoveries are being made on a regular basis at Charnwood through the continued research by BGS investigators and others, and these discoveries will need to be placed within an accurate and precise chronostratigraphy that is being updated. Such refinements to the chronostratigraphy are necessary as they will help facilitate correlation with an emerging Ediacaran chronology worldwide. An assessment of the geochronology potential of all available ash beds in the Maplewell Group was beyond the scope of this study and there remains much to be done. Finally, the data presented for the Hanging Rocks Formation provides a useful preliminary age but suitable zircons for dating were exhausted before high precision ages by CA-ID-TIMS could be obtained. Further geochronology investigation of this formation will lead to insights into the nature of the minimum age of the Charnwood Precambrian fossils as well as nature of the Precambrian-Cambrian transition that is represented by the Hanging Rocks Formation and overlying Brand Formation.

CONCLUSIONS

High precision U-Pb zircon dating of multiple levels within the ca. 3200 m thick Charnian Supergroup of central England has generated a better resolved chronostratigraphy for the fossiliferous succession. The oldest division, the Blackbrook Group, has a prominent late Neoproterozoic 620-611 Ma zircon population; notable is the complete absence of ca. 570-560 Ma zircons. The overlying Maplewell Group shows a dual distribution of zircon ages: an older population that is statistically indistinguishable from the main zircon population in the Blackbrook Group, and a younger one ranging between 569 Ma and ca. 557 ± 6 Ma, interpreted here to reflect the age of deposition. Thus, there is very considerable temporal overlap with the fossiliferous successions on the Avalon Peninsula of Newfoundland (Narbonne, 2005). Observed differences in the structure and composition of their respective coeval communities are therefore most parsimoniously interpreted as evidence of ecological specialization (*cf* Wilby et al., 2011).

On the basis of the new zircon age interpretations, the oldest fossiliferous horizon in Charnwood Forest, consisting entirely of ivesheadiomorphs, is constrained to the interval <611 Ma and >569 Ma. Given that the fossils lie >600 m below the 569 Ma Benscliffe Breccia Member, they are likely to be significantly older than 570 Ma, perhaps of comparable or greater antiquity to the oldest known Ediacaran macro-fossils in Newfoundland (dated at ca. 579 Ma). The highest diversity biotas in Charnwood Forest, which lie within the upper part of the Maplewell Group, are constrained to the interval ≤562 Ma-ca. 557 Ma. They therefore broadly overlap to post-date the currently recognized acme of diversity in the Newfoundland succession, based on the published ca. 565 Ma age (Benus, 1988) for the famous E surface in the Mistaken Point Formation. U-Pb data suggest that the youngest biotas in Charnwood Forest probably temporally overlap with taxonomically very different biotas in the Longmynd (Shropshire, UK), constrained between ca. <567 Ma and ca. 556 Ma (Compston et al., 2002), and possibly also White Sea assemblages in Russia dated at ca. 558 Ma (Grazhdankin, 2004) and 555 Ma (Martin et al., 2000) and the Zigan Formation assemblage (South Urals) dated at 548.2 ± 7.6 Ma (Grazhdankin et al., 2011).

ACKNOWLEDGMENTS

Analytical work was supported by funding under NIGFSC project IP/564/0998; PRW was supported by NERC grant NE/I005927/1. We thank our NIGL colleagues Adrian Wood, Nicola Atkinson, Laura Braccali and Neil Boulton for laboratory support; Stephen Parry and Gren Turner at BGS for zircon imaging; Sue Martin, Louise Neep, Paul Shepherd, Mark Dean from BGS, and GeoEd for molding and casting the fossils; and specimen photography of some of the samples by Paul Witney and Charlotte Kenchington from BGS. We gratefully acknowledge the assistance in facilitating site access given by Natural England, the Mistaken Point Ecological Reserve (Parks and Natural Areas Division, Government of Newfoundland

and Labrador) and landowners in Charnwood Forest. Stephen Parry and Helen Boynton are thanked for their constructive comments on early versions of the manuscript. Alex Liu, an anonymous reviewer and the associate editor Rob Rainbird are thanked for their generous, helpful and detailed reviews and suggestions. SRN, DJC, JNC, PRW and TCP publish with the permission of the Executive Director of the British Geological Survey (NERC).

REFERENCES CITED

Bamforth, E.L., Narbonne, G.M., and Anderson, M.M., 2008, Growth and ecology of an Ediacaran multibranched rangeomorph from the Mistaken Point Assemblage, Newfoundland: Journal of Paleontology, v. 82, p. 763-777.

Benus, A. P., 1988, Sedimentological context of a deep-water Ediacaran fauna (Mistaken Point, Avalon Zone, eastern Newfoundland), *in* Landing, E., Narbonne, G. M., and Myrow, P., eds., Trace Fossils, Small Shelly Fossils and the Precambrian-Cambrian Boundary, Volume 463, New York State Museum and Geological Survey Bulletin.

Bland, B.H., and Goldring, R., 1995, *Teichichnus* Seilacher 1955 and other trace fossils (Cambrian?) from the Charnian of Central England: Neues Jahrbuch for Geologie und Palaeontologie (Seilacher Festschrift), v. 195, p. 5-23.

Bowring, S., Myrow, P., Landing, E., and Ramezani, J., 2003, Geochronological constraints on terminal Neoproterozoic events and the rise of metazoans: Geophysical Research Abstracts, v. 5, no. 13, p. 219.

Boynton, H.E. 1978. Fossils from the Precambrian of Charnwood Forest, Leicestershire. Mercian Geologist, v. 6, p. 291-296.

Boynton, H.E., and Ford, T.D., 1995, Ediacaran fossils from the Precambrian (Charnian Supergroup) of Charnwood Forest, Leicestershire, England: Mercian Geologist, v. 13, p. 165-183.

Boynton, H.E., and Moseley, J., 1999, The geology of The Brand, Charnwood Forest, Leicestershire: Transactions of the Leicester Literary and Philosophical Society, v. 93, p. 32-38.

Brasier, M. D., 1980, The Lower Cambrian transgression and glauconite-phosphate facies in Western-Europe: Journal of the Geological Society [London], v. 137, p. 695-703.

Brasier, M. D., 2009, Darwin’s Lost World: the Hidden History of Animal Life, Oxford University Press, 304 p.

Brasier, M.D., and Antcliffe, J.B., 2009, Evolutionary relationships within the Avalonian Ediacara biota: new insights from laser analysis: Journal of the Geological Society [London], v. 166, p. 363-384.

Brasier, M.D., Antcliffe, J.B., and Liu, A.G., 2012, The architecture of Ediacaran fronds: Palaeontology, v. 55, p. 1105-1124.

Bridge, D. M., Carney, J. N., Lawley, R. S., and Rushton, A. W. A., 1998, Geology of the country around Coventry and Nuneaton. Memoir for 1:50 000 Geological Sheet 169 (England and Wales), British Geological Survey, 185 p.

Callow, R.H.T., McIlroy, D., and Brasier, M.D., 2011, John Salter and the Ediacara Fauna of the Longmyndian Supergroup: Ichnos, v. 18, p. 176-187.

Canfield, D.E., Poulton, S.W., and Narbonne, G.M., 2007, Late-Neoproterozoic deep-ocean oxygenation and the rise of animal life: Science, v. 315, p. 92-95.

Carney, J.N., 1999, Revisiting the Charnian Supergroup: new advances in understanding old rocks: Geology Today, Nov-Dec, p. 221-229.

Carney, J.N., 2000a, Blackbrook Reservoir, Geological Conservation Review Series No. 20, Joint Nature Conservation Committee, Peterborough, p. 28-30.

Carney, J.N., 2000b, Igneous processes within late Precambrian volcanic centres near Whitwick, north-western Charnwood Forest: Mercian Geologist, v. 15, p. 7-28.

Carney, J.N., 2000c, Outwoods-Hangingstone Hills, Geological Conservation Review Series No. 20, Joint Nature Conservation Committee, Peterborough, p. 43-48.

Carney, J.N., 2000d, Beacon Hill, Geological Conservation Review Series No. 20, Joint Nature Conservation Committee, Peterborough, p. 30-32.

Carney, J. N., and Noble, S. R., 2007, Geological setting, environment and age of the Charnwood biota: Transactions of the Leicester Literary and Philosophical Society, v. 101, p. 49-51.

Carney, J. N., and Pharaoh, T. C., 2000a, Bardon Hill, In Carney, J.N., Horak, J.M., Pharaoh, T.C., Gibbons, W., Wilson, D., Barclay, W.J., and Bevins, R.E. Precambrian rocks of England and Wales, Geological Conservation Review Series No. 20, Joint Nature Conservation Committee, Peterborough, p. 40-43.

Carney, J. N., and Pharaoh, T. C., 2000b, Cliffe Hill Quarry, In Carney, J.N., Horak, J.M., Pharaoh, T.C., Gibbons, W., Wilson, D., Barclay, W.J., and Bevins, R.E. Precambrian rocks of England and Wales, Geological Conservation Review Series No. 20, Joint Nature Conservation Committee, Peterborough, p. 48-52.

Cas, R.A.F., and Wright, J.V., 1991, Subaqueous pyroclastic flows and ignimbrites: an assessment: Bulletin of Volcanology, v. 53, p. 357-380.

Clapham, M. E., and Narbonne, G. M., 2002, Ediacaran epifaunal tiering: Geology, v. 30, p. 627-630.

Clapham, M. E., Narbonne, G. M., and Gehling, J. G., 2003, Paleoecology of the oldest known animal communities: Ediacaran assemblages at Mistaken Point, Newfoundland: Paleobiology, v. 29, p. 527-544.

Clapham, M.E., Narbonne, G.M., Gehling, J.G., Greentree, C., and Anderson, M.M., 2004, *Thectardis avalonensis*: A new Ediacaran fossil from the Mistaken Point Biota, Newfoundland: Journal of Paleontology, v. 78, p. 1031-1036.

Compston, W., Wright, A. E., and Toghill, P., 2002, Dating the Late Precambrian volcanicity of England and Wales: Journal of the Geological Society [London], v. 159, p. 323-339.

Condon., D.J. and Bowring, S.A., 2011, A user's guide to Neoproterozoic geochronology. Geological Society [London] Memoirs, v. 36, p. 135-149.

Condon, D., Schoene, B., Bowring, S., Parrish, R., McLean, N., Noble, S., and Crowley, Q., 2007, EARTHTIME; isotopic tracers and optimized solutions for high-precision U-Pb ID-TIMS geochronology: Eos, Transactions, American Geophysical Union, v. 88, no. 52, Suppl.

Erwin, D.H., Laflamme, M., Tweedt, S.M., Sperling, E.A., Pisani, D., Peterson, K.J., 2011, The Cambrian conundrum: early divergence and later ecological success in the early history of animals: Science, v. 334, p. 1091-1097.

Eyles, N., and Eyles, C.H., 1989, Glacially-influenced deep-marine sedimentation of the Late Precambrian Gaskiers Formation, Newfoundland, Canada: Sedimentology, v. 36, p. 601-620.

Ford, T. D., 1958, Pre-Cambrian fossils from Charnwood Forest: Proceedings of the Yorkshire Geological Society, v. 31, p. 211-217.

Gehling, J.G., and Narbonne, G.M., 2007, Spindle-shaped Ediacara fossils from the Mistaken Point Assemblage, Avalon Zone, Newfoundland: Canadian Journal of Earth Sciences, v. 44, p. 367-387.

Gehling, J.G, and Droser, M.L., 2013, How well do fossil assemblages of the Ediacara Biota tell time? Geology, v. 41, p. 447-450.

Gibbons, W., 1990, Transcurrent ductile shear zones and the dispersal of the Avalon superterrane, *in* D'Lemos, R. S., Strachan, R. A., and Topley, C. G., eds., The Cadomian orogeny, Geological Society [London] Special Publication 51, p.

Gibbons, W., and Horak, J. M., 1996, The evolution of the Neoproterozoic Avalonian subduction system: Evidence from the British Isles, *in* Nance, R. D., and Thompson, M. D., eds., Geological Society of America Special Paper 304, p. 269-280.

Grazhdankin, D., 2004, Patterns of distribution in the Ediacaran biotas: facies versus biogeography and evolution: Paleobiology, v. 30, p. 203-221.

Grazhdankin, D.V., Marusin, V.V., Meert, J., Krupenin, M.T., and Maslov, A.V., 2011, Kotlin regional stage in the south Urals: Doklady Earth Sciences, v. 440, p. 1222-1226.

Halverson, G.P., Hoffman, P.F., Schrag, D.P., Maloof, A.C., and Rice, A.H.N., 2005, Toward and Neoproterozoic composite carbon-isotope record: Geological Society of America Bulletin, v. 117, p. 1181-1207.

Hiess, J., Condon, D. J., McLean, N., and Noble, S. R., 2012, $^{238}U/^{235}U$ Systematics in Terrestrial Uranium-Bearing Minerals: Science, v. 335, p. 1610-1614.

Hofmann, H.J., and Mountjoy, E.W., 2001, Namacalathus-Cloudina assemglage in Neoproterozoic Miette Group (Byng Formation), British Columbia: Canada's oldest shelly fossils: Geology, v. 29, p. 1091-94.

Hofmann, H.J., and Mountjoy, E.W., 2010, Ediacaran body and trace fossils in the Miette Group (Windermere Supergroup) near Salient Mountain, British Columbia, Canada: Canadian Journal of Earth Sciences, v. 47, p. 1305-1325.

Hofmann, H. J., O'Brien, S. J., and King, A. F., 2008, Ediacaran biota on Bonavista Peninsula, Newfoundland, Canada: Journal of Paleontology, v. 82, p. 1-36.

Horstwood, M. S. A., Foster, G. L., Parrish, R. R., Noble, S. R., and Nowell, G. M., 2003, Common-Pb corrected in situ U-Pb accessory mineral geochronology by LA-MC-ICP-MS: Journal of Analytical Atomic Spectrometry, v. 18, p. 837-846.

Howe, M.P.A., Evans, M., Carney, J.N., and Wilby, P.R., 2012, New perspectives on the globally important Ediacaran fossil discoveries in Charnwood Forest, UK: Harley's 1848 prequel to Ford (1958): Proceedings of the Yorkshire Geological Society, v. 59, p. 137-144.

Hua, H., Pratt, B.R., Zhang, L.-Y., 2003, Borings in Cloudina shells: complex predator-prey dynamics in the terminal Neoproterozoic: Palaios, v. 18, p. 454-459.

Jaffey, A. H., Flynn, K. F., Glendenin, L. E., Bentley, W. C., and Essling, A. M., 1971, Precision measurement of half-lives and specific of ^{235}U and ^{238}U: Physics Reviews, v. C4, p. 1889-1906.

Jensen, S., Droser, M.L., and Gehling, J.G., 2005, Trace fossil preservation and the early evolution of animals: Palaeogeography, Palaeoclimatology, Palaeoecology, v. 220, p. 19-29.

Laflamme, M., Schiffbauer, J.D., and Narbonne, G.M., 2011, Deep-water Microbially Induced Sedimentary Structures (MISS) in deep time: the Ediacaran fossil Ivesheadia: In Noffke, N.K., and Chafetz, H. (Eds) Microbial Mats in Siliciclastic Depositional Systems Through Time, SEPM Special Publication 101, p. 111-123.

Laflamme, M., Flude, L.I., and Narbonne, G.M., 2012, Ecological tiering and the evolution of a stem: the oldest stemmed frond from the Ediacaran of Newfoundland, Canada: Journal of Paleontology, v. 86, p. 193-200.

Laflamme, M., Darroch, S.A.F., Tweedt, S.M., Peterson, K.J., and Erwin, D.H., 2013, The end of the Ediacara biota: Extinction, biotic replacement, or Cheshire Cat?: Gondwana Research, v. 23, p. 558-573.

Landing, E., Narbonne, G.M., Myrow, P., Benus, A.P., and Anderson, M.M., 1988, Faunas and depositional environments of the Upper Precambrian through Lower Cambrian, southeastern Newfoundland, *in* Landing, E., et al., eds., Trace fossils, small shelly fossils, and the Precambrian-Cambrian boundary: New York State Museum Bulletin, v. 463, p. 18-52.

Le Bas, M.J., 1996, Mount Bardon volcanism: Transactions of the Leicester Literary and Philosophical Society, v. 90, p. 26-34.

Li, Z.X., Bogdanova, S.V., Collins, A.S., Davidson, A., De Waele, B., Ernst, R.E., Fitzsimons, I.C.W., Fuck, R.A., Gladkochub, D.P., Jacobs, J., Karlstrom, K.E., Lu, S., Natapov, L.M., Pease, V., Pisarevsky, S.A., Thrane, K., and Vernikovsky, V., 2008, Assembly, configuration and breakup history of Rodina; a synthesis: Precambrian Research, v. 160, p. 179-210.

Liu, A. G., McIlroy, D., and Brasier, M. D., 2010, First evidence for locomotion in the Ediacara biota from the 565 Ma Mistaken Point Formation, Newfoundland: Geology, v. 38, p.123-126.

Liu, A. G., McIlroy, D., Antcliffe, J. B., and Brasier, M. D., 2011, Effaced preservation in the Ediacara biota and its implications for the early macrofossil record: Palaeontology, v. 54, p. 607-630.

Liu, A. G., McIlroy, D., Mathews, J.J., and Brasier, M. D., 2012, A juvenile assemblage of Ediacaran fronds from the Drook Formation, Newfoundland: Journal of the Geological Society [London], v. 169, p.395-403.

Ludwig, K. R., 2003, Isoplot 3.00. A geochronological toolkit for Microsoft Excel: Berkeley Geochronology Center Special Publication 4, 71p.

Ludwig, K. R., and Mundil, R., 2002, Extracting reliable U-Pb ages and errors from complex populations of zircons from Phanerozoic tuffs: Geochimica et Cosmochimica Acta, v. 66, no. Supplement 1. The Goldschmidt Conference Abstracts, p. A463.

Maloof, A. C., Rose, C.V., Beach, R., Samuels, B.M., Calmet, C.C., Erwin, D.H., Poirier, G.R., Yao, N., and Simons, F.J., 2010, Possible animal-body fossils in pre-Marinoan limestones from South Australia: Nature Geoscience, v. 3, p. 653-659.

Martin, M. W., Grazhdankin, D. V., Bowring, S. A., Evans, D. A. D., Fedonkin, M. A., and Kirschvink, J. L., 2000, Age of Neoproterozoic bilatarian body and trace fossils, White Sea, Russia: Implications for metazoan evolution: Science, v. 288, p. 841-845.

Mattinson, J. M., 2005, Zircon U-Pb chemical abrasion ("CA-TIMS") method: Combined annealing and multi-step partial dissolution analysis for improved precision and accuracy of zircon ages: Chemical Geology, v. 220, p. 47-66.

McIlroy, D., Brasier, M. D., and Moseley, J. B., 1998, The Proterozoic-Cambrian transition within the 'Charnian supergroup' of central England and the antiquity of the Ediacara fauna: Journal of the Geological Society [London], v. 155, p. 401-411.

Meert, J.G., and Lieberman, B.S., 2008, The Neoproterozoic assembly of Gondwana and its relationship to the Ediacaran-Cambrian radiation: Gondwana Research, v. 14, p. 5-21.

Moseley, J.B., and Ford, T.D., 1985, A stratigraphic revision of the Late Precambrian rocks of the Charnwood Forest, Leicestershire: Mercian Geologist, v. 10, p. 1-18.

Moseley, J.B., and Ford, T.D., 1989, The sedimentology of the Charnian Supergroup: Mercian Geologist, v. 11, p. 251-274.

Murphy, J. B., Fernandez-Suarez, J., Jeffries, T. E., and Strachan, R. A., 2004, U-Pb (LA-ICP-MS) dating of detrital zircons from Cambrian clastic rocks in Avalonia: erosion of a Neoproterozoic arc along the northern Gondwanan margin: Journal of the Geological Society [London], v. 161, p. 243-254.

Nance, R. D., Murphy, J. B., and Strachan, R. A., 2008, Neoproterozoic - early Palaeozoic tectonostratigraphy of the peri-Gondwanan terranes: Amazonian v. West African connections: The Boundaries of the West African Craton. Geological Society [London] Special Publication 297, p. 345-384.

Narbonne, G. M., 2004, Modular construction of Early Ediacaran complex life forms: Science, v. 305, p. 1141-1144.

Narbonne, G.M., 2005, The Ediacaran biota: Neoproterozoic origin of animals and their ecosystems: Annual Review of Earth and Planetary Sciences, v. 33, p. 421-442.

Narbonne, G.M., 2010, Neoproterozoic oceans and early animals: Science, v. 328, p. 53-54.

Narbonne, G. M., and Gehling, J. G., 2003, Life after snowball: the oldest complex Ediacaran fossils: Geology, v. 31, p. 27-30.

Narbonne, G. M., Xiao, S., Shields, G. A., and Gehling, J. G., 2012, Chapter 18 - The Ediacaran Period, The Geologic Time Scale: Boston, Elsevier, p. 413-435.

Noble, S. R., Tucker, R. D., and Pharaoh, T. C., 1993, Lower Paleozoic and Precambrian igneous rocks from Eastern England, and their bearing on late Ordovician closure of the Tornquist Sea - constraints from U-Pb and Nd isotopes: Geological Magazine, v. 130, p. 835-846.

O'Brien, S. J., O'Brien, B. H., Dunning, G. R., and Tucker, R. D., 1996, Late Neoproterozoic Avalonian and related peri-Gondwanan rocks of the Newfoundland Appalachians, *in* Nance, R. D., and Thompson, M. D., eds., Avalonian and related peri-Gondwanan terranes of the Circum-North Atlantic, Geological Society of America Special Paper 304, p. 9-28.

Pharaoh, T.C., and Evans, C.J., 1987, Morley Quarry No. 1 Borehole: Geological well completion report: Investigation of the geothermal potential of the UK, British Geological Survey Report WJ/GE/87/5, 43 p.

Pharaoh, T. C., and Carney, J. N., 2000, Introduction to the Precambrian rocks of England and Wales., Precambrian Rocks of England and Wales. Geological Conservation Review Series No. 20, Joint Nature Conservation Committee, Peterborough, p. 3-17.

Pharaoh, T.C., Webb, P.C., Thorpe, R.S., and Beckinsale, R.D., 1987, Geochemical evidence for the tectonic setting of late Proterozoic volcanic suites in central England: In Geochemistry and Mineralisation of Proterozoic volcanic suites (eds T.C. Pharaoh, R.D. Beckinsale and D. Rickard), Geological Society [London] Special Publication 33, p. 541-552.

Pharoah, T.C., Merriman, R.J., Evans, J.A., Brewer, T.S., Webb, P.C. and Smith, N.J.P., 1991, Early Palaeozoic arc-related volcanism in the concealed Caledonides of southern Britain. Annales de la Société Géologique de Belgique, T114, p. 63-91.

Runnegar, B., 2000, Loophole for snowball earth. Nature, v. 405, p. 403-404.

Schmitz, M.D., 2012, Radiometric ages used in GTS 2012, *in* Gradstein, F.M., Ogg, J.G., and Schmitz, M.D., eds., The Geologic Time Scale 2012: Oxford, UK, Elsevier, p. 1045-1082.

Schneider, J. L., Le Ruyet, A., Chanier, F., Buret, C., Ferriere, J., Proust, J. N., and Rosseel, J. B., 2001, Primary or secondary distal volcaniclastic turbidites: how to make the distinction? An example from the Miocene of New Zealand (Mahia Peninsula, North Island): Sedimentary Geology, v. 145, p. 1-22.

Schofield, D. I., Evans, J. A., Millar, I. L., Wilby, P. R., and Aspden, J. A., 2008, New U-Pb and Rb-Sr constraints on pre-Acadian tectonism in North Wales: Journal of the Geological Society [London], v. 165, p. 891-894.

Schofield, D. I., Millar, I. L., Wilby, P. R., and Evans, J. A., 2010, A new, high precision U-Pb date from the oldest known rocks in southern Britain: Geological Magazine, v. 147, p. 145-150.

Shen, B., Dong, L., Xiao, S., and Kowalewski, M., 2008, The Avalon explosion: evolution of Ediacara morphospace: Science, v. 319, p. 81-84.

Stix, J., 1991, Subaqueous, intermediate to silicic-composition explosive volcanism: a review: Earth-Science Reviews, v. 31, p. 21-53.

Strachan, R. A., Nance, R. D., Dallmeyer, R. D., D’Lemos, R. S., Murphy, J. B., and Watt, G. R., 1996, Late Precambrian tectonothermal evolution of the Malverns Complex: Journal of the Geological Society [London], v. 153, p. 589-600.

Strachan, R. A., Collins, A. S., Buchan, C., Nance, R. D., Murphy, J. B., and D'Lemos, R. S., 2007, Terrane analysis along a Neoproterozoic active margin of Gondwana: insights from U-Pb zircon geochronology: Journal of the Geological Society [London], v. 164, p. 57-60.

Sutherland, D.S., Boynton, H.E., Ford, T.D., Le Bas, M.J., and Moseley, J., 1994, A guide to the geology of the Precambrian rocks of Bradgate Park in Charnwood Forest, Leicestershire: Transactions of the Leicester Literary and Philosophical Society, v. 87, p. 1-36.

Trofimovs, J., Amy, L., Boudon, G., Deplus, C., Doyle, E., Fournier, N., Hart, M.B., Komorowski, J.C., Le Friant, A., Lock, E.J., Pudsey, C., Ryan, G., Sparks, R.S.J., and Talling, P.J., 2006, Submarine pyroclastic deposits formed at the Soufrière Hills volcano, Montserrat (1995-2003): What happens when pyroclastic flows enter the ocean?: Geology, v. 34, p. 549-552.

Tucker, R. D., and Pharaoh, T. C., 1991, U-Pb zircon ages for Late Precambrian igneous rocks in southern Britain: Journal of the Geological Society [London], v. 148 , p. 435-443.

Waggoner, B.M., 2003, The Ediacaran biotas in space and time: Integrated and Comparative Biology, v. 43, p. 104-113.

Watts, W.W., 1903, Charnwood Forest: A buried Triassic landscape: The Geographical Journal, v. 21, p. 623-633.

Waldron, J.W.F., Schofield, D.I., White, C.E., and Barr, S.M., 2011, Cambrian successions of the Meguma Terrane, Nova Scotia, and Harlech Dome, North Wales: dispersed fragments of a peri-Gondwanan basin?: Journal of the Geological Society [London], v. 168, p. 83-97.

Wilby, P. R., Carney, J. N., and Howe, M. P. A., 2011, A rich Ediacaran assemblage from eastern Avalonia: Evidence of early widespread diversity in the deep ocean: Geology, v. 39, p. 655-658.

Wood, D. A., Dalrymple, R. W., Narbonne, G. M., Gehling, J. G., and Clapham, M. E., 2003, Paleoenvironmental analysis of the late Neoproterozoic Mistaken Point and Trepassey formations, southeastern Newfoundland: Canadian Journal of Earth Sciences, v. 40, p. 1375-1391.

Worssam, B. C., and Old, R. A., 1988, Geology of the country around Coalville, Memoir of the British Geological Survey, Sheet 155 (England and Wales), 161 p.

Xiao, S., and Laflamme, M., 2009, On the eve of animal radiation: phylogeny, ecology, and evolution of the Ediacara biota: Trends in Ecology and Evolution, v. 24, p. 31-40.

Yuan, X., Chen, Z., Xiao, S, Zhou, C., and Hua, H., 2011, An early Ediacaran assemblage of macroscopic and morphologically differentiated eukaryotes: Nature, v. 470, p. 390-393.

FIGURE CAPTIONS

Figure 1. Simplified geological map of the Neoproterozoic and Cambrian rocks of the Charnwood Forest area, modified from Carney (1999), showing geochronological sample locations. Inset: Location of Charnwood Forest in relation to the Neoproterozoic ‘Avalonian’ terranes of southern Britain (modified from Pharaoh and Carney, 2000). Ox, Or, G: Oxendon, Orton and Glinton boreholes (see also DR section 4). In the inset map, MCT is the Monian Complex Terrane. Other Precambrian exposures include the Malverns (MV), Longmynd and Wrekin (LM&W), NT (Nuneaton) and CF (Charnwood Forest). The Cambrian Harlech Dome (HD) is also indicated (proposed part of Megumia, Waldron et al., 2011).

Figure 2. Simplified stratigraphy of the Charnian Supergroup (after Carney, 1999), showing the stratigraphic context of the U-Pb samples dated in this study. SQB, BBr, SSBr: South Quarry Breccia, Benscliffe Breccia and Sliding Stone Slump Breccia members.

Figure 3. Microphotographs (ppl) of tuffaceous horizons in the Beacon Hills Formation. A: Beacon Hill Formation at Buck Hills showing crystal-rich and very fine-grained vitric tuff layers, the latter with relict glass shards. Scale bar is 1 mm. B: close-up of relict glass shards, scale bar is 250 µm.

Figure 4. Representative Ediacaran fossils from the Charnian Supergroup of Charnwood Forest (UK). All specimens are casts, except F (in situ), and are housed at the British Geological Survey, Keyworth. Specimens are from different stratigraphic levels: A-E and G, Bradgate Formation; F, Beacon Hill Formation; H-I, Ives Head Formation. A: *Charnia masoni*, holotype (GSM106160). B: *Charniodiscus concentricus*, holotype (GSM106161).

C: *Bradgatia linfordensis*, holotype (GSM106163). D: Discoidal fossil, assigned to *Cyclomedusa sp*. by Boynton (1978) (VEN 11.0). E: Small *Charniodiscus sp.*, presumed juvenile (VEN 1.2). F: *Aspidella sp*. G: Closely associated, current-aligned fronds, including *C. masoni* and *B. linfordensis* (GSM105873). H: The ivesheadiomorph '*Ivesheadia lobata*' (Boynton and Ford, 1995) (GSM119699). I: The ivesheadiomorph '*Blackbrookia oaksi*' (Boynton and Ford, 1995) (GSM119700). Scales: A–3 cm; B–3 cm; C–10 cm; D–5 cm; E–0.5 cm; F–1 cm; G–10 cm; H–4 cm; I–5 cm.

Figure 5. Plot of ^{238}U/^{206}Pb ages for the Park Breccia samples JNC 912 (this study) and CH2 (Compston et al., 2002) showing individual data points, single spots for the SHRIMP U-Pb data and single zircon crystal/fragment for the CA-ID-TIMS data, respectively.

Figure 6. Simplified stratigraphic column of the Charnian Supergroup (see also Fig. 2) showing the U-Pb data for samples as follows: black data boxes correspond to LA-ICP-MS analyses and associated uncertainties for ca. 600 Ma zircons; purple data boxes indicate LA-ICP-MS analyses of probable 570-550 Ma grains; CA-ID-TIMS data shown in red for analyses using the EARTHTIME ^{205}Pb-^{233}U-^{235}U tracer and green for the Tom Krogh ^{205}Pb-^{235}U Carnegie tracer. Also indicated is the CA-ID-TIMS ca. 618-611 Ma zircon population (horizontal grey band) and the calculated age with uncertainty for the upwardly younging trend of the youngest volcanic grain populations recovered from successive levels in the Maplewell Group (short horizontal darker grey bands). BBr (BH), BH, BG, HR: Benscliffe Breccia (Beacon Hill Formation), Beacon Hill Formation, Bradgate Formation, Hanging Rocks Formation.

Figure 7. Chronostratigraphic frameworks for the late Neoproterozoic successions in A) Newfoundland, and B) Charnwood Forest, showing known local ranges of selected shared taxa and respective endemic forms. Dates for the Newfoundland succession are from Benus (1988) and Bowring et al. (2003), and related taxonomic ranges are based on Liu et al. (2012, fig. 8). Note that the age of the upper part of the Newfoundland succession and the lower part of the Charnwood succession are not as yet well constrained, leading to uncertainty in correlation.

TABLE 1: Summary of sample details and interpretations. For further petrographic details and locations, see Data Repository. [1]*Sensu* Schneider et al. (2001); [2]*Sensu* Stix (1991).

Sample details	Description	Sedimentary architecture	Interpretation
Maplewell Group			
Hanging Rocks Formation JNC 846 (Fig. DR 1e)	Sandstone, poorly sorted; mainly sand-size grains and rounded granules of dacitic tuff	Medium-bedded, internally massive	Turbidite carrying detritus initially worked in fluvial or nearshore environments
Park Breccia, Bradgate Formation, JNC 912 (Fig. DR 1d)	Mudstone slivers and rafts in a medium-grained volcaniclastic sandstone matrix; latter mainly andesitic grains	Thickly bedded	Secondary monomagmatic volcaniclastic turbidite[1], probable subaqueous slump of pyroclastic material
Beacon Hill Formation, JNC 911	Fine-grained tuffaceous siltstone with a flinty fracture; abundant vitric shards in unresolvable silt-grade base	Fine-scale parallel lamination, with local slight syn-sedimentary disturbances	Subaqueous vitric tuff deposited from the settling-out of ash through water column
Beacon Hill Formation (Bardon Quarry), JNC 907	Volcaniclastic sandstone, siltstone and mudstone; abundant glassy andesite grains and some sedimentary fragments in coarser sandstones	Massive to thinly bedded, common normal grading; individual beds and laminae are parallel-sided but locally convoluted	Turbidite facies, in part resedimented peperite derived from subaqueous andesitic domes of the Bardon Hill Complex
Benscliffe Breccia Member, Beacon Hill Formation, JNC 918 (Fig. DR 1c)	Abundant andesite lapilli and small blocks in a coarse-grained, crystal-rich volcaniclastic sandstone matrix	Massive, very poorly sorted, no visible stratification	Long run-out subaqueous pyroclastic flow
Blackbrook Group			
South Quarry Breccia Member, Ives Head Formation, JNC 917 (Fig. DR 1b)	Contorted rafts of mudstone and siltstone in a coarse, crystal-rich volcaniclastic sandstone matrix; andesitic grains show limited textural variation	Massively bedded	Volcaniclastic turbidite, epiclastic/pyroclastic origin is indeterminant: if pyroclastic then possible secondary volcaniclastic turbidite[1], probable subaqueous slump
Ives Head Formation, JNC 836 (DR Fig. 1a)	Medium-grained volcaniclastic sandstone; dominantly composed of monolithological andesite grains	Middle part of a bed ca. 3 m thick showing pronounced normal grading	Volcaniclastic turbidite, epiclastic/pyroclastic origin is indeterminant: if pyroclastic then possible primary mass flow of pyroclastic debris[2]

Ives Head Formation, JNC 916	Medium-grained volcaniclastic sandstone; dominantly composed of monolithological andesite grains	From a thickly bedded succession of normally graded sandstones, siltstones and mudstones	Volcaniclastic turbidite, epiclastic/pyroclastic origin is indeterminant: if pyroclastic then possible primary mass flow of pyroclastic debris[2]

TABLE 2. Summary of interpreted U-Pb (zircon) dates (millions of years)

Sample ID	Stratigraphic Position	$^{206}Pb/^{238}U$ date	± X	± Y	± Z	N	MSWD	Interpretation
846	Hanging Rocks Formation	556.6	6.4			4	-	Deposition
912	Bradgate Formation	561.85	0.34	0.66	0.89	7/12	1.2	Eruption/deposition
907	Beacon Hill Formation	565.22	0.33	0.65	0.89	2/5	0.42	Eruption/deposition
911	Beacon Hill Formation	ca. 613		-	-	-	-	Inherited, out of order
918	Benscliffe Breccia	569.08	0.45	0.73	0.94	2/12	0.8	Eruption/deposition
917	Ives Head Formation	611.28	0.57	0.83	1.06	youngest U-Pb date	-	Maximum age
836	Ives Head Formation	611.71	0.55	0.83	1.05	youngest U-Pb date	-	Maximum age
916	Ives Head Formation	612.15	0.70	0.93	1.14	youngest U-Pb date	-	Maximum age

(X) Internal or analytical uncertainty (abs, Myr).

(Y) Includes quadratic addition of tracer calibration error.

(Z) Includes quadratic addition of both tracer calibration and ^{238}U decay constant errors.

[1] GSA Data Repository item 2014xxx, Sample descriptions, U-Pb methods, data and interpretation is available online at www.geosociety.org/pubs/ft2014.htm, or on request from editing@geosociety.org or Documents Secretary, GSA, P.O. Box 9140, Boulder, CO 80301, USA.

Figure 1

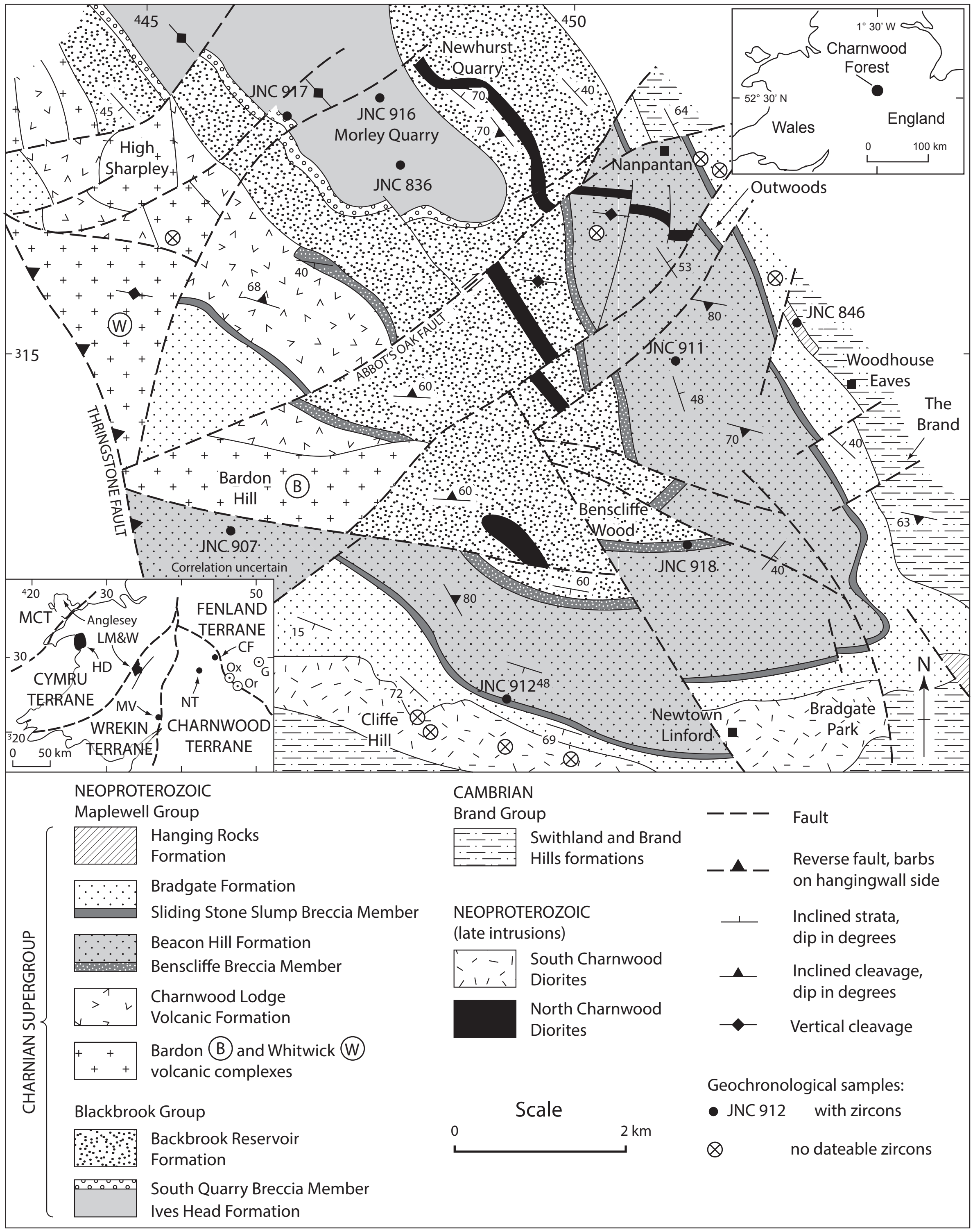
445
450
315
Newhurst Quarry
JNC 917
JNC 916
Morley Quarry
JNC 836
High Sharpley
Nanpantan
Outwoods
JNC 846
JNC 911
Woodhouse Eaves
The Brand
ABBOT'S OAK FAULT
THRINGSTONE FAULT
Bardon Hill
JNC 907
Correlation uncertain
Benscliffe Wood
JNC 918
JNC 912
Cliffe Hill
Newtown Linford
Bradgate Park
N
Charnwood Forest
1° 30' W
52° 30' N
Wales
England
0
100 km
MCT
Anglesey
LM&W
HD
CYMRU TERRANE
MV
WREKIN TERRANE
NT
CHARNWOOD TERRANE
FENLAND TERRANE
CF
Ox
Or
G
50 km
NEOPROTEROZOIC
Maplewell Group
Hanging Rocks Formation
Bradgate Formation
Sliding Stone Slump Breccia Member
Beacon Hill Formation
Benscliffe Breccia Member
Charnwood Lodge Volcanic Formation
Bardon B and Whitwick W volcanic complexes
Blackbrook Group
Backbrook Reservoir Formation
South Quarry Breccia Member
Ives Head Formation
CHARNIAN SUPERGROUP
CAMBRIAN
Brand Group
Swithland and Brand Hills formations
NEOPROTEROZOIC
(late intrusions)
South Charnwood Diorites
North Charnwood Diorites
Scale
0
2 km
Fault
Reverse fault, barbs on hangingwall side
Inclined strata, dip in degrees
Inclined cleavage, dip in degrees
Vertical cleavage
Geochronological samples:
JNC 912 with zircons
no dateable zircons

Figure 2

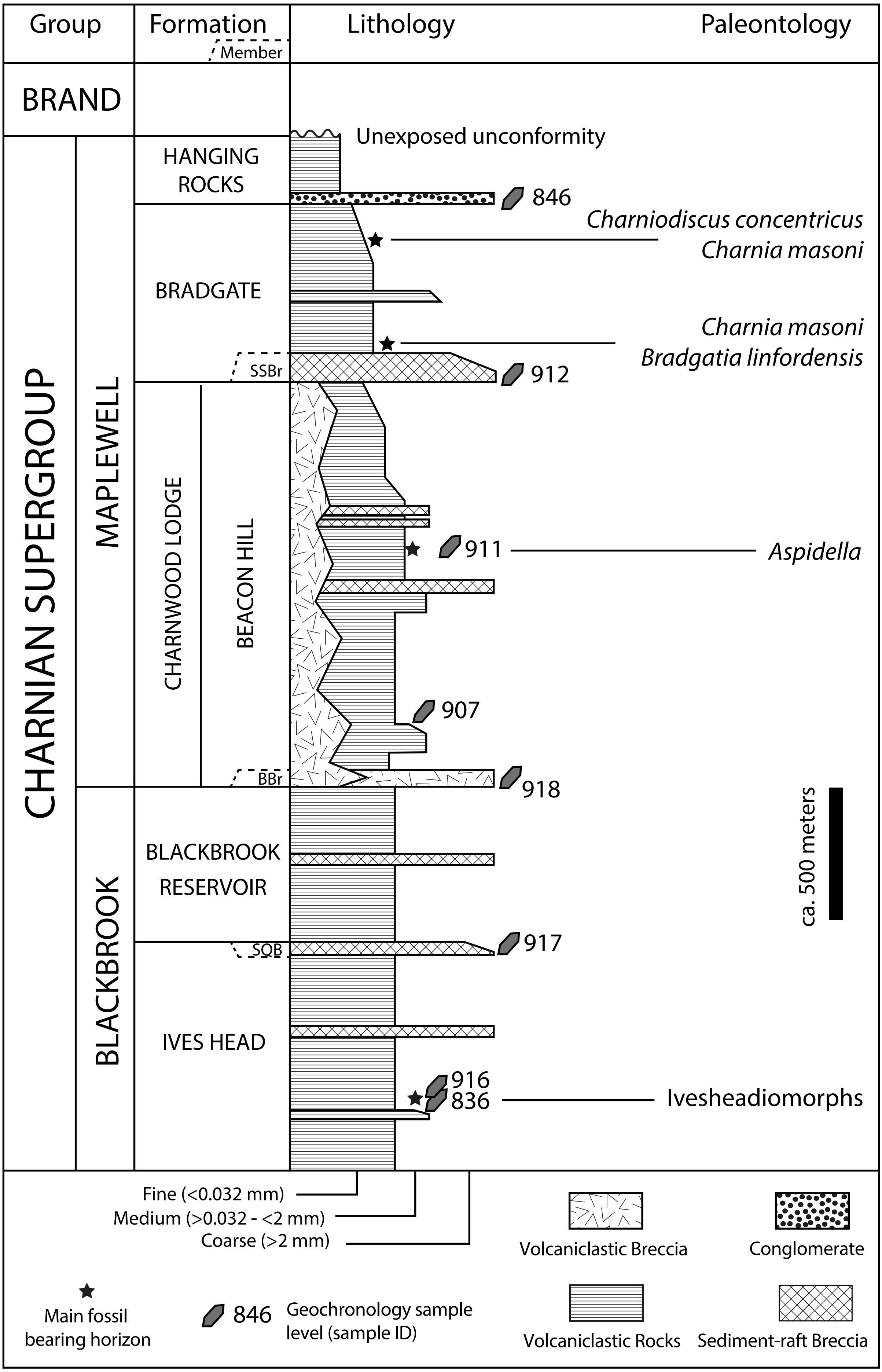
Group
Formation
Member
Lithology
Paleontology
BRAND
CHARNIAN SUPERGROUP
MAPLEWELL
BLACKBROOK
HANGING ROCKS
BRADGATE
SSBr
CHARNWOOD LODGE
BEACON HILL
BBr
BLACKBROOK RESERVOIR
SQB
IVES HEAD
Unexposed unconformity
846
Charniodiscus concentricus
Charnia masoni
Charnia masoni
Bradgatia linfordensis
912
911
Aspidella
907
918
917
916
836
Ivesheadiomorphs
ca. 500 meters
Fine (<0.032 mm)
Medium (>0.032 - <2 mm)
Coarse (>2 mm)
Volcaniclastic Breccia
Conglomerate
Main fossil bearing horizon
846 Geochronology sample level (sample ID)
Volcaniclastic Rocks
Sediment-raft Breccia

Figure 3a

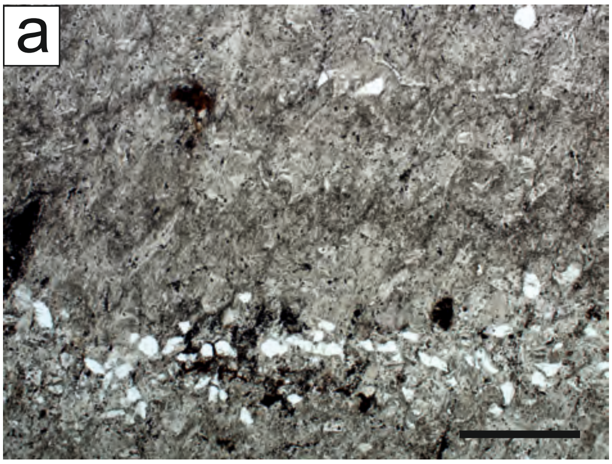

Figure 3b

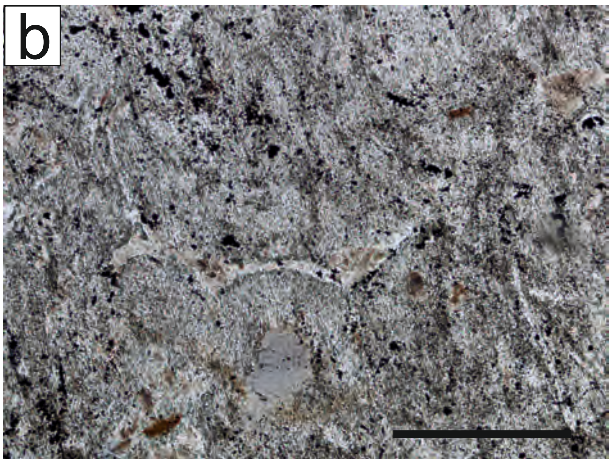

Figure 4

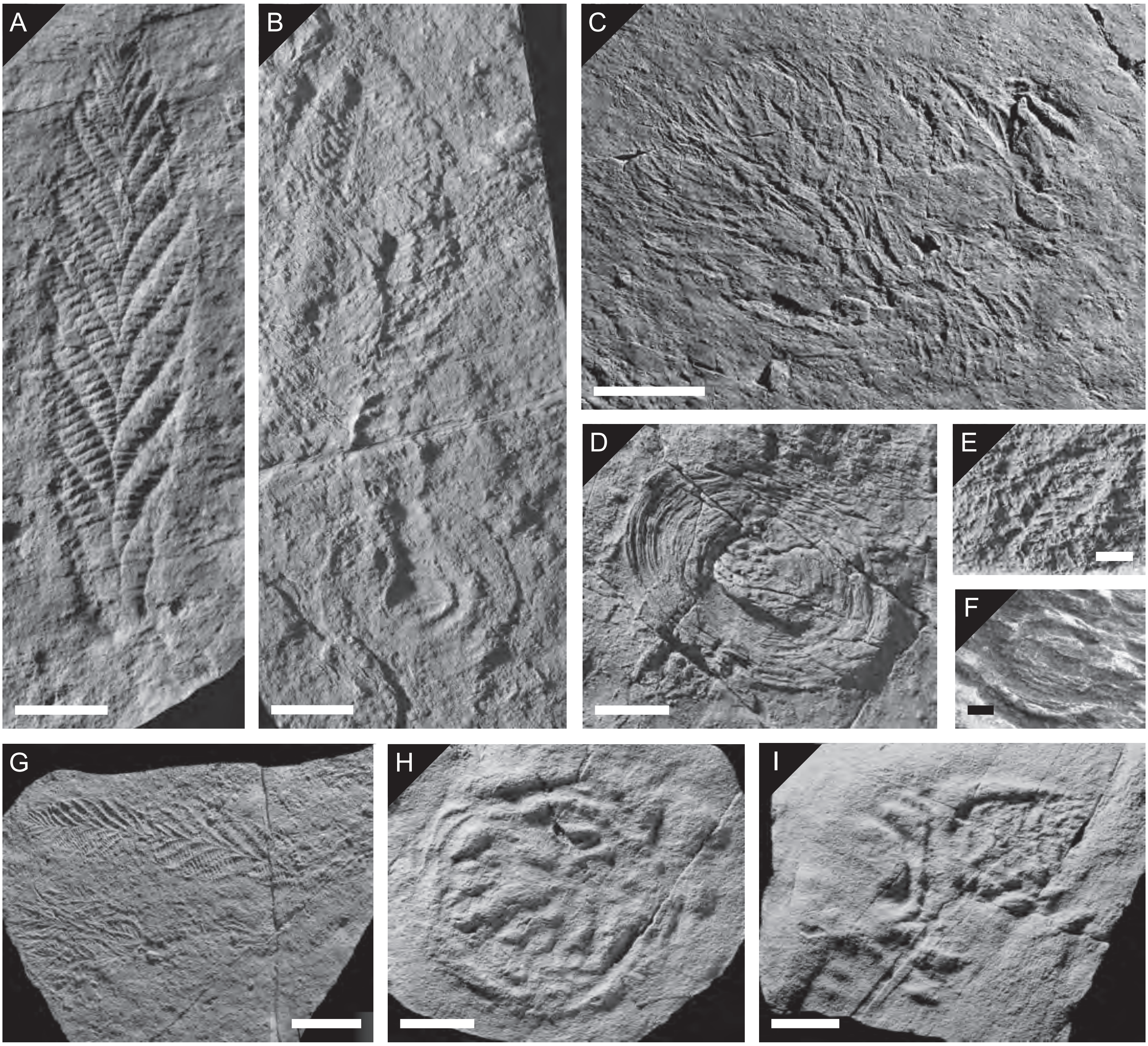

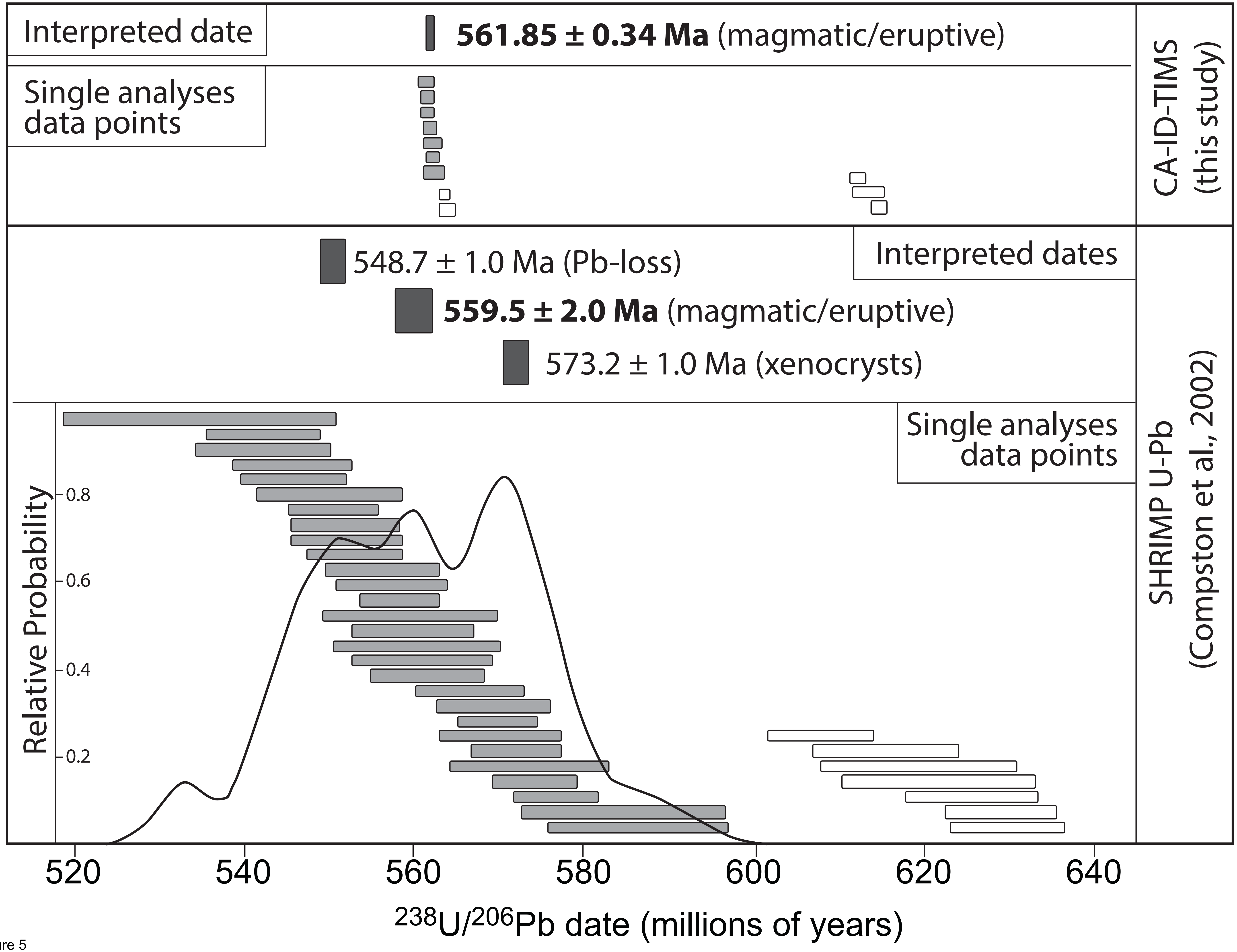
Interpreted date
561.85 ± 0.34 Ma (magmatic/eruptive)
Single analyses data points
CA-ID-TIMS (this study)
548.7 ± 1.0 Ma (Pb-loss)
Interpreted dates
559.5 ± 2.0 Ma (magmatic/eruptive)
573.2 ± 1.0 Ma (xenocrysts)
Single analyses data points
SHRIMP U-Pb (Compston et al., 2002)
Relative Probability
0.8
0.6
0.4
0.2
520
540
560
580
600
620
640
$^{238}U/^{206}Pb$ date (millions of years)

Figure 5

Figure 6

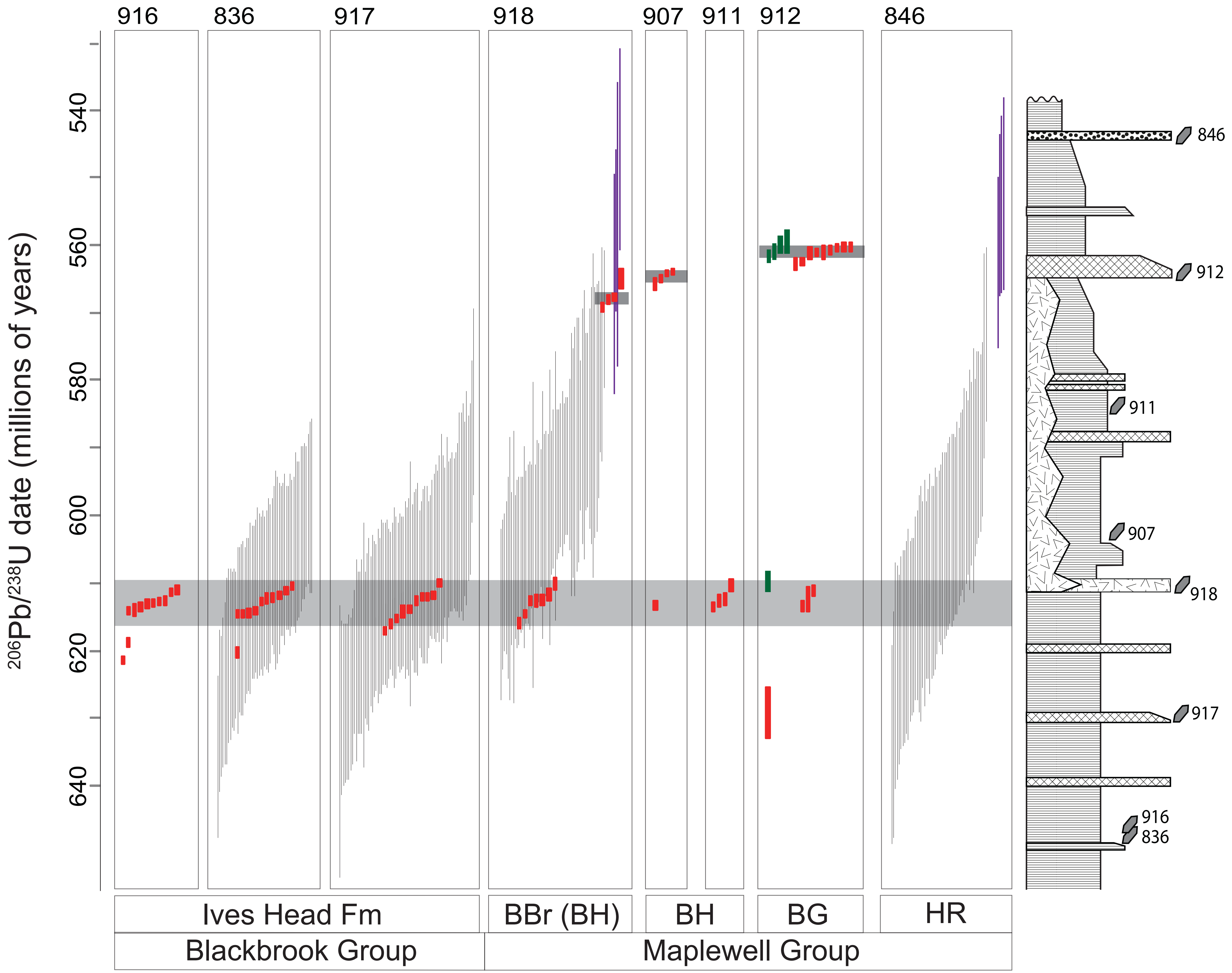
916
836
917
918
907
911
912
846
540
560
580
600
620
640
$^{206}Pb/^{238}U$ date (millions of years)
Ives Head Fm
BBr (BH)
BH
BG
HR
Blackbrook Group
Maplewell Group
846
912
911
907
918
917
916
836

Figure 7

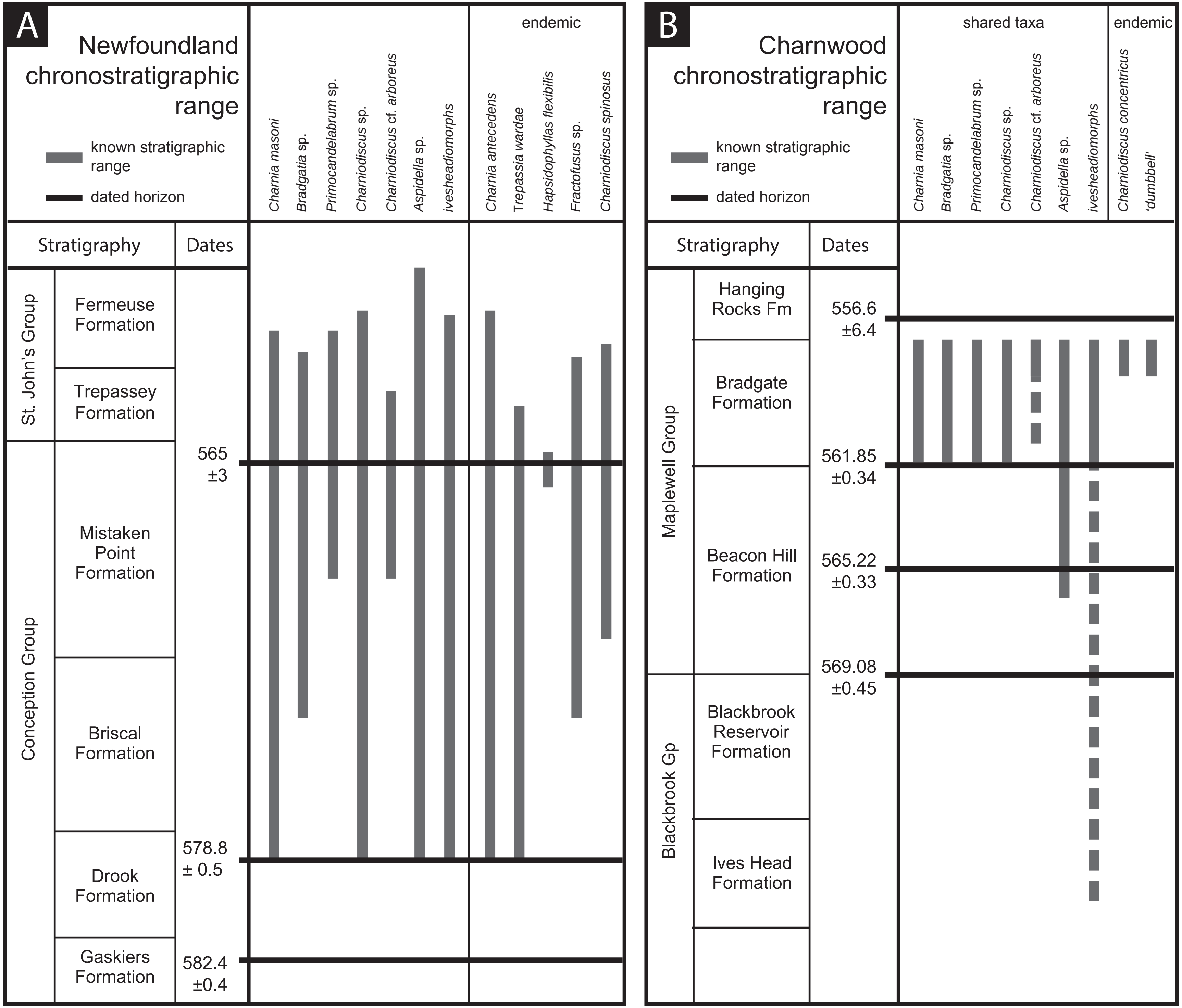

A
Newfoundland chronostratigraphic range
known stratigraphic range
dated horizon
endemic
Charnia masoni
Bradgatia sp.
Primocandelabrum sp.
Charniodiscus sp.
Charniodiscus cf. arboreus
Aspidella sp.
ivesheadiomorphs
Charnia antecedens
Trepassia wardae
Hapsidophyllas flexibilis
Fractofusus sp.
Charniodiscus spinosus
Stratigraphy
Dates
St. John's Group
Fermeuse Formation
Trepassey Formation
Conception Group
Mistaken Point Formation
Briscal Formation
Drook Formation
Gaskiers Formation
565 ±3
578.8 ± 0.5
582.4 ±0.4
B
Charnwood chronostratigraphic range
known stratigraphic range
dated horizon
shared taxa
endemic
Charnia masoni
Bradgatia sp.
Primocandelabrum sp.
Charniodiscus sp.
Charniodiscus cf. arboreus
Aspidella sp.
ivesheadiomorphs
Charniodiscus concentricus
'dumbbell'
Stratigraphy
Dates
Maplewell Group
Hanging Rocks Fm
Bradgate Formation
Beacon Hill Formation
Blackbrook Gp
Blackbrook Reservoir Formation
Ives Head Formation
556.6 ±6.4
561.85 ±0.34
565.22 ±0.33
569.08 ±0.45

DATA REPOSITORY

Analytical methods

Mineral Separation

Samples (5 to ~50 kg) were jaw-crushed and disk-milled to <420 μm and heavy mineral concentrates prepared using a Gemini table, heavy liquids (methylene iodide) and Frantz LB-1 separator. Grains selected for LA-ICPMS were mounted in epoxy blocks and imaged in BSE and CL modes by SEM prior to analysis by Dr. S. Parry and Mr. G. Turner of the British Geological Survey.

Laser ablation ICP-MS

Laser ablation data were obtained on a Nu Instruments multiple collector inductively coupled plasma mass spectrometer (MC-ICP-MS). The NIGL Nu MC-ICP-MS collector block permits simultaneous collection of masses relevant to U-Pb chronology (masses 202 through 207, 235, and 238). Further details are given for an almost identical collector configuration by Simonetti et al. (2005). Data collection, reduction and propagation of uncertainties follow Horstwood et al. (2003) and Bauer et al. (2011). Discrete dynode secondary electron multipliers were used to measure ^{204}Pb+^{204}Hg, ^{206}Pb and ^{207}Pb, with other isotopes of interest measured on Faraday cups. Targeted zircons were sampled using a New Wave Research UP193-FX 193 nm ArF excimer laser microprobe system. Zircons were ablated for 20 seconds using a 25 μm static spot at a laser fluence of ca. 2.5 J cm^{-2}. These ablation protocols provided reconnaissance level data with ^{206}Pb/^{238}U ratio uncertainties generally <2%. Instrumental mass fractionation was monitored using a mixed natural Tl-^{235}U solution introduced via a Nu Instruments DSN 100 desolvating nebulizer. Fractionation related to laser ablation was corrected in unknowns by analyzing zircon reference materials. During the course of this study the following zircon standards were used: 91500 dated at 1062.4 ± 0.4 Ma (Wiedenbeck et al., 1995), GJ-1 dated at 600.4 ± 0.6 Ma, (Jackson et al., 2004) and 602.3 ± 1 Ma (current value from NIGL TIMS data using the EARTHTIME ^{205}Pb-^{233}U-^{235}U tracer), and the 337.33 ± 0.38 Ma Plesovice zircon (Sláma et al., 2008). Raw data was reduced using an in-house Excel data reduction worksheet. Given the reconnaissance nature of the LA-ICP-MS analytical work, data with <10% discordance were accepted for age calculations where the contaminant was deemed most likely to be common Pb from the abundant melt inclusions in many of the zircons (see DR Fig 2). Zircon data were rejected in instances where mixing was along obvious <3000 Ma – non-zero discordia lines, and grains where sufficient common Pb was present to result in >10% discordance.

U-Pb (zircon) Chemical Abrasion Isotope Dilution Thermal Ionisation Mass Spectrometry (CA-ID-TIMS)

Zircons analysed by TIMS were subjected to “chemical abrasion” (thermal annealing and subsequent leaching pre-treatment; Mattinson, 2005) to effectively eliminate Pb-loss. Zircons were heated in a muffle furnace at 900 ± 20°C for ~60 hours in quartz beakers before being transferred to 3 ml Hex Savillex beakers, which were in turn placed in a Parr vessel, and leached in a ~5:1 mix of 29M HF + 30% HNO_3 for 12 hours at ~180°C. The acid solution was removed, fractions rinsed in ultrapure H_2O, fluxed on a hotplate at ~80°C for 1 hr in 6 M HCl, ultrasonically cleaned for 1 hr, and then placed back on the hotplate for an additional 30 min. The HCl solution was removed and the fractions (single zircon crystals or a single fragment) were selected, photographed (in transmitted light) and again rinsed (in ultrapure acetone) prior to being transferred to 300 µl Teflon PFA microcapsules and spiked with the mixed EARTHTIME ^{233}U–^{235}U–^{205}Pb tracer. The single zircons or fragments were dissolved in ~ 120 µl of 29 M HF with a trace amount of 30% HNO_3 at ~220°C for 48 hours, with the microcapsules housed within Parr vessels. The zircon digests were subsequently dried to fluorides and then converted to chlorides in 3M HCl at ~180°C overnight. U and Pb were separated using standard HCl-based anion-exchange chromatographic procedures on 0.05 ml PTFE columns manufactured in-house (Corfu and Noble, 1992). Isotope ratios were measured using NIGL's Thermo-Electron Triton Thermal Ionisation Mass-Spectrometer (TIMS) dedicated to low-blank U-Pb geochronology (Triton 2). Pb and U were loaded together on a single Re filament in a silica-gel/phosphoric acid mixture (Gerstenberger and Haase, 1997). Pb isotopes were measured by peak-hopping on a single SEM detector. U isotope measurements were made in static Faraday mode. Age calculations and uncertainty estimation (including U/Th disequilibrium) were based upon the algorithms of Schmitz and Schoene (2007). All acids were prepared by sub-boiling distillation: HCl and HNO_3 were double-distilled in quartz and HF was double-distilled in Teflon. Ultrapure water with a resistivity of 18 MΩ was prepared with a Milli-Q system. All reagents were blank-checked prior to use.

$^{206}Pb/^{238}U$ dates are calculated using the ^{238}U and ^{235}U decay constants of Jaffey et al. (1971) and corrected for initial U/Th disequilibrium using an assumed magma Th/U ratio of 4, typical for magmatic systems. A value of $^{238}U/^{235}U_{zircon} = 137.818 \pm 0.045$ (Hiess et al., 2012) was used in the data reduction calculations. Compared to calculations using the old 'consensus' value ($^{238}U/^{235}U = 137.88$) this has the effect of reducing $^{207}Pb/^{206}Pb$ dates by ca. 0.98 Myr at the age range of interest (ca. 560 to 620 Ma) and reduces the $^{206}Pb/^{238}U$ dates by <5 kyr. For U–Pb dates of this age, the $^{206}Pb/^{238}U$ dates are the most precise and robust. In contrast, the ^{207}Pb-based dates ($^{207}Pb/^{235}U$ and $^{206}Pb/^{207}Pb$) are considerably less precise and hence are only used to assess concordance of the U–Pb (zircon) systematics.

Detailed geochronology sample descriptions

Blackbrook Group

Three Blackbrook Group samples were examined in this study. Sample JNC 916 was collected at Morley Quarry (BNG SK 4766 1787) from a several meters-thick succession of volcaniclastic sandstones, siltstones and mudstones, just above the exposed base of the Ives Head Formation. At Morley Quarry, individual graded units (Bouma A-E divisions) typically commence in structureless, very coarse-grained volcaniclastic sandstone in which are embedded sporadic angular fragments of laminated volcaniclastic siltstone ripped up from the underlying beds. They show an upward transition into medium-grained sandstone, which in turn develops a diffuse parallel-stratification before passing up to parallel-laminated siltstone and mudstone. An outstanding petrographical feature of JNC 916 is the general uniformity of the angular to subrounded dacitic volcanic grains, which enclose small quartz and plagioclase phenocrysts; their groundmasses are extremely fine-grained and microcrystalline although some show a slightly coarser, microgranular texture. Plagioclase and quartz also occur as discrete, fragmented euhedra between the lithic grains. This graded bed is comparable to the 'secondary monomagmatic volcaniclastic turbidites' of Schneider et al. (2001) which show mild reworking and clast heterogeneity.

JNC 836 was sampled (BNG SK 4772 1700) from the middle part of a 2.5 m thick volcaniclastic turbidite (see Fig. 3a of Carney, 1999). The position of this turbidite is critical in terms of palaeontology, since its uppermost bedding plane contains impressions of *Ivesheadia*, *Blackbrookia* and *Shepshedia* (Boynton and Ford, 1995; Liu et al., 2011). Sand-size, angular to subrounded volcanic grains predominate in this sample. These grains are remarkably homogeneous with ~85 per cent having uniformly microcrystalline groundmasses and the remainder exhibiting varying degrees of patchy coarsening to microgranular or faintly spherulitic textures truncated at grain edges (DR Fig. 1a). Many grains contain quartz microphenocrysts indicating a dacitic composition for the parental magmas; one grain was also seen to contain a euhedral, acicular zircon crystal. Sharply angular to locally subhedral quartz and plagioclase phenocryst fragments are particularly common within the matrix to the lithic grains. These petrographic characteristics strongly resemble those of JNC 916 and thus JNC 836 is interpreted to have had a similar origin.

JNC 917 is from the South Quarry Breccia Member located about 600 m stratigraphically above the other two samples. The sample was obtained from the South Quarry type locality (BNG SK 4637 1712). Exposed faces in the quarry consist of a few meters of stratified to massive coarse-grained volcaniclastic sandstone, passing upwards into a breccia with large contorted rafts of laminated mudstone embedded in a volcaniclastic sandstone matrix. In thin section, the analysed sample contains about 50-60% plagioclase and quartz, present as phenocrysts in dacitic lithic volcanic grains, or as fragmented to partially-fragmented crystals concentrated within the matrix between the grains. Lithic grains show a range of crystallinities from exceedingly fine-grained, virtually aphanitic, to more coarsely crystalline varieties with microgranular textures. Patchy recrystallization is commonly seen within the confines of a single grain (DR Fig. 1b). Some lithic grains contain very large embayed quartz euhedra surrounded by a thin 'skin' consisting of the microcrystalline matrix. In other outcrops, a degree of heterogeneity is shown by the lithic volcanic grains, and some examples possess a perlitic texture (Carney, 1994). The sedimentary features of the South Quarry Member are consistent with a history of secondary reworking involving submarine slumping of incompletely consolidated volcaniclastic strata.

Maplewell Group

The oldest sample in the Maplewell Group to yield dateble zircons is JNC 918 from the Benscliffe Breccia, a highly distinctive unit at the base of the Beacon Hill Formation (Fig. 1). Sample JNC 918 was collected from the Benscliffe Breccia Member at the 'Pillar Rock' type locality in Benscliffe Wood (BNG SK 5146 1246). These exposures show 3+ meters of massive breccia in which lapilli- to small block-size fragments of andesite are set in a poorly sorted matrix of crystal-rich, coarse-grained volcaniclastic sandstone (see Fig. 3b of Carney, 1999). The andesite lapilli and blocks are angular to subrounded, with rather diffuse margins when viewed in polished slabs, with only limited petrographic variation. Many have coarsely microgranular textures, but some possess local areas containing small, stubby plagioclase laths with random orientation. A minor proportion of the lapilli and blocks have finely microcrystalline texture. In some of the larger andesitic blocks the degree of crystallinity decreases outwards to rims of finely microcrystalline material which, as with the exposed rock surfaces, are somewhat poorly defined against the matrix. When compared with the andesite fragments, the matrix is notably enriched in plagioclase and quartz crystals (DR Fig. 1c); these are small and most are shattered and/or fragmented, appearing to have been granulated during their entrainment between the andesite blocks. The essentially monolithological nature of the andesite fragments would satisfy the criterion of Stix (1991) for a primary mass flow of pyroclastic debris, and the unit was interpreted by Carney (1999) as a long-runout subaqueous pyroclastic block flow marking a major eruptive event at the base of the Maplewell Group.

Volcaniclastic strata from the western flank of the Charnwood anticlinal structure were sampled (JNC 907) in the southern part of Bardon Hill Quarry (BNG SK 4572 1289) from a well-bedded volcaniclastic sequence faulted against the Bardon Hill Volcanic Complex. On the basis of regional correlations, it was originally thought that this sequence was from the middle part of the Bradgate Formation. Correlation with horizons sitting close to the base of the Beacon Hill Formation (Fig. 2), however, is equally likely based on our further mapping and is our preferred interpretation. Zircons were extracted from ca. 20 kg bulk sample of normally graded volcaniclastic siltstones and sandstones showing varying degrees of coarseness and bedding. In thin section, the sampled coarse grey-green volcaniclastic sandstone contains abundant angular quartz and plagioclase crystal fragments, although the dominant constituents are tightly packed subrounded to highly angular lithic volcanic grains. These are heterogeneous in terms of their lithology with some consisting of peripherally ragged fragments of oxidised andesite and locally with spherulitic and shardic textures. Most of the fragments are andesite or low-silica dacite, with textures ranging from aphanitic to microgranular and fluxional/intergranular.

Sample JNC 911 was collected from the summit of Beacon Hill (BNC SK 5091 1488) and is the type locality for the Beacon Tuff Member of the Beacon Hill Formation (Moseley and Ford, 1985). The Beacon Hill tuffs are typically siliceous with a flinty appearance, and are generally fine- to medium-grained and laminated; some intervals show large-scale load structures (Carney, 2000b). In thin section, vitric shards are concentrated within silty laminae and the larger examples show blocky, sliver and y-shapes and internal replacement by grainy amorphous material. The matrix between the shards, and dominating laminae devoid of such shards, consists of exceedingly fine grained microcrystalline quartzo-feldspathic material. Abundant but faint and shadowy shardic outlines and bubble-wall textures are visible in this microcrystalline material and is interpreted here as finely comminuted ash. These tuffs probably originated as primary fall-out from ash clouds followed by settling out through the water column to the sea-floor.

The overlying Bradgate Formation is dated by the only sample out of several collected from this formation that yielded datable zircons (JNC 912), from the 'Park Breccia' unit at the base of the Bradgate Formation. This unit (Worssam and Old, 1988) denotes a particularly prominent sedimentary breccia horizon that typically occurs a few to several meters below the Sliding Stone Slump Breccia Member. The latter unit is prominent and mappable, but in detail there are many thinner and more discontinuous breccias of this type (Moseley and Ford, 1985), including the Park Breccia, which is developed over a thickness of about 100 m. The term 'Sliding Stone Slump Breccia Member' is therefore used here to cover the whole of this interval (see Fig. 1). Stratigraphic equivalence of the Park Breccia and Sliding Stone Slump Breccia is important. A precise age for the Park Breccia therefore places a good temporal constraint on the Ediacaran macrofossils preserved on the Mercian Assemblage bedding plane described in detail by Wilby et al. (2011). This bedding plane, with over 200 fossil impressions including the holotypes of *Bradgatia linfordensis* and *Charnia grandis* (Boynton and Ford, 1995) occurs only ca. 5 metres above the Sliding Stone Slump Breccia as seen in Bradgate Park.

The Park Breccia sample, JNC 912, was collected from a cutting on the A50 road (BNG SK 4860 1095) at the same locality as sample CH2 of Compston et al. (2002). It is a massive, medium-grained, volcaniclastic sandstone containing generally small cm-scale discrete mudstone rafts. In thin section, the matrix to these rafts is crammed with fine sand-size, angular to subrounded lithic volcanic grains. About 50% of these are composed of sparsely porphyritic andesite in which plagioclase laths and microlites show fluxional to decussate orientation; the remainder consist of andesite with non-oriented textures ranging from aphanitic through to microcrystalline and microgranular types. Between these grains are angular fragments of quartz and feldspar (DR Fig. 1d). The sedimentary clasts consist of volcaniclastic mudstone and siltstone. Like the Sliding Stone Slump Breccia, the Park Breccia is interpreted as being deposited from sediment gravity flows generated by submarine slumping of only partially lithified volcaniclastic material.

The Hanging Rocks Formation was analysed for its detrital zircon characteristics because it provides evidence of epiclastic sedimentation in the terminal part of the Charnian Supergroup. It also occupies an important and somewhat controversial stratigraphical position (Fig. 2) at the top of the Maplewell Group. Sample JNC 846 was collected from the type locality on Charnwood Forest Golf Course (BNG SK 5244 1502). It is a medium-grained poorly sorted micaceous sandstone, with abundant rounded granules and small pebbles and aligned slivers of siltstone (DR Fig. 1e). Thin sections show that many granules and pebbles have lithologies ‘exotic’ to those found in the underlying Charnian strata. These exotic grains include meta-quartzite with sutured grain boundaries and muscovite laths, various polycrystalline quartz aggregates, and perthitic alkali feldspar. The majority of the other lithic grains are volcanic and include andesites and dacites with microcrystalline, microgranular, and in a few cases, intergranular textures. These resemble the lithic grains in the underlying Charnian formations. Other volcanic grains in the rock, however, do not and include various types of welded tuff with fluidal and shardic textures, some with marginally melted quartz xenocrysts (Carney, 1994; 2000c). The good to moderate rounding and sphericity of lithic grains and individual crystals in this formation is a further feature setting this unit apart from lithologies in the underlying formations (see also discussion on the geochemistry of the pebbles, below).

U-Pb Results

Blackbrook Group

LA-ICP-MS results are summarised in DR Table 1. The dominant zircon population of JNC 836 has a $^{206}Pb/^{238}U$ age of 611^{+2}_{-4} Ma (n=55, coherent group of 49) for <5% discordant zircons (as calculated with the TuffZirc age extraction algorithm; Ludwig, 2003; Ludwig and Mundil, 2002). Also present are xenocrystic grain cores with $^{206}Pb/^{238}U$ ages of 630 ± 12 Ma, 703 ± 14 Ma, 1045 ± 18 Ma, 1228 ± 20 Ma and 1484 ± 29 Ma. The stratigraphically younger South Quarry Breccia sample, JNC 917, has a zircon population with a weighted mean $^{206}Pb/^{238}U$ age of 611 ± 2 Ma (TuffZirc, n = 76, coherent group of 68), indistinguishable from the age of the JNC 836 zircons.

A summary of the CA-ID-TIMS ages and the entire data set are presented in Tables 2 and DR Table 2, respectively. Almost all of the data for JNC 916, 836 and 917 cluster on or near concordia between ca. 611 Ma and ca. 620 Ma. This mirrors the main cluster of LA-ICP-MS data for these three rocks. The CA-TIMS data for all three samples completely overlaps, as does the age of the youngest grain analysed from each stratigraphic horizon. For purposes of TIMS-ICP comparison, the pooled CA-TIMS data yield a TuffZirc $^{206}Pb/^{238}U$

age of 613.9$^{+1.4}_{-0.5}$ Ma (n = 38). Separate from this main group are two data points with slightly older ^{206}U/^{238}U ages of ca. 622 Ma.

Beacon Hill Formation (Maplewell Group)

LA-ICP-MS analysis of JNC 918 reveals a zircon population differing from the underlying Blackbrook Group samples by virtue of the presence of a younger ca. 570 Ma component. ^{206}Pb/^{238}U ages of <5% discordant grains form an asymmetric distribution with a TuffZirc ^{206}Pb/^{238}U age of 599$^{+3}_{-5}$ Ma (n = 61, coherent group of 52). The Isoplot age population unmixing utility based on Sambridge and Compston (1994) yields two age components at 600 ± 2 Ma and 569 ± 7 Ma.

CA-ID-TIMS data for JNC 918 includes analyses of <600 Ma grains identified by LA-ICP-MS that were extracted from the epoxy grain mount as well as additional unmounted grains. CA-TIMS confirms the presence of <600 Ma grains, and two analyses have ^{206}U/^{238}U ages of ca. 569 Ma. One further analysis is younger than the two overlapping concordant ca. 569 Ma grains but is imprecise and concordant by virtue of its large uncertainties. It was included here to further illustrate the presence of <600 Ma zircons but is not used in the calculation of the age of this volcaniclastic rock because of its proportionally large common Pb correction and consequent diminished reliability. Also present are a main zircon population at 611-618 Ma that overlaps completely with the dominant zircon populations of the underlying Blackbrook Group rocks.

Carney and Noble (2007) reported CA-ID-TIMS data for JNC 911 that substantiates the ca. 600 Ma and younger zircon ages yielded by JNC 918 from the Beacon Hill Formation. The JNC 911 data were obtained prior to the development of the EARTHTIME tracer and instead used the original T. Krogh ^{205}Pb-^{235}U tracer that was prepared at the Department of Terrestrial Magnetism, Carnegie Institution, Washington D.C. in the 1970's. The calibration of this older spike was checked using U-Pb gravimetric solutions at the Jack Satterley Geochronology Laboratory, Toronto. These same gravimetric solutions were in turn shown to be accurate compared to other more recently mixed U-Pb gravimetric solutions used to calibrate the EARTHTIME ^{205}Pb-^{233}U-^{235}U tracer. Potential bias in data produced using either of the tracers is therefore not significant at the level of the quoted uncertainties for these legacy data. Of the four analyses obtained for JNC 911, two grains give a ^{206}Pb/^{238}U age of 611.6 ± 1.4 Ma, while two younger discordant grains give ^{206}Pb/^{238}U ages of 582.5 ± 0.4 and 590.5 ± 0.3 Ma, either reflecting Pb-loss from ca. 600 Ma or probably more likely analysed mixtures of ≥611 Ma cores and younger rims not completely removed by air abrasion. Additional data produced during the present study using the EARTHTIME tracer revealed only >611 Ma zircons.

Of the limited number of grains (n = 5) analysed from JNC 907, CA-ID-TIMS data indicate an old ca. 613 Ma component and a younger ca. 567-565 Ma component. Two of the younger grains overlap within uncertainty (^{206}Pb/^{238}U = 565.2 ± 0.3 Ma) which are interpreted to be the age of this rock.

Bradgate Formation (Maplewell Group)

For JNC 912, sampled from the Park Breccia at the base of the Bradgate Formation, CA-ID-TIMS analysis reveals two widely differing age groups. The oldest, represented by three concordant analyses, yields a ^{206}Pb/^{238}U age of 613.5 ± 3.4 Ma, consistent with the zircons dated from the underlying volcanic and volcaniclastic rocks. The younger zircons in the Park Breccia, also concordant, yield a ^{206}Pb/^{238}U age of 561.9 ± 0.3 Ma based on seven concordant analyses. The coherence of this group of analyses strongly indicates that this horizon was deposited during a single eruptive event. These new data generated with the EARTHTIME tracer are in agreement with previously reported legacy TIMS data (561.9 ± 1.9 Ma, n = 4) on similar zircon grains produced with the T. Krogh Carnegie $^{205}Pb/^{235}U$ tracer (Carney and Noble, 2007, Wilby et al., 2011).

Hanging Rocks Formation (Maplewell Group)

JNC 846 LA-ICP-MS detrital zircon ages concentrate in the range 750-560 Ma, with a very few Mesoproterozoic to Archaean grains (n = 78). Pre-Neoproterozoic grains are dated at 1176 ± 36 Ma, 2076 ± 55 Ma and 2597 ± 76 Ma. Unmixing calculations on the Neoproterozoic data yield peaks at 729 ± 9 Ma, 673 ± 19 Ma, 608 ± 2 Ma and 562 ± 6 Ma. Focussing further on the youngest zircons (n = 4), these have a mean $^{206}Pb/^{238}U$ age of 557 ± 6 Ma, interpreted as dating (albeit imprecisely), the youngest material sampled within the Maplewell Group. CA-TIMS analysis of young grains extracted from the LA-ICP-MS grain mount was attempted but abandoned due to a mismatch in grain indexing. Further work on this formation will be pursued, but was beyond the scope of this study.

Chemical compositions of Hanging Rocks Formation volcanic pebbles

The conglomerates of this formation represent the first appearance of unequivocally epiclastic material in the Charnian Supergroup. Although the rounded pebbles and granules indicate an early history of reworking in shallow waters by wave or current agitation, the overall sedimentary architecture of the Hanging Rocks Formation suggests that final transport to the Charnian depo-basin was by the agency of turbidity currents (Carney, 2000c). Geochemical data from three volcanic pebbles separated from a conglomerate sample were investigated by two of us (TCP and JNC) to better characterize the sources of volcanogenic detritus available to the Charnwood region late in the development of the volcanic and sedimentary activity. Whole-rock chemical compositions for the pebbles are reported in DR Table 3, and their geochemistry indicates that the pebbles have major and trace element compositions akin to those of igneous rocks from the concealed ca. 600-620 Ma Fenland

Terrane (Noble et al., 1993; Pharaoh et al., 1991; Pharaoh and Carney, 2000). The latter are chemically more evolved than the Charnian Supergroup (e.g. higher SiO2, LILE's), and this relationship is reflected by HFSE trace element distributions for Zr and Y shown in DR Fig. 5. On this diagram, the Hanging Rocks pebbles plot in a field outlined by igneous rocks of the Fenland Terrane, and are quite distinct from the more HFSE-depleted Charnwood igneous and volcanic rocks. Note that the crystal-rich Caldecote Formation volcaniclastic strata exposed at Nuneaton (Fig. 1, inset) have similar Zr-Y characteristics to these Charnwood rocks, supporting their position within the Charnwood Terrane.

We conclude from this that the volcanic pebbles in the Hanging Rocks Formation most likely reflect a significant episode of uplift, emergence and fluviatile and/or shoreline reworking within the Fenland Terrane, which lay adjacent to the Charnwood Terrane (Fig. 1, inset). For reference, geochemical data from Warren House Formation and Uriconian Group volcanic rocks of the Wrekin Terrane are also plotted in DR figure 5. These rocks are contemporaries of the Maplewell Group, with U-Pb ages in the range 565-560 Ma and (Tucker and Pharaoh, 1991), and although the Uriconian samples compare geochemically with those from the Fenland Terrane/Hanging Rocks Formation cluster on DR Fig. 5, the Wrekin Terrane lies at a considerably greater distance from Charnwood than does the Fenland Terrane, and is thus less likely to be a source of the pebbles. Moreover, the Wrekin Terrane as a whole does not contain the c. 620-600 Ma zircon population that is characteristic of the Fenland Terrane and Hanging Rocks Formation. We note that the Padarn Tuff from the Cymru Terrane of north Wales has yielded U-Pb TIMS ages of c. 616 Ma (Tucker and Pharaoh, 1991) and SHRIMP ages of c. 605 Ma (Compston et al. 2002) and so, in terms of age at least, it represents an alternative potential source for the Hanging Rocks pebbles, albeit much more distal than the Fenland Terrane.

Figure DR 1: Volcaniclastic rock textures

A. JNC 836 volcaniclastic sandstone Ives Head Formation (XPL). Close-packed andesite/dacite grains with microgranular and microcrystalline textures; quartz grains (white) show highly angular outlines (lower right) and magmatic rounding (crystal at top image). B. JNC 917 South Quarry Breccia volcaniclastic matrix (XPL). Centre of image shows close-packed microcrystalline andesite/dacite grains. Individual plagioclase crystals have angular outlines and subgrain development; quartz crystals (white areas) are angular with one grain (lower right) interpreted as a magmatically abraded euhedra with marginal gas bubble incursion. C. JNC 918 Benscliffe Breccia crystal-enriched matrix (PPL). 'Trains' of close-packed plagioclase and quartz crystals separate andesitic and dacitic lapilli. Crystals are euhedral to sharply angular, with no evidence of abrasion other than that which can be ascribed to collisions during mass-transport. D. JNC 912 Park Breccia volcaniclastic sandstone matrix (XPL). Angular plagioclase and quartz crystals, abundant angular to subangular andesite and dacite grains; textures of latter show variation between microcrystalline and finely microgranular, with fluxional texture visible in the grain at top-right. E. JNC 846 Hanging Rocks Formation sandstone (PPL). Sandstone is poorly sorted, with silt-size to medium sand-size andesite and dacite grains; elliptical clast shows tectonic foliation (top-centre of image). Larger well-rounded grains are embedded in silt- to mud-rich matrix.

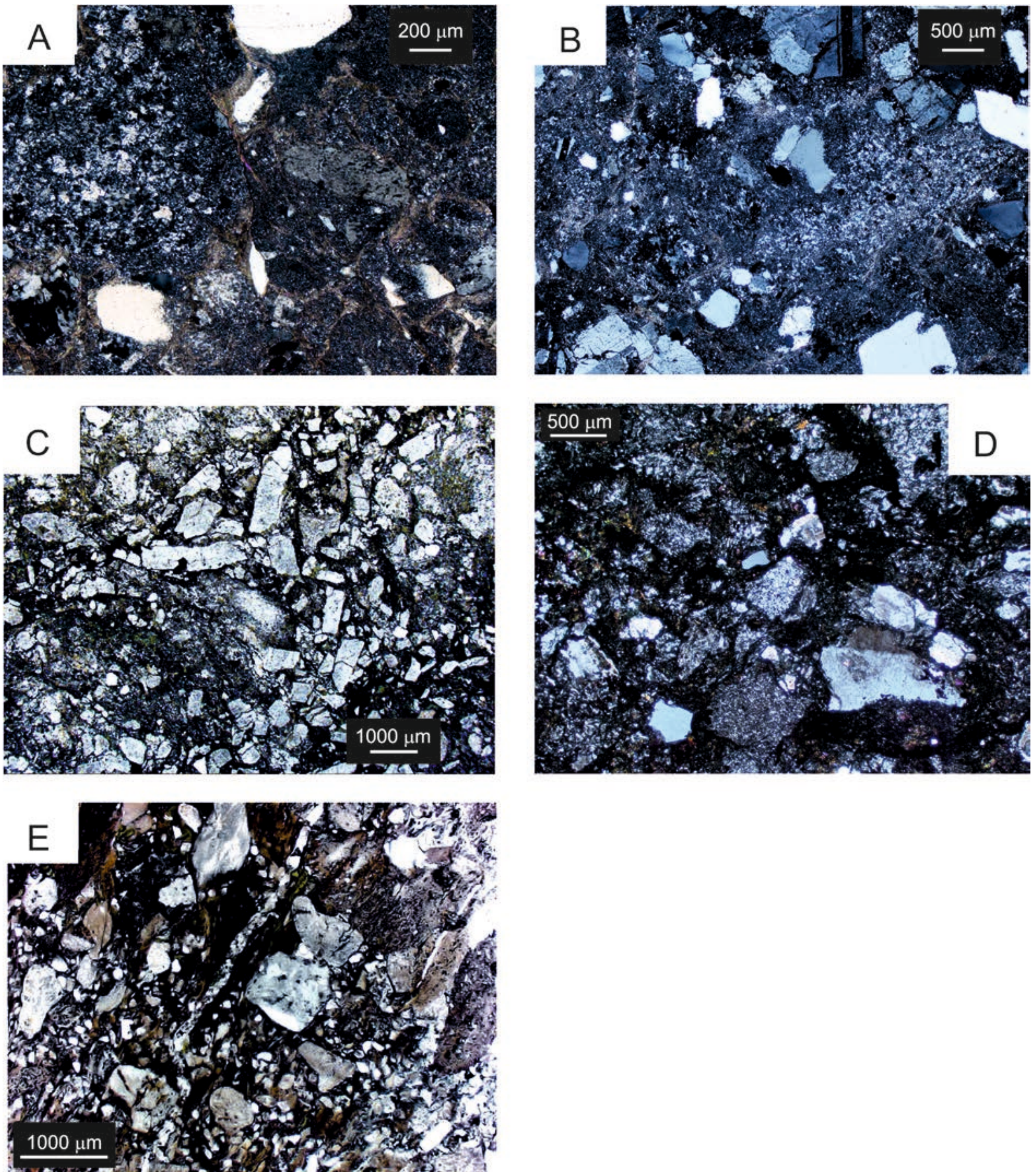
A
200 µm
B
500 µm
C
1000 µm
D
500 µm
E
1000 µm

Figure DR 2. SEM-CL images for typical Charnwood zircons. A-F: Euhedral zircons typical of the Blackbrook Group rocks, showing melt/mineral inclusions and typical zoning. G: Euhedral zircon with prominent xenocrystic core. H: Rare rounded zircon. I-N: Euhedral zircons typical of all the Maplewell Group rocks. O-P: Rounded detrital zircons specifically from the Hanging Rocks Formation, Maplewell Group. Scale bars are 25 µm.

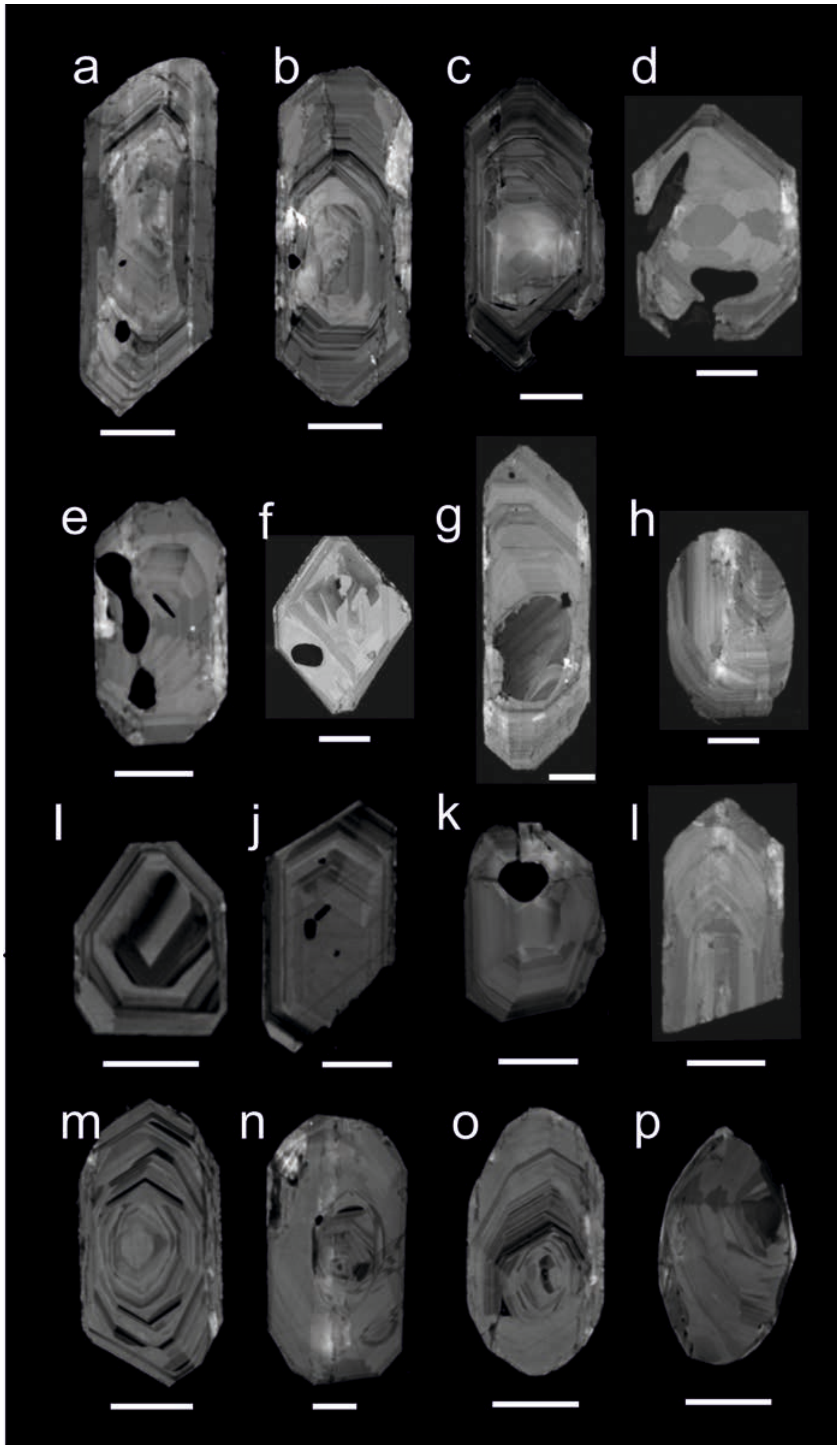

Figure DR 3. Tera-Wasserburg diagrams for LA-ICPMS zircon U-Pb data. Data are plotted at the ± 1σ level, and are the <5% discordant grains in Table DR2. Insets illustrate c. 600 Ma data in detail.

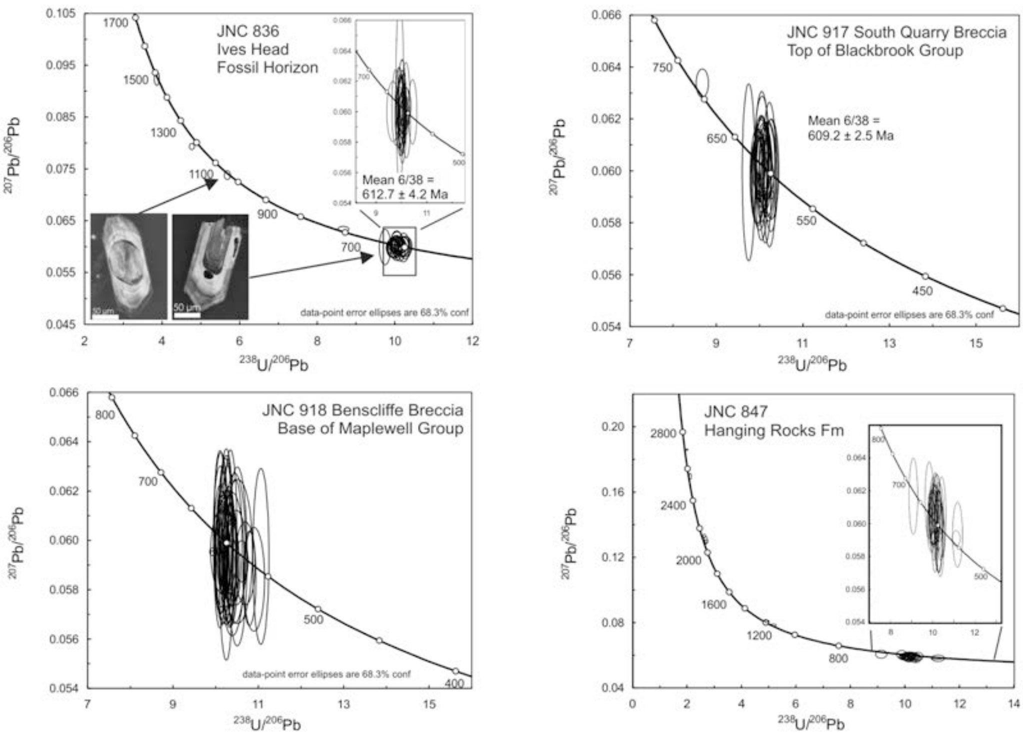

Figure DR 4. Concordia diagrams for CA-TIMS zircon U-Pb data. Data are plotted at the ± 2σ level. Insets illustrate data used to calculate deposition ages.

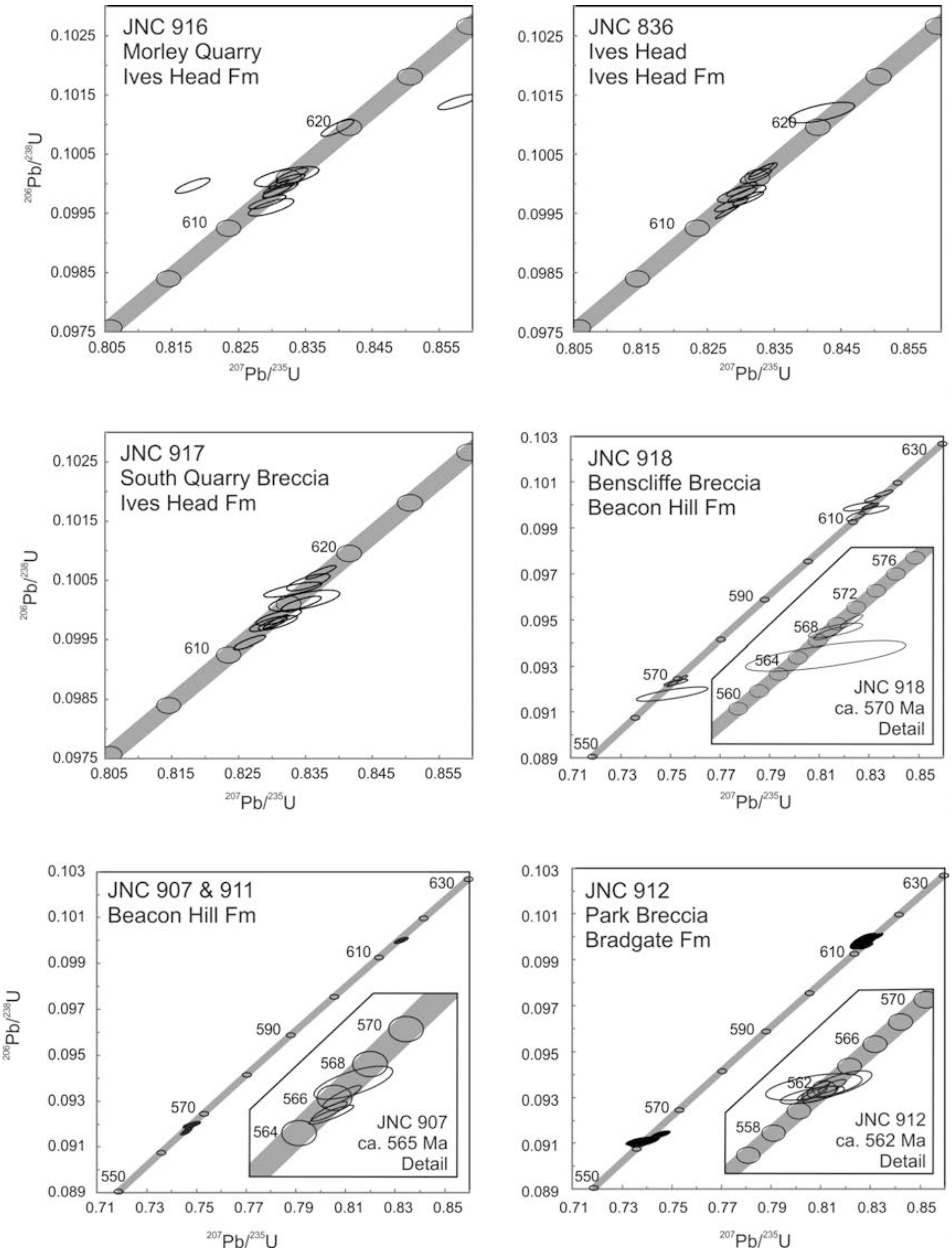

Figure DR 5. Midlands Microcraton Zr and Y characteristics. Data sources are (1) DR Table 3 ; (2) Pharaoh et al., (1987; primary igneous rocks); Carney (2000); (3) Pharaoh and Evans (1987); (4) Bridge et al. (1998); (5) Pharaoh et al. (1991), and (6) Bevins et al. (1995).

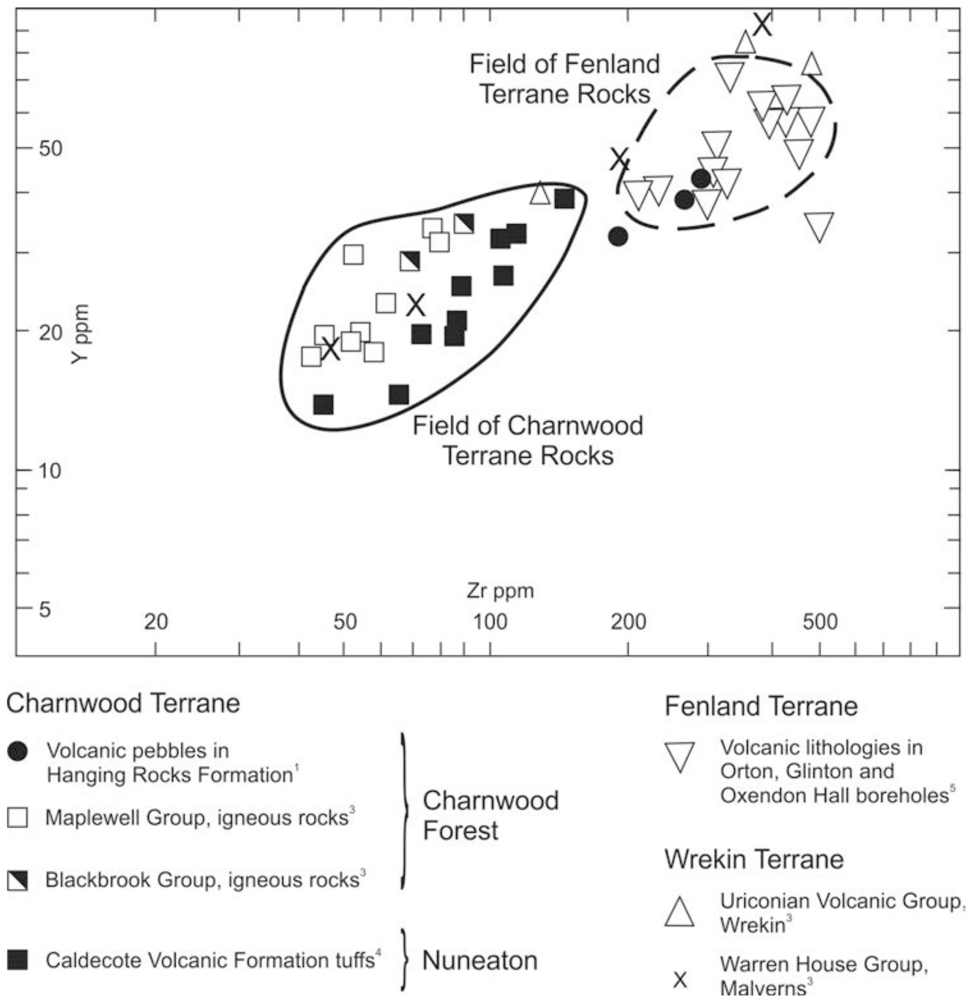

Table DR 1. U-Pb LA-ICP-MS U-Pb isotope data (≤ 10% discordant).

Sample and grain	Ion Beam Intensities (mV) ^{206}Pb	^{207}Pb	^{238}U	Concentrations U (ppm)	Pb (ppm)	Isotope Ratios (not corrected for common Pb) $^{238}U/^{206}Pb$	± 1σ % err	$^{207}Pb/^{206}Pb$	± 1σ % err	$^{207}Pb/^{235}U$	± 1σ % err	$^{206}Pb/^{238}U$	± 1σ % err	corr. coef.	Age (Ma) $^{206}Pb/^{238}U$	± 2σ abs
JNC 836 (BNG SK 4772 1700), Blackbrook Group, Ives Head Fm at Ives Head, turbidite bed, volcaniclastic sandstone																
1	0.7	0.04	10	109	11	9.89	0.99	0.0589	2.18	0.821	2.40	0.1011	0.99	0.41	621	12
2	1.0	0.05	15	152	16	9.88	1.08	0.0590	1.63	0.824	1.96	0.1012	1.08	0.55	621	13
4	0.8	0.04	12	125	12	9.98	0.99	0.0588	1.99	0.813	2.22	0.1002	0.99	0.45	616	12
5	0.4	0.03	6	65	7	9.84	1.16	0.0628	3.21	0.880	3.41	0.1016	1.16	0.34	624	14
6	0.8	0.05	13	132	13	9.92	1.19	0.0591	1.84	0.821	2.19	0.1008	1.19	0.54	619	14
7	0.6	0.04	10	105	10	10.13	1.10	0.0591	2.30	0.805	2.55	0.0987	1.10	0.43	607	13
10 (rim)	0.7	0.04	11	116	12	10.10	1.10	0.0587	2.14	0.801	2.40	0.0990	1.10	0.46	609	13
11	0.7	0.04	11	116	11	10.13	1.04	0.0591	2.13	0.804	2.37	0.0987	1.04	0.44	607	12
12	1.1	0.10	7	69	18	3.86	1.11	0.0925	0.97	3.300	1.48	0.2589	1.11	0.75	1484	29
13	0.7	0.04	11	112	11	10.00	1.08	0.0597	2.15	0.823	2.41	0.1000	1.08	0.45	614	13
14	1.0	0.05	15	159	16	10.13	0.93	0.0588	1.59	0.800	1.85	0.0987	0.93	0.51	607	11
16	0.7	0.04	11	114	11	10.03	0.97	0.0591	2.12	0.812	2.33	0.0997	0.97	0.42	613	11
18	0.9	0.05	14	144	14	10.04	1.09	0.0604	1.73	0.830	2.05	0.0996	1.09	0.53	612	13
19	0.9	0.05	14	142	14	10.10	1.20	0.0603	1.75	0.823	2.12	0.0990	1.20	0.57	609	14
20 - core	4.6	0.35	34	353	73	4.82	0.99	0.0838	0.32	2.398	1.04	0.2075	0.99	0.95	1215	22
20 – rim	0.6	0.03	10	102	10	10.26	0.99	0.0598	2.39	0.804	2.59	0.0975	0.99	0.38	599	11
21	0.6	0.03	9	92	9	10.13	0.92	0.0596	2.59	0.811	2.75	0.0987	0.92	0.33	607	11
22	0.6	0.03	9	96	10	9.95	1.12	0.0587	2.51	0.814	2.75	0.1005	1.12	0.41	618	13
23	0.9	0.05	13	135	14	9.64	1.00	0.0587	1.79	0.839	2.05	0.1038	1.00	0.49	636	12
24	0.8	0.04	12	128	13	10.06	1.03	0.0603	1.90	0.827	2.16	0.0994	1.03	0.48	611	12
25	0.7	0.04	11	115	12	9.89	1.02	0.0585	2.12	0.816	2.35	0.1011	1.02	0.43	621	12
26	0.7	0.04	10	108	11	9.81	1.02	0.0583	2.23	0.819	2.45	0.1019	1.02	0.42	626	12
28	1.2	0.07	19	194	19	10.02	0.97	0.0588	1.35	0.809	1.66	0.0998	0.97	0.58	613	11
31	1.8	0.13	16	167	29	5.68	0.93	0.0738	0.78	1.791	1.21	0.1760	0.93	0.77	1045	18
32	0.4	0.02	6	58	6	9.75	1.01	0.0599	3.76	0.848	3.90	0.1026	1.01	0.26	630	12
33	1.0	0.06	16	168	17	10.04	1.04	0.0592	1.55	0.813	1.87	0.0996	1.04	0.56	612	12
34	0.8	0.04	12	123	12	10.10	0.94	0.0591	2.01	0.807	2.22	0.0990	0.94	0.42	609	11
35	0.8	0.05	13	131	13	9.76	0.88	0.0594	1.84	0.840	2.04	0.1025	0.88	0.43	629	11
36	0.6	0.03	9	91	9	9.88	1.11	0.0584	2.55	0.816	2.78	0.1012	1.11	0.40	622	13

Sample and grain	Ion Beam Intensities (mV)			Concentrations		Isotope Ratios (not corrected for common Pb)									Age (Ma)	
	^{206}Pb	^{207}Pb	^{238}U	U (ppm)	Pb (ppm)	$^{238}U/^{206}Pb$	± 1σ % err	$^{207}Pb/^{206}Pb$	± 1σ % err	$^{207}Pb/^{235}U$	± 1σ % err	$^{206}Pb/^{238}U$	± 1σ % err	corr. coef.	$^{206}Pb/^{238}U$	± 2σ abs
JNC 836 (BNG SK 4772 1700), Blackbrook Group, Ives Head Fm at Ives Head, turbidite bed, volcaniclastic sandstone.																
37	3.1	0.23	23	239	50	4.77	0.91	0.0793	0.51	2.295	1.04	0.2098	0.91	0.87	1228	20
38	0.5	0.03	7	75	7	10.18	1.03	0.0590	3.16	0.799	3.32	0.0983	1.03	0.31	604	12
39	1.0	0.06	16	166	16	10.04	1.06	0.0587	1.57	0.806	1.89	0.0996	1.06	0.56	612	12
40	0.7	0.04	11	116	11	10.27	1.13	0.0601	2.12	0.807	2.40	0.0974	1.13	0.47	599	13
41	0.5	0.03	8	87	8	10.26	1.12	0.0612	2.72	0.823	2.95	0.0974	1.12	0.38	599	13
42	0.6	0.03	9	90	9	10.04	0.96	0.0597	2.64	0.820	2.81	0.0996	0.96	0.34	612	11
43	0.5	0.03	7	77	7	10.23	1.00	0.0599	3.08	0.807	3.23	0.0978	1.00	0.31	601	11
44	0.7	0.04	11	115	11	10.21	1.07	0.0600	2.11	0.810	2.37	0.0980	1.07	0.45	603	12
46	0.5	0.03	8	85	8	10.05	1.02	0.0605	2.73	0.831	2.92	0.0995	1.02	0.35	612	12
47	0.6	0.03	9	98	10	10.06	1.12	0.0606	2.44	0.831	2.69	0.0994	1.12	0.42	611	13
48	1.4	0.08	22	229	23	10.10	1.27	0.0603	1.13	0.824	1.70	0.0990	1.27	0.75	609	15
49	1.0	0.05	15	157	15	10.17	1.19	0.0604	1.61	0.819	2.00	0.0983	1.19	0.59	605	14
50	0.8	0.04	12	128	13	9.96	0.99	0.0596	1.92	0.825	2.16	0.1004	0.99	0.46	617	12
51	0.9	0.05	13	134	14	9.94	1.04	0.0596	1.83	0.827	2.11	0.1006	1.04	0.49	618	12
52	1.2	0.07	19	198	19	10.04	0.97	0.0609	1.34	0.837	1.65	0.0996	0.97	0.59	612	11
53	1.2	0.07	19	195	19	9.98	0.98	0.0603	1.31	0.833	1.63	0.1002	0.98	0.60	615	11
54	0.8	0.04	10	113	11	9.79	0.93	0.0584	2.04	0.822	2.24	0.1021	0.93	0.41	627	11
55	0.8	0.04	11	115	11	9.90	0.94	0.0588	2.04	0.819	2.24	0.1010	0.94	0.42	620	11
57	3.0	0.18	36	394	41	8.67	1.08	0.0634	0.57	1.007	1.22	0.1153	1.08	0.88	703	14
58	1.3	0.07	17	189	17	10.01	0.98	0.0593	1.30	0.816	1.63	0.0999	0.98	0.60	614	11
59	0.8	0.04	10	111	10	9.95	1.09	0.0598	2.02	0.829	2.30	0.1005	1.09	0.47	618	13
60	1.1	0.06	15	163	15	10.10	1.07	0.0603	1.45	0.823	1.80	0.0990	1.07	0.59	609	12
61	1.2	0.07	17	181	16	10.17	1.02	0.0595	1.36	0.806	1.70	0.0983	1.02	0.60	604	12
62	1.1	0.06	16	169	15	10.12	0.98	0.0598	1.41	0.814	1.72	0.0988	0.98	0.57	607	11
63	0.7	0.04	9	102	9	10.22	0.98	0.0586	2.25	0.791	2.46	0.0978	0.98	0.40	602	11
64	0.8	0.04	11	115	10	10.24	0.92	0.0591	2.03	0.795	2.23	0.0977	0.92	0.41	601	11
65	0.5	0.03	7	77	7	10.12	0.96	0.0589	2.88	0.802	3.03	0.0988	0.96	0.32	607	11
66	1.2	0.06	16	176	16	10.15	0.95	0.0590	1.39	0.801	1.69	0.0986	0.95	0.56	606	11
67	0.8	0.04	11	119	11	10.14	0.95	0.0580	2.02	0.788	2.23	0.0986	0.95	0.42	606	11

	Ion Beam Intensities (mV)			Concentrations		Isotope Ratios (not corrected for common Pb)									Age (Ma)	
Sample and grain	^{206}Pb	^{207}Pb	^{238}U	U (ppm)	Pb (ppm)	$^{238}U/^{206}Pb$	± 1σ % err	$^{207}Pb/^{206}Pb$	± 1σ % err	$^{207}Pb/^{235}U$	± 1σ % err	$^{206}Pb/^{238}U$	± 1σ % err	corr. coef.	$^{206}Pb/^{238}U$	± 2σ abs
JNC 917 (BNG SK 4637 1712) Blackbrook Group, Ives Head Fm, South Quarry Breccia, volcaniclastic sandstone and mudstone breccia.																
1	0.7	0.04	10	128	12	9.67	1.68	0.0600	2.18	0.856	2.75	0.1034	1.68	0.61	635	20
2	0.9	0.05	13	173	16	10.24	1.33	0.0589	1.80	0.792	2.24	0.0976	1.33	0.60	601	15
3-1	0.7	0.04	11	143	13	10.31	1.11	0.0589	2.22	0.788	2.49	0.0970	1.11	0.45	597	13
3-3	0.4	0.02	6	85	8	9.87	1.27	0.0590	3.28	0.824	3.52	0.1014	1.27	0.36	622	15
4	0.3	0.02	5	62	6	10.04	1.02	0.0589	4.35	0.810	4.47	0.0996	1.02	0.23	612	12
5	0.5	0.03	8	104	10	9.96	1.13	0.0596	2.73	0.824	2.95	0.1004	1.13	0.38	617	13
6	0.4	0.03	6	81	8	9.76	1.00	0.0735	4.33	1.039	4.44	0.1025	1.00	0.23	629	12
7	0.4	0.03	7	87	8	9.76	0.98	0.0639	2.98	0.903	3.14	0.1024	0.98	0.31	629	12
8	0.6	0.03	9	115	11	9.78	0.95	0.0589	2.48	0.830	2.65	0.1022	0.95	0.36	627	11
9-1	0.4	0.02	6	85	8	9.78	1.04	0.0576	3.27	0.812	3.43	0.1023	1.04	0.30	628	12
9-2	0.7	0.04	11	143	13	9.80	0.99	0.0597	2.04	0.840	2.27	0.1020	0.99	0.44	626	12
10	0.9	0.05	14	180	17	9.89	1.01	0.0596	1.69	0.831	1.97	0.1011	1.01	0.51	621	12
11	0.4	0.02	6	78	7	9.98	1.00	0.0593	3.58	0.819	3.72	0.1002	1.00	0.27	616	12
12	0.6	0.03	9	119	11	9.97	0.93	0.0601	2.40	0.830	2.58	0.1003	0.93	0.36	616	11
13	0.5	0.03	7	96	9	10.04	0.93	0.0592	2.99	0.814	3.13	0.0996	0.93	0.30	612	11
14	0.5	0.03	7	99	9	10.01	1.07	0.0573	2.97	0.789	3.16	0.0999	1.07	0.34	614	13
15	0.3	0.02	4	57	5	9.90	1.54	0.0874	8.74	1.217	8.88	0.1010	1.54	0.17	620	18
16	0.4	0.02	6	74	7	10.15	1.04	0.0564	3.83	0.766	3.97	0.0986	1.04	0.26	606	12
17	0.7	0.04	10	134	12	9.93	1.24	0.0596	2.21	0.828	2.54	0.1007	1.24	0.49	618	15
18-1	0.6	0.03	9	124	11	10.17	1.33	0.0590	2.43	0.800	2.77	0.0983	1.33	0.48	604	15
18-2	0.5	0.03	8	105	9	10.15	1.21	0.0591	2.85	0.803	3.10	0.0985	1.21	0.39	606	14
19	0.3	0.02	5	61	6	10.09	1.14	0.0586	4.44	0.801	4.58	0.0991	1.14	0.25	609	13
20-1	0.3	0.02	5	61	6	10.09	1.14	0.0586	4.44	0.801	4.58	0.0991	1.14	0.25	609	13
20-1	0.5	0.03	8	109	10	10.29	1.08	0.0610	2.76	0.818	2.97	0.0972	1.08	0.36	598	12
21	0.6	0.04	9	126	12	10.06	1.56	0.0586	2.31	0.803	2.79	0.0994	1.56	0.56	611	18
22	1.2	0.07	19	251	23	10.15	1.49	0.0604	1.28	0.820	1.96	0.0985	1.49	0.76	606	17
23	0.9	0.06	14	192	17	10.29	1.42	0.0652	2.01	0.873	2.46	0.0972	1.42	0.58	598	16
24	1.2	0.07	19	247	22	10.07	0.89	0.0597	1.32	0.817	1.59	0.0993	0.89	0.56	610	10
25-1	0.7	0.04	10	139	13	10.01	1.04	0.0594	2.12	0.818	2.36	0.0999	1.04	0.44	614	12

	Ion Beam Intensities (mV)			Concentrations		Isotope Ratios (not corrected for common Pb)									Age (Ma)	
Sample and grain	^{206}Pb	^{207}Pb	^{238}U	U (ppm)	Pb (ppm)	$^{238}U/^{206}Pb$	± 1σ % err	$^{207}Pb/^{206}Pb$	± 1σ % err	$^{207}Pb/^{235}U$	± 1σ % err	$^{206}Pb/^{238}U$	± 1σ % err	corr. coef.	$^{206}Pb/^{238}U$	± 2σ abs
JNC 917 (BNG SK 4637 1712) Blackbrook Group, Ives Head Fm, South Quarry Breccia, volcaniclastic sandstone and mudstone breccia.																
25-2	0.9	0.05	14	184	17	10.02	0.88	0.0598	1.68	0.823	1.90	0.0998	0.88	0.46	613	10
26	0.5	0.03	8	100	9	9.97	0.99	0.0614	2.86	0.849	3.02	0.1003	0.99	0.33	616	12
27	0.5	0.03	8	104	9	10.01	0.97	0.0599	2.75	0.826	2.92	0.0999	0.97	0.33	614	11
28	0.8	0.04	11	151	14	10.04	0.96	0.0609	1.96	0.836	2.18	0.0996	0.96	0.44	612	11
29-1	0.4	0.02	6	84	7	10.19	1.00	0.0611	3.29	0.827	3.44	0.0981	1.00	0.29	603	12
29-2	0.4	0.02	6	76	7	10.05	1.05	0.0629	3.39	0.863	3.55	0.0995	1.05	0.30	612	12
30	0.5	0.03	8	106	10	10.06	1.00	0.0621	2.60	0.851	2.78	0.0994	1.00	0.36	611	12
31-1	0.5	0.03	8	104	10	10.05	1.13	0.0693	3.20	0.951	3.39	0.0995	1.13	0.33	612	13
31-2	0.7	0.04	11	145	13	10.25	1.29	0.0617	2.05	0.830	2.42	0.0975	1.29	0.53	600	15
33-1	0.6	0.04	10	130	12	10.09	0.94	0.0627	2.18	0.857	2.38	0.0991	0.94	0.40	609	11
33-2	0.4	0.03	6	86	8	10.55	1.26	0.0670	3.18	0.876	3.42	0.0948	1.26	0.37	584	14
34	0.4	0.02	6	75	7	10.14	1.15	0.0628	3.60	0.854	3.78	0.0986	1.15	0.30	606	13
35-1	0.5	0.03	8	107	10	9.98	1.12	0.0591	2.69	0.816	2.92	0.1002	1.12	0.38	616	13
35-2	0.5	0.03	7	96	9	9.92	1.09	0.0602	2.93	0.837	3.12	0.1008	1.09	0.35	619	13
36	0.6	0.05	9	124	11	9.75	1.09	0.0816	2.34	1.154	2.59	0.1026	1.09	0.42	629	13
37	1.3	0.08	21	274	24	10.25	1.41	0.0621	1.20	0.836	1.86	0.0975	1.41	0.76	600	16
38	0.5	0.03	7	91	8	10.16	1.21	0.0622	2.97	0.844	3.20	0.0985	1.21	0.38	605	14
40	0.4	0.03	7	88	8	10.20	1.03	0.0630	3.08	0.851	3.25	0.0981	1.03	0.32	603	12
41	0.5	0.03	7	94	8	10.17	0.96	0.0617	2.97	0.837	3.13	0.0983	0.96	0.31	605	11
42	0.6	0.03	9	114	10	10.20	0.97	0.0625	2.48	0.845	2.66	0.0981	0.97	0.37	603	11
43	0.7	0.04	11	144	13	10.11	0.91	0.0620	2.01	0.845	2.20	0.0990	0.91	0.41	608	11
44	0.4	0.02	6	85	7	10.26	1.13	0.0624	3.19	0.839	3.39	0.0975	1.13	0.34	600	13
45	0.4	0.03	6	81	7	10.21	1.09	0.0824	3.08	1.113	3.27	0.0980	1.09	0.33	602	12
46-1	0.3	0.02	4	54	5	9.16	1.47	0.0724	4.31	1.090	4.56	0.1091	1.47	0.32	668	19
46-2	0.3	0.02	5	60	5	10.08	1.12	0.0641	4.26	0.877	4.41	0.0992	1.12	0.25	610	13
48-1	0.7	0.04	10	137	13	9.94	0.96	0.0604	2.14	0.838	2.35	0.1006	0.96	0.41	618	11
48-2	0.6	0.04	10	126	12	9.91	0.93	0.0608	2.28	0.846	2.46	0.1009	0.93	0.38	620	11
49	0.3	0.02	5	66	6	9.89	1.02	0.0594	4.06	0.829	4.19	0.1011	1.02	0.24	621	12
50	0.5	0.03	8	106	10	9.77	0.96	0.0603	2.72	0.851	2.89	0.1024	0.96	0.33	628	12
51-1	0.4	0.02	6	83	7	10.02	0.99	0.0604	3.37	0.830	3.52	0.0998	0.99	0.28	613	12

	Ion Beam Intensities (mV)			Concentrations		Isotope Ratios (not corrected for common Pb)									Age (Ma)	
Sample and grain	^{206}Pb	^{207}Pb	^{238}U	U (ppm)	Pb (ppm)	$^{238}U/^{206}Pb$	± 1σ % err	$^{207}Pb/^{206}Pb$	± 1σ % err	$^{207}Pb/^{235}U$	± 1σ % err	$^{206}Pb/^{238}U$	± 1σ % err	corr. coef.	$^{206}Pb/^{238}U$	± 2σ abs
JNC 917 (BNG SK 4637 1712) Blackbrook Group, Ives Head Fm, South Quarry Breccia, volcaniclastic sandstone and mudstone breccia.																
51-2	0.4	0.02	6	83	8	9.86	0.92	0.0594	3.41	0.830	3.54	0.1014	0.92	0.26	622	11
52	1.2	0.07	19	252	22	10.13	1.05	0.0599	1.30	0.816	1.68	0.0987	1.05	0.63	607	12
53	0.3	0.02	5	67	6	10.13	1.02	0.0588	4.25	0.801	4.37	0.0988	1.02	0.23	607	12
54	0.6	0.03	9	116	10	10.20	1.03	0.0593	2.57	0.801	2.77	0.0981	1.03	0.37	603	12
55	0.7	0.05	11	149	14	9.90	1.10	0.0673	2.52	0.937	2.75	0.1010	1.10	0.40	620	13
56	1.1	0.06	18	241	21	10.07	1.24	0.0598	1.42	0.819	1.88	0.0993	1.24	0.66	610	14
57	0.3	0.02	5	68	6	10.06	1.15	0.0573	4.20	0.785	4.36	0.0994	1.15	0.26	611	13
58-1	1.3	0.07	19	257	23	10.07	1.01	0.0602	1.28	0.824	1.63	0.0993	1.01	0.62	610	12
58-2	0.5	0.03	8	107	9	10.04	0.97	0.0591	2.78	0.812	2.95	0.0996	0.97	0.33	612	11
59	0.6	0.04	10	127	11	10.03	1.03	0.0602	2.32	0.828	2.53	0.0997	1.03	0.41	613	12
60	0.6	0.04	10	133	12	10.44	1.08	0.0600	2.34	0.792	2.58	0.0958	1.08	0.42	590	12
61-1	0.5	0.03	7	96	9	10.00	1.11	0.0692	3.78	0.954	3.94	0.1000	1.11	0.28	614	13
61-2	0.4	0.02	6	74	7	10.05	1.14	0.0617	3.73	0.846	3.90	0.0995	1.14	0.29	611	13
62	0.5	0.03	8	101	9	10.01	1.03	0.0597	2.83	0.822	3.01	0.0999	1.03	0.34	614	12
63	0.8	0.05	13	170	15	10.02	1.15	0.0653	1.66	0.898	2.02	0.0998	1.15	0.57	613	13
64	0.6	0.03	9	115	10	10.18	1.01	0.0608	2.59	0.824	2.78	0.0983	1.01	0.36	604	12
66	0.3	0.02	5	64	6	10.07	1.17	0.0620	4.12	0.849	4.28	0.0993	1.17	0.27	611	14
JNC 918 (BNG SK 5146 1246) Maplewell Group, Beacon Hill Fm, Benscliffe Breccia at Pillar Rock, Massive andesite breccia and coarse grained volcaniclastic sandstone.																
1	1.9	0.11	30	110	9	10.90	1.51	0.0584	2.37	0.739	2.81	0.0918	1.51	0.54	566	16
2	1.9	0.11	30	86	8	10.11	1.77	0.0619	2.67	0.845	3.20	0.0990	1.77	0.55	608	21
3	0.8	0.05	7	110	9	11.08	1.99	0.0578	2.45	0.720	3.16	0.0903	1.99	0.63	557	21
4	0.8	0.06	7	85	8	10.10	1.69	0.0587	2.77	0.801	3.25	0.0990	1.69	0.52	609	20
5	3.5	0.17	100	123	11	10.19	1.98	0.0596	1.97	0.806	2.80	0.0981	1.98	0.71	603	23
6	3.0	0.15	86	78	7	10.26	1.78	0.0582	3.07	0.782	3.55	0.0974	1.78	0.50	599	20
8	2.0	0.11	30	81	7	10.24	1.62	0.0592	2.89	0.797	3.31	0.0976	1.62	0.49	601	19
9	1.9	0.11	30	93	8	10.54	1.66	0.0605	2.51	0.791	3.01	0.0949	1.66	0.55	584	18
12	0.9	0.06	8	71	6	10.52	2.18	0.0596	3.24	0.781	3.90	0.0951	2.18	0.56	586	24
13	0.9	0.06	8	72	6	10.39	1.79	0.0590	3.25	0.784	3.71	0.0963	1.79	0.48	592	20
15	3.3	0.16	96	140	12	10.69	1.44	0.0591	1.88	0.762	2.37	0.0935	1.44	0.61	576	16

Sample and grain	Ion Beam Intensities (mV) ^{206}Pb	^{207}Pb	^{238}U	Concentrations U (ppm)	Pb (ppm)	Isotope Ratios (not corrected for common Pb) $^{238}U/^{206}Pb$	± 1σ % err	$^{207}Pb/^{206}Pb$	± 1σ % err	$^{207}Pb/^{235}U$	± 1σ % err	$^{206}Pb/^{238}U$	± 1σ % err	corr. coef.	Age (Ma) $^{206}Pb/^{238}U$	± 2σ abs
JNC 918 (BNG SK 5146 1246) Maplewell Group, Beacon Hill Fm, Benscliffe Breccia at Pillar Rock, Massive andesite breccia and coarse grained volcaniclastic sandstone.																
16	3.4	0.17	100	123	11	10.38	1.53	0.0613	2.04	0.814	2.55	0.0963	1.53	0.60	593	17
17	0.7	0.04	11	121	11	10.53	1.68	0.0611	2.13	0.801	2.71	0.0950	1.68	0.62	585	19
18	0.6	0.03	8	55	5	10.49	1.80	0.0573	4.22	0.754	4.59	0.0954	1.80	0.39	587	20
19	0.6	0.03	11	75	7	10.45	1.62	0.0597	3.36	0.788	3.73	0.0957	1.62	0.43	589	18
20	0.5	0.03	8	74	7	10.51	1.70	0.0612	2.98	0.802	3.44	0.0951	1.70	0.50	586	19
21	0.8	0.04	12	47	4	10.38	1.73	0.0566	4.89	0.752	5.19	0.0963	1.73	0.33	593	20
22	0.5	0.03	8	80	7	10.44	1.69	0.0565	3.07	0.746	3.51	0.0958	1.69	0.48	590	19
23	1.1	0.07	17	121	11	10.49	1.56	0.0593	2.13	0.780	2.64	0.0954	1.56	0.59	587	17
24	0.5	0.03	8	41	4	10.59	1.46	0.0565	5.67	0.736	5.85	0.0944	1.46	0.25	582	16
25	0.6	0.03	9	90	7	11.32	1.44	0.0576	3.02	0.701	3.35	0.0883	1.44	0.43	546	15
26	6.6	0.42	106	105	9	10.24	1.07	0.0594	2.30	0.799	2.53	0.0976	1.07	0.42	600	12
27	0.6	0.03	9	140	12	10.08	1.29	0.0594	1.80	0.812	2.21	0.0992	1.29	0.58	610	15
28	1.9	0.10	29	107	9	10.16	0.98	0.0600	2.25	0.814	2.45	0.0984	0.98	0.40	605	11
30	1.8	0.10	29	116	10	10.22	1.10	0.0596	2.10	0.804	2.37	0.0979	1.10	0.47	602	13
32	0.8	0.05	7	170	15	10.32	1.76	0.0609	1.52	0.814	2.33	0.0969	1.76	0.76	596	20
33	0.9	0.06	7	89	8	10.46	1.01	0.0600	2.70	0.791	2.88	0.0956	1.01	0.35	589	11
34	2.7	0.13	80	133	12	10.12	1.09	0.0623	2.02	0.848	2.29	0.0988	1.09	0.47	608	13
36	3.2	0.16	96	43	4	10.50	1.14	0.0613	4.94	0.805	5.07	0.0952	1.14	0.23	586	13
37	1.0	0.07	9	63	5	11.06	1.13	0.0593	3.97	0.740	4.12	0.0904	1.13	0.27	558	12
40	2.7	0.13	79	60	5	10.25	1.01	0.0602	3.83	0.810	3.96	0.0976	1.01	0.26	600	12
41	2.7	0.13	77	79	7	10.33	0.95	0.0579	3.13	0.772	3.27	0.0968	0.95	0.29	595	11
42	0.4	0.02	7	71	6	10.16	1.09	0.0569	3.33	0.772	3.50	0.0984	1.09	0.31	605	13
43	0.5	0.02	7	94	8	9.98	1.09	0.0592	2.63	0.818	2.85	0.1002	1.09	0.38	615	13
44	0.3	0.02	6	63	6	10.12	1.09	0.0603	3.55	0.822	3.72	0.0988	1.09	0.29	607	13
45	0.8	0.05	14	143	12	10.38	0.92	0.0581	1.81	0.772	2.03	0.0964	0.92	0.45	593	10
46	0.8	0.04	12	84	7	10.14	0.99	0.0578	2.93	0.786	3.09	0.0986	0.99	0.32	606	11
47	0.7	0.04	12	66	6	10.16	1.32	0.0566	3.67	0.768	3.90	0.0985	1.32	0.34	605	15
48	0.3	0.02	5	69	6	10.03	0.96	0.0633	3.29	0.869	3.43	0.0997	0.96	0.28	613	11
49	0.5	0.03	7	81	7	10.37	0.90	0.0574	3.02	0.763	3.15	0.0964	0.90	0.29	593	10
50	0.5	0.03	7	120	11	10.06	0.89	0.0584	2.02	0.801	2.21	0.0994	0.89	0.40	611	10

	Ion Beam Intensities (mV)			Concentrations		Isotope Ratios (not corrected for common Pb)									Age (Ma)	
Sample and grain	^{206}Pb	^{207}Pb	^{238}U	U (ppm)	Pb (ppm)	$^{238}U/^{206}Pb$	± 1σ % err	$^{207}Pb/^{206}Pb$	± 1σ % err	$^{207}Pb/^{235}U$	± 1σ % err	$^{206}Pb/^{238}U$	± 1σ % err	corr. coef.	$^{206}Pb/^{238}U$	± 2σ abs
JNC 918 (BNG SK 5146 1246) Maplewell Group, Beacon Hill Fm, Benscliffe Breccia at Pillar Rock, Massive andesite breccia and coarse grained volcaniclastic sandstone.																
51	0.3	0.02	5	51	4	10.50	1.19	0.0567	4.65	0.744	4.80	0.0952	1.19	0.25	586	13
55	0.7	0.04	12	57	5	10.10	0.98	0.0600	3.96	0.820	4.08	0.0990	0.98	0.24	609	11
56	0.2	0.01	4	175	15	10.23	0.91	0.0592	1.49	0.798	1.75	0.0977	0.91	0.52	601	10
57	0.5	0.03	9	311	27	10.61	0.94	0.0592	0.93	0.769	1.32	0.0943	0.94	0.71	581	10
58	1.0	0.07	9	75	7	10.31	1.05	0.0594	3.07	0.795	3.25	0.0970	1.05	0.32	597	12
59	1.0	0.07	9	63	6	10.18	0.93	0.0613	3.55	0.830	3.67	0.0982	0.93	0.25	604	11
61	1.1	0.07	9	138	12	10.38	1.14	0.0590	1.87	0.784	2.19	0.0964	1.14	0.52	593	13
62	1.1	0.07	9	87	7	10.35	1.09	0.0590	2.80	0.786	3.01	0.0966	1.09	0.36	595	12
63	1.0	0.07	9	319	28	10.19	0.89	0.0612	1.13	0.827	1.43	0.0981	0.89	0.62	603	10
64	2.6	0.13	75	79	7	10.32	1.00	0.0591	2.98	0.790	3.14	0.0969	1.00	0.32	596	11
65	2.5	0.13	74	48	4	10.25	1.07	0.0593	4.63	0.798	4.75	0.0976	1.07	0.23	600	12
66	2.5	0.12	72	78	7	10.23	1.03	0.0606	2.95	0.817	3.13	0.0978	1.03	0.33	601	12
67	2.7	0.13	79	76	7	10.08	0.97	0.0579	3.04	0.793	3.20	0.0992	0.97	0.30	610	11
68	2.7	0.13	79	123	10	10.79	0.93	0.0585	2.16	0.747	2.35	0.0927	0.93	0.39	571	10
69	2.5	0.12	73	65	6	10.35	0.94	0.0605	3.48	0.806	3.60	0.0966	0.94	0.26	595	11
70	1.0	0.08	9	204	18	10.36	0.91	0.0590	1.31	0.786	1.59	0.0966	0.91	0.57	594	10
72	0.9	0.07	8	81	7	10.16	1.03	0.0592	2.92	0.803	3.10	0.0984	1.03	0.33	605	12
73	2.4	0.13	71	101	9	10.14	1.00	0.0595	2.40	0.809	2.60	0.0986	1.00	0.38	606	12
75	2.3	0.13	68	115	10	10.11	0.92	0.0611	2.06	0.834	2.26	0.0989	0.92	0.41	608	11
77	1.0	0.07	8	70	6	10.28	0.94	0.0600	3.33	0.805	3.46	0.0973	0.94	0.27	599	11
JNC 846 (BNG SK 5244 1502) Maplewell Group, Hanging Rocks Fm, medium grained poorly sorted micaceous sandstone.																
1	0.8	0.05	12	144	14	9.66	1.22	0.0592	1.88	0.845	2.24	0.1035	1.22	0.54	635	15
2	0.6	0.03	9	105	10	10.01	1.51	0.0588	2.55	0.810	2.97	0.0999	1.51	0.51	614	18
3	0.8	0.05	13	158	14	10.18	1.21	0.0609	2.26	0.825	2.56	0.0982	1.21	0.47	604	14
4	0.9	0.05	13	161	15	9.93	1.33	0.0599	1.73	0.831	2.18	0.1007	1.33	0.61	618	16
5	1.5	0.08	23	272	25	9.96	1.10	0.0610	1.11	0.845	1.57	0.1004	1.10	0.71	617	13
7	0.6	0.03	9	107	10	10.06	1.22	0.0601	2.52	0.823	2.80	0.0994	1.22	0.44	611	14
8	0.8	0.04	12	146	13	10.07	1.23	0.0603	1.90	0.826	2.26	0.0993	1.23	0.54	610	14

Sample and grain	Ion Beam Intensities (mV) ^{206}Pb	^{207}Pb	^{238}U	Concentrations U (ppm)	Pb (ppm)	Isotope Ratios (not corrected for common Pb) $^{238}U/^{206}Pb$	± 1σ % err	$^{207}Pb/^{206}Pb$	± 1σ % err	$^{207}Pb/^{235}U$	± 1σ % err	$^{206}Pb/^{238}U$	± 1σ % err	corr. coef.	Age (Ma) $^{206}Pb/^{238}U$	± 2σ abs
JNC 846 (BNG SK 5244 1502) Maplewell Group, Hanging Rocks Fm, medium grained poorly sorted micaceous sandstone.																
9	0.6	0.03	9	110	10	10.13	1.10	0.0601	2.47	0.818	2.70	0.0987	1.10	0.41	607	13
10	1.3	0.07	20	240	22	10.04	1.15	0.0610	1.22	0.837	1.68	0.0996	1.15	0.68	612	13
11	0.8	0.05	13	152	14	10.00	1.19	0.0604	1.86	0.833	2.21	0.1000	1.19	0.54	614	14
12	0.4	0.02	6	73	7	10.06	1.24	0.0593	3.55	0.813	3.76	0.0994	1.24	0.33	611	14
13	0.6	0.03	9	105	10	9.84	1.34	0.0614	2.50	0.861	2.84	0.1016	1.34	0.47	624	16
15	0.4	0.03	7	81	7	10.36	1.61	0.0644	3.08	0.856	3.48	0.0965	1.61	0.46	594	18
16	0.6	0.03	8	95	10	9.09	1.50	0.0617	2.49	0.936	2.91	0.1101	1.50	0.52	673	19
18	0.7	0.04	12	143	13	10.30	1.41	0.0607	1.98	0.813	2.43	0.0971	1.41	0.58	598	16
19	1.2	0.07	11	227	20	10.04	1.44	0.0599	1.33	0.823	1.96	0.0996	1.44	0.73	612	17
20	0.8	0.05	8	152	14	9.93	1.24	0.0594	1.84	0.826	2.22	0.1007	1.24	0.56	619	15
21	0.4	0.02	12	80	7	10.01	1.22	0.0592	3.33	0.816	3.55	0.0999	1.22	0.34	614	14
23	0.7	0.04	17	125	11	10.10	1.30	0.0597	2.29	0.815	2.63	0.0990	1.30	0.49	608	15
24	0.3	0.02	8	64	6	10.17	1.18	0.0585	4.04	0.794	4.21	0.0984	1.18	0.28	605	14
25	0.7	0.04	9	135	12	10.04	1.19	0.0606	2.06	0.833	2.38	0.0996	1.19	0.50	612	14
26	1.0	0.05	106	186	16	10.24	1.16	0.0610	1.74	0.821	2.10	0.0977	1.16	0.56	601	13
27	1.0	0.06	9	198	17	10.48	1.16	0.0609	1.54	0.802	1.93	0.0954	1.16	0.60	588	13
28	0.4	0.02	29	79	7	10.11	1.14	0.0601	3.35	0.819	3.54	0.0989	1.14	0.32	608	13
29	0.5	0.03	29	105	9	10.42	1.28	0.0604	2.70	0.799	2.99	0.0959	1.28	0.43	591	14
30	0.9	0.15	29	36	16	2.08	1.27	0.1696	0.67	11.267	1.44	0.4817	1.27	0.89	2535	53
31	2.2	0.16	7	198	36	4.89	1.14	0.0816	0.61	2.302	1.29	0.2045	1.14	0.88	1200	25
32	0.6	0.04	7	115	10	10.23	1.24	0.0630	2.44	0.849	2.74	0.0977	1.24	0.45	601	14
33	1.7	0.20	7	84	29	2.67	1.47	0.1301	0.51	6.717	1.55	0.3745	1.47	0.94	2050	51
34	0.4	0.02	80	70	6	10.43	1.23	0.0584	3.96	0.772	4.15	0.0959	1.23	0.30	590	14
35	0.6	0.07	78	30	10	2.65	1.48	0.1309	1.22	6.806	1.92	0.3770	1.48	0.77	2062	52
36	0.5	0.03	96	95	9	9.89	1.23	0.0595	2.83	0.829	3.08	0.1011	1.23	0.40	621	14
37	0.5	0.03	9	101	9	9.90	1.22	0.0639	2.50	0.890	2.78	0.1010	1.22	0.44	620	14
38	1.8	0.11	9	276	31	8.17	1.15	0.0637	0.89	1.075	1.45	0.1225	1.15	0.79	745	16
40	1.0	0.05	79	179	16	9.94	1.14	0.0601	1.61	0.834	1.98	0.1006	1.14	0.58	618	13
41	0.8	0.05	79	145	13	9.90	1.24	0.0648	2.11	0.903	2.45	0.1010	1.24	0.51	620	15
42	0.6	0.03	77	108	9	10.36	1.21	0.0591	2.64	0.787	2.90	0.0966	1.21	0.42	594	14

	Ion Beam Intensities (mV)			Concentrations		Isotope Ratios (not corrected for common Pb)									Age (Ma)	
Sample and grain	^{206}Pb	^{207}Pb	^{238}U	U (ppm)	Pb (ppm)	$^{238}U/^{206}Pb$	± 1σ % err	$^{207}Pb/^{206}Pb$	± 1σ % err	$^{207}Pb/^{235}U$	± 1σ % err	$^{206}Pb/^{238}U$	± 1σ % err	corr. coef.	$^{206}Pb/^{238}U$	± 2σ abs
JNC 846 (BNG SK 5244 1502) Maplewell Group, Hanging Rocks Fm, medium grained poorly sorted micaceous sandstone.																
43	0.8	0.05	7	160	14	10.37	1.18	0.0595	1.89	0.791	2.23	0.0964	1.18	0.53	593	13
44	2.1	0.12	7	390	35	9.95	1.13	0.0613	0.81	0.848	1.39	0.1005	1.13	0.81	617	13
45	1.7	0.21	6	84	29	2.59	1.17	0.1335	0.51	7.095	1.27	0.3854	1.17	0.92	2101	42
46	12.8	1.55	14	676	216	2.82	1.11	0.1306	0.16	6.378	1.13	0.3541	1.11	0.99	1954	37
47	1.0	0.06	12	192	17	10.14	1.29	0.0609	1.53	0.828	2.00	0.0986	1.29	0.64	606	15
48	0.6	0.04	12	120	11	10.20	1.26	0.0608	2.33	0.822	2.65	0.0980	1.26	0.48	603	14
49	2.8	0.17	5	438	47	8.40	1.09	0.0648	0.60	1.063	1.25	0.1190	1.09	0.87	725	15
50	1.7	0.10	7	341	29	10.44	1.18	0.0607	0.95	0.802	1.52	0.0958	1.18	0.78	590	13
52	0.5	0.03	7	86	8	9.84	1.19	0.0590	3.08	0.826	3.30	0.1016	1.19	0.36	624	14
54	3.7	0.20	8	761	62	11.10	1.14	0.0591	0.52	0.734	1.25	0.0901	1.14	0.91	556	12
55	1.4	0.08	12	221	23	8.48	1.19	0.0653	1.11	1.061	1.62	0.1179	1.19	0.73	718	16
56	0.7	0.04	4	142	13	10.27	1.21	0.0602	2.05	0.808	2.37	0.0974	1.21	0.51	599	14
58	1.3	0.08	9	273	22	11.14	1.25	0.0630	1.35	0.780	1.84	0.0898	1.25	0.68	554	13
59	0.6	0.04	9	115	10	10.34	1.46	0.0634	2.40	0.845	2.81	0.0968	1.46	0.52	595	17
60	0.2	0.01	9	35	3	10.74	1.19	0.0625	7.09	0.801	7.19	0.0931	1.19	0.17	574	13
63	5.9	0.56	9	389	99	3.54	1.29	0.1043	0.22	4.060	1.31	0.2822	1.29	0.99	1602	37
66	0.5	0.03	72	101	9	10.28	1.17	0.0595	2.73	0.798	2.97	0.0972	1.17	0.39	598	13
67	0.9	0.05	79	168	15	10.21	1.16	0.0616	1.70	0.831	2.06	0.0979	1.16	0.56	602	13
69-1 core	2.3	0.24	79	146	39	3.36	1.35	0.1097	0.45	4.501	1.43	0.2977	1.35	0.95	1680	40
69-2 rim	0.6	0.03	73	120	10	10.96	1.19	0.0621	2.43	0.782	2.70	0.0912	1.19	0.44	563	13
70	5.5	0.95	9	201	93	1.95	1.26	0.1858	0.17	13.111	1.27	0.5117	1.26	0.99	2664	55
71	3.1	0.35	9	176	53	3.08	1.34	0.1226	0.32	5.488	1.38	0.3246	1.34	0.97	1812	42
72	1.0	0.06	8	198	17	10.32	1.26	0.0582	1.65	0.778	2.08	0.0969	1.26	0.61	596	14
73	0.5	0.03	71	98	8	10.69	1.40	0.0574	3.06	0.741	3.37	0.0936	1.40	0.41	577	15
74	0.6	0.03	68	109	10	9.83	1.42	0.0573	2.57	0.804	2.94	0.1017	1.42	0.49	625	17
75	2.4	0.18	68	232	41	5.13	1.26	0.0794	0.57	2.136	1.38	0.1950	1.26	0.91	1149	26
77	0.8	0.05	8	157	14	10.06	1.43	0.0631	2.34	0.865	2.74	0.0994	1.43	0.52	611	17
78	0.8	0.05	8	161	14	10.21	1.21	0.0576	1.93	0.778	2.28	0.0979	1.21	0.53	602	14
79	0.9	0.05	67	175	16	10.14	1.17	0.0575	1.74	0.782	2.10	0.0986	1.17	0.56	606	14
80	2.4	0.14	68	466	40	10.32	1.14	0.0607	0.77	0.811	1.38	0.0969	1.14	0.83	596	13
81	0.5	0.03	69	95	9	10.16	1.21	0.0571	2.99	0.775	3.22	0.0984	1.21	0.38	605	14

Sample and grain	Ion Beam Intensities (mV) ^{206}Pb	^{207}Pb	^{238}U	Concentrations U (ppm)	Pb (ppm)	Isotope Ratios (not corrected for common Pb) $^{238}U/^{206}Pb$	± 1σ % err	$^{207}Pb/^{206}Pb$	± 1σ % err	$^{207}Pb/^{235}U$	± 1σ % err	$^{206}Pb/^{238}U$	± 1σ % err	corr. coef.	Age (Ma) $^{206}Pb/^{238}U$	± 2σ abs
JNC 846 (BNG SK 5244 1502) Maplewell Group, Hanging Rocks Fm, medium grained poorly sorted micaceous sandstone.																
82	0.8	0.04	10	170	14	11.18	1.38	0.0593	2.21	0.732	2.60	0.0895	1.38	0.53	552	15
83	0.7	0.04	14	142	12	10.20	1.21	0.0585	2.11	0.791	2.43	0.0980	1.21	0.50	603	14
84	0.4	0.02	11	70	6	10.01	1.38	0.0552	3.95	0.761	4.19	0.0999	1.38	0.33	614	16
85	1.1	0.07	6	198	18	9.71	1.42	0.0658	1.49	0.934	2.06	0.1030	1.42	0.69	632	17
86	1.4	0.09	11	224	24	8.34	1.29	0.0656	1.15	1.085	1.73	0.1199	1.29	0.75	730	18
87	0.9	0.08	5	75	16	4.29	1.75	0.0947	1.13	3.041	2.08	0.2330	1.75	0.84	1350	43

383

Table DR 2. CA-ID-TIMS U-Pb isotope data.

	Compositional Parameters						Radiogenic Isotope Ratios								Isotopic Ages					
Sample	$\frac{Th}{U}$ (a)	$^{206}Pb^*$ x10^{-13} mol	mol % $^{206}Pb^*$	$\frac{Pb^*}{Pb_c}$ (b)	Pb_c (pg)	$\frac{^{206}Pb}{^{204}Pb}$ (c)	$\frac{^{208}Pb}{^{206}Pb}$ (d)	$\frac{^{207}Pb}{^{206}Pb}$ (d)	% err (e)	$\frac{^{207}Pb}{^{235}U}$ (d)	% err (e)	$\frac{^{206}Pb}{^{238}U}$ (d)	% err (e)	corr. coef.	$\frac{^{207}Pb}{^{206}Pb}$ (f)	± (g)	$\frac{^{207}Pb}{^{235}U}$ (f)	± (g)	$\frac{^{206}Pb}{^{238}U}$ (f)	± (g)
JNC 916 (BNG SK 4766 1787) Blackbrook Group, Ives Head Fm, Morley Quarry, volcaniclastic turbidite, coarse to medium grained volcaniclastic sandstone bed.																				
916-1	0.818	0.9041	97.68%	14	1.78	784	0.254	0.060311	0.399	0.832198	0.474	0.100121	0.139	0.647	613.50	8.62	614.83	2.19	615.19	0.81
916-2	0.772	0.8731	98.96%	31	0.76	1747	0.240	0.060361	0.195	0.832210	0.268	0.100039	0.104	0.796	615.31	4.21	614.84	1.23	614.71	0.61
916-3	1.015	1.7281	99.25%	45	1.08	2424	0.316	0.060354	0.164	0.832966	0.237	0.100142	0.101	0.823	615.08	3.55	615.26	1.09	615.31	0.59
916-4	1.200	1.2275	99.33%	53	0.68	2727	0.372	0.060364	0.160	0.839782	0.238	0.100944	0.115	0.810	615.47	3.46	619.03	1.10	620.00	0.68
916-5	0.870	4.9560	99.68%	102	1.33	5643	0.270	0.060299	0.101	0.830639	0.186	0.099954	0.097	0.939	613.08	2.18	613.97	0.86	614.21	0.57
916-6	0.776	0.9826	98.95%	30	0.87	1727	0.244	0.061388	0.199	0.857714	0.269	0.101380	0.097	0.809	651.64	4.28	628.87	1.26	622.56	0.57
916-7	0.809	0.9824	98.90%	29	0.91	1656	0.252	0.060361	0.205	0.829311	0.275	0.099691	0.096	0.806	615.30	4.44	613.23	1.27	**612.67**	**0.56**
916-8	0.776	0.7048	98.50%	21	0.89	1215	0.242	0.060454	0.260	0.829855	0.335	0.099602	0.120	0.734	618.63	5.61	613.53	1.54	**612.15**	**0.70**
916-9	0.690	1.3007	99.32%	47	0.74	2687	0.215	0.060354	0.145	0.830851	0.224	0.099887	0.104	0.862	615.05	3.12	614.08	1.03	**613.82**	**0.61**
916-10	1.066	0.9138	99.16%	41	0.64	2178	0.327	0.059382	0.187	0.818128	0.260	0.099968	0.104	0.800	579.91	4.06	607.00	1.19	614.29	0.61
916-11	0.718	0.8734	99.05%	33	0.69	1919	0.223	0.060378	0.182	0.831247	0.257	0.099895	0.104	0.816	615.91	3.94	614.30	1.18	**613.87**	**0.61**
JNC 836 (BNG SK 4772 1700), Blackbrook Group, Ives Head Fm at Ives Head, turbidite bed, volcaniclastic sandstone.																				
836-1	0.810	4.9699	99.73%	120	1.12	6708	0.252	0.060308	0.174	0.832253	0.228	0.100133	0.099	0.701	613.40	3.76	614.86	1.05	615.26	0.58
836-2	0.804	4.6447	99.57%	75	1.67	4214	0.250	0.060335	0.128	0.833300	0.212	0.100213	0.114	0.859	614.38	2.77	615.44	0.98	615.73	0.67
836-3	1.101	0.7845	97.66%	15	1.56	778	0.342	0.060380	0.401	0.842139	0.477	0.101202	0.140	0.647	616.01	8.66	620.33	2.22	621.51	0.83
836-4	1.033	1.3642	98.44%	22	1.79	1168	0.321	0.060339	0.286	0.830166	0.358	0.099831	0.122	0.700	614.53	6.18	613.70	1.65	613.48	0.71
836-5	0.900	3.6772	99.77%	146	0.70	7970	0.280	0.060311	0.098	0.833126	0.179	0.100232	0.091	0.943	613.53	2.12	615.35	0.83	615.84	0.53
836-6	0.790	7.9385	99.81%	173	1.23	9733	0.246	0.060365	0.091	0.828011	0.177	0.099528	0.095	0.953	615.45	1.96	612.51	0.81	**611.71**	**0.55**
836-7	0.757	1.8113	99.07%	35	1.40	1967	0.236	0.060336	0.176	0.828618	0.248	0.099648	0.098	0.831	614.41	3.79	612.85	1.14	**612.42**	**0.57**
836-8	0.873	1.8599	99.30%	47	1.08	2613	0.272	0.060457	0.152	0.831118	0.226	0.099749	0.096	0.859	618.74	3.28	614.23	1.04	**613.01**	**0.56**
836-9	0.938	0.9852	99.32%	49	0.56	2667	0.292	0.060289	0.149	0.830135	0.224	0.099909	0.096	0.864	612.74	3.22	613.69	1.03	613.94	0.56
836-10	0.845	1.0035	99.49%	64	0.43	3535	0.263	0.060355	0.134	0.830210	0.214	0.099809	0.104	0.870	615.10	2.89	613.73	0.99	**613.36**	**0.61**
JNC 917 (BNG SK 4637 1712) Blackbrook Group, Ives Head Fm, South Quarry Breccia, volcaniclastic sandstone and mudstone breccia.																				
917-1	0.818	1.3654	98.88%	29	1.28	1632	0.255	0.060421	0.218	0.830881	0.287	0.099781	0.099	0.782	617.43	4.71	614.10	1.32	**613.20**	**0.58**
917-2	0.888	1.3073	99.19%	41	0.89	2247	0.276	0.060311	0.163	0.826647	0.237	0.099454	0.097	0.845	613.50	3.53	611.75	1.09	**611.28**	**0.57**
917-3	0.837	0.7527	98.80%	27	0.76	1522	0.261	0.060476	0.223	0.834390	0.292	0.100111	0.099	0.784	619.40	4.82	616.05	1.35	615.13	0.58

	Compositional Parameters						Radiogenic Isotope Ratios								Isotopic Ages					
Sample	$\frac{Th}{U}$ (a)	$^{206}Pb^*$ $x10^{-13}$ mol	mol % $^{206}Pb^*$	$\frac{Pb^*}{Pb_c}$ (b)	Pb_c (pg)	$\frac{^{206}Pb}{^{204}Pb}$ (c)	$\frac{^{208}Pb}{^{206}Pb}$ (d)	$\frac{^{207}Pb}{^{206}Pb}$ (d)	% err (e)	$\frac{^{207}Pb}{^{235}U}$ (d)	% err (e)	$\frac{^{206}Pb}{^{238}U}$ (d)	% err (e)	corr. coef.	$\frac{^{207}Pb}{^{206}Pb}$ (f)	± (g)	$\frac{^{207}Pb}{^{235}U}$ (f)	± (g)	$\frac{^{206}Pb}{^{238}U}$ (f)	± (g)
JNC 917 (BNG SK 4637 1712) Blackbrook Group, Ives Head Fm, South Quarry Breccia, volcaniclastic sandstone and mudstone breccia																				
917-4	0.874	1.4134	98.42%	21	1.88	1151	0.272	0.060369	0.265	0.830974	0.336	0.099877	0.109	0.744	615.61	5.73	614.15	1.55	**613.76**	**0.64**
917-5	0.804	3.3230	99.75%	132	0.68	7394	0.250	0.060383	0.098	0.830544	0.183	0.099802	0.096	0.939	616.09	2.12	613.91	0.84	**613.32**	**0.56**
917-6	0.758	1.4526	98.96%	31	1.26	1756	0.236	0.060328	0.208	0.829462	0.279	0.099764	0.104	0.781	614.10	4.49	613.31	1.28	**613.10**	**0.61**
917-7	0.996	0.3395	97.21%	12	0.81	653	0.310	0.060479	0.438	0.834828	0.520	0.100158	0.145	0.658	619.55	9.46	616.29	2.40	615.40	0.85
917-8	1.029	0.8713	97.70%	15	1.70	791	0.319	0.060243	0.352	0.833103	0.426	0.100343	0.104	0.771	611.09	7.60	615.33	1.96	616.49	0.61
917-9	0.958	0.5610	98.69%	25	0.62	1389	0.297	0.060337	0.244	0.835428	0.316	0.100467	0.116	0.734	614.45	5.28	616.62	1.46	617.21	0.68
917-10	1.181	1.2504	99.27%	49	0.76	2507	0.367	0.060370	0.149	0.837311	0.223	0.100637	0.092	0.873	615.69	3.22	617.66	1.03	618.20	0.54
JNC 918 (BNG SK 5146 1246) Maplewell Group, Beacon Hill Fm, Benscliffe Breccia at Pillar Rock, Massive andesite breccia and coarse grained volcaniclastic sandstone.																				
918-1	0.813	1.5478	98.91%	30	1.42	1665	0.253	0.060400	0.263	0.831346	0.337	0.099871	0.150	0.662	616.69	5.68	614.36	1.56	613.73	0.88
918-2	0.823	0.2736	90.82%	3	2.30	198	0.258	0.059363	1.360	.751061	0.542	.091802	0.275	0.710	579.16	29.55	568.84	6.71	566.26	0.49
918-3	0.600	0.5695	97.34%	11	1.29	684	0.187	0.059168	0.436	.752816	0.522	.092320	0.132	0.727	571.98	9.48	569.86	2.28	**569.32**	**0.72**
918-4	0.490	0.7836	99.46%	55	0.36	3349	0.153	0.059269	0.126	.755601	0.220	.092504	0.119	0.890	575.67	2.75	571.47	0.96	**570.41**	**0.65**
918-5	1.155	0.3340	98.61%	25	0.39	1308	0.359	0.060167	0.281	.824720	0.374	.099459	0.169	0.709	608.38	6.07	610.68	1.72	611.30	0.99
918-6	0.841	0.8034	99.04%	34	0.64	1904	0.262	0.059104	0.188	.751434	0.267	.092250	0.111	0.809	569.67	4.10	569.06	1.16	**568.90**	**0.60**
918-7	0.942	1.1857	96.79%	10	3.28	562	0.292	0.060022	0.551	0.826189	0.637	0.099876	0.160	0.629	603.16	11.92	611.50	2.93	613.75	0.94
918-8	0.770	1.1994	99.01%	32	0.99	1839	0.239	0.060189	0.220	0.831416	0.290	0.100230	0.103	0.779	609.13	4.75	614.40	1.34	615.83	0.61
918-9	0.613	0.6635	98.23%	17	0.99	1025	0.190	0.060383	0.301	0.835880	0.386	0.100444	0.138	0.726	616.08	6.50	616.87	1.78	617.09	0.81
918-10	1.006	0.4393	97.93%	16	0.77	879	0.314	0.060534	0.515	0.832075	0.598	0.099738	0.156	0.627	621.49	11.11	614.76	2.76	612.94	0.91
918-11	1.025	0.8994	98.57%	24	1.08	1273	0.319	0.060325	0.253	0.830539	0.329	0.099898	0.111	0.772	614.04	5.48	613.91	1.52	613.88	0.65
JNC 911 (BNG SK 5091 1488) Maplewell Group, Beacon Hill Fm, Beacon Tuff member, fine grained vitric tuff																				
911-1	0.853	0.2204	97.00%	11	0.57	608	0.266	0.060382	0.551	0.830848	0.624	0.099841	0.167	0.548	616.05	11.89	614.08	2.88	613.55	0.98
911-2	0.959	0.2888	98.70%	26	0.31	1404	0.300	0.060748	0.362	0.836241	0.436	0.099883	0.163	0.601	629.12	7.81	617.07	2.02	613.79	0.95
911-3	0.728	0.3385	98.21%	18	0.51	1015	0.227	0.060593	0.515	0.830965	0.584	0.099507	0.163	0.539	623.57	11.11	614.15	2.69	611.59	0.95
911-4	0.892	0.8723	99.15%	39	0.62	2154	0.277	0.060355	0.203	0.832170	0.267	0.100045	0.106	0.727	615.08	4.39	614.82	1.23	614.74	0.62

	Compositional Parameters						Radiogenic Isotope Ratios								Isotopic Ages					
Sample	Th/U (a)	^{206}Pb* x10^{-13} mol	mol % ^{206}Pb*	Pb*/Pb$_c$ (b)	Pb$_c$ (pg)	^{206}Pb/^{204}Pb (c)	^{208}Pb/^{206}Pb (d)	^{207}Pb/^{206}Pb (d)	% err (e)	^{207}Pb/^{235}U (d)	% err (e)	^{206}Pb/^{238}U (d)	% err (e)	corr. coef.	^{207}Pb/^{206}Pb (f)	± (g)	^{207}Pb/^{235}U (f)	± (g)	^{206}Pb/^{238}U (f)	± (g)
JNC 907 (BNG SK 4572 1289) Maplewell Group, Bradgate Fm, Bardon Hill Quarry, volcaniclastic sandstone-siltstone.																				
907-1	0.728	1.0034	99.57%	74	0.36	4250	0.227	0.059034	0.121	0.745624	0.197	0.091645	0.091	0.907	567.08	2.63	565.68	0.86	**565.34**	**0.49**
907-2	1.381	0.5476	99.00%	37	0.46	1828	0.430	0.060407	0.191	0.832527	0.264	0.100000	0.110	0.781	617.03	4.13	615.01	1.22	614.46	0.64
907-3	0.786	0.1982	98.29%	19	0.29	1065	0.245	0.059038	0.322	0.747964	0.405	0.091928	0.151	0.680	567.21	7.02	567.04	1.76	**567.00**	**0.82**
907-4	0.526	0.9329	99.53%	65	0.36	3884	0.164	0.059039	0.124	0.746907	0.200	0.091795	0.091	0.900	567.24	2.71	566.43	0.87	**566.23**	**0.49**
907-5	0.988	0.8248	99.21%	43	0.54	2313	0.308	0.059072	0.168	0.745812	0.247	0.091609	0.088	0.931	568.51	3.66	565.79	1.07	**565.11**	**0.47**
JNC 912 (BNG SK 4860 1095) Maplewell Group, Bradgate Fm, Park Breccia, medium grained volcaniclastic sandstone with mudstone rafts.																				
912-1	0.958	1.7591	96.41%	9	5.47	500	0.299	0.059189	0.364	0.745734	0.444	0.091419	0.157	0.641	572.80	7.91	565.75	1.92	563.99	0.85
912-2	0.975	1.4672	98.19%	18	2.24	1004	0.304	0.059074	0.269	0.743811	0.340	0.091360	0.095	0.803	568.59	5.86	564.63	1.47	563.65	0.51
912-3	0.959	1.1188	96.53%	9	3.35	519	0.299	0.059012	0.381	0.741328	0.479	0.091151	0.188	0.664	566.29	8.30	563.18	2.07	**562.41**	**1.01**
912-4	0.897	0.3926	99.20%	41	0.26	2283	0.279	0.060394	0.211	0.832673	0.289	0.100040	0.135	0.737	616.50	4.55	615.09	1.34	614.71	0.79
912-5	0.739	0.3679	99.22%	41	0.24	2337	0.230	0.060321	0.254	0.828301	0.325	0.099635	0.130	0.686	613.88	5.48	612.67	1.49	612.34	0.76
912-6	0.645	0.1324	98.08%	16	0.22	946	0.200	0.060141	0.415	0.827562	0.556	0.099845	0.300	0.679	607.39	8.98	612.26	2.56	613.58	1.76
912-7	0.925	0.9862	90.88%	3	8.27	196	0.288	0.058757	0.636	0.737863	0.718	0.091119	0.188	0.545	556.85	13.86	561.16	3.10	**562.22**	**1.01**
912-8	0.841	0.4506	97.70%	14	0.88	792	0.262	0.058822	0.416	0.737648	0.486	0.090993	0.128	0.639	559.22	9.07	561.03	2.09	**561.48**	**0.69**
912-9	0.968	1.1579	99.62%	90	0.36	4832	0.302	0.058948	0.142	0.740356	0.214	0.091130	0.103	0.826	563.94	3.08	562.61	0.93	**562.29**	**0.55**
912-10	0.978	0.7051	99.36%	52	0.38	2830	0.305	0.058813	0.155	0.737693	0.231	0.091012	0.101	0.848	558.92	3.37	561.06	0.99	**561.59**	**0.54**
912-11	1.020	1.3312	99.35%	52	0.73	2780	0.318	0.058897	0.221	0.738713	0.280	0.091008	0.116	0.663	562.04	4.82	561.65	1.21	**561.56**	**0.62**
912-12	0.707	1.3966	99.60%	80	0.46	4585	0.220	0.058818	0.117	0.738201	0.221	0.091067	0.131	0.903	559.06	2.54	561.36	0.95	**561.92**	**0.70**
912-13tk	0.921	1.3740	99.17%	40	0.95	2195	0.288	0.058953	0.396	0.738231	0.573	0.090862	0.318	0.747	564.09	8.63	561.37	2.47	**560.70**	**1.71**
912-2tk	0.980	2.1717	99.44%	60	1.02	3236	0.306	0.058923	0.369	0.740830	0.449	0.091228	0.183	0.602	563.00	8.05	562.89	1.94	**562.86**	**0.99**
912-3tk	0.707	0.2218	89.49%	3	2.16	173	0.218	0.060231	1.605	0.852674	2.534	0.102720	0.638	1.315	610.65	34.68	626.12	11.84	630.40	3.83
912-4tk	1.020	1.2248	98.82%	29	1.21	1546	0.319	0.059069	0.434	0.741640	0.573	0.091102	0.216	0.756	568.40	9.44	563.36	2.48	**562.12**	**1.16**
912-5tk	0.905	0.8641	99.01%	33	0.72	1840	0.282	0.058796	0.190	0.736851	0.515	0.090934	0.242	1.154	558.29	4.15	560.57	2.22	**561.13**	**1.30**
912-6tk	1.025	0.5127	97.94%	16	0.89	884	0.320	0.059719	0.753	0.776568	1.084	0.094354	0.348	0.967	592.18	16.32	583.52	4.81	581.30	1.93
912-7tk	0.820	0.6422	98.05%	16	1.06	934	0.254	0.060034	0.255	0.822386	0.674	0.099396	0.262	1.295	603.57	5.53	609.38	3.09	610.94	1.53

Notes: *(a) calculated from measured ^{208}Pb/^{206}Pb assuming concordance, (b) radiogenic/common Pb in sample (c) corrected for fractionation and spike, (d) corrected for fractionation, spike and blank (Stacey and Kramers (1975), (e) uncertainty is ± 2 SE %, (f) calculated using decay constants of Jaffey et al., (1971) and ^{238}U/^{235}U for crustal zircon from Hiess et al., (2013), (g) uncertainty is ± 2 SD absolute.*

Table DR 3. Chemical compositions of volcanic pebbles separated from Hanging Rocks Formation conglomerate sample JNC 685. Due to the small size of each sample (3-4 grams) only a limited range of trace elements could be determined. Analysis was conducted at the BGS using a Fisons/ARL 3580 inductively-coupled plasma-atomic emission spectrometer.

	JNC 685A	JNC685B	JNC685C
SiO_2 (wt%)	67.41	67.64	64.44
TiO_2	0.22	0.51	0.52
Al_2O_3	17.94	18.07	18.34
Fe_2O_3(tot.)	2.05	1.21	4.25
MnO	0.06	0.02	0.09
MgO	0.46	0.19	1.07
CaO	0.17	0.22	0.50
Na_2O	9.19	9.52	8.20
K_2O	1.02	0.81	1.16
P_2O_5	0.00	0.03	0.03
LOI	0.72	0.83	1.37
Total	99.24	99.05	99.97
Sr (ppm)	179	196	228
Ba	357	317	429
V	27	36	91
Zn	28	15	57
Cu	9	8	12
Pb	18	21	16
Zr	185	285	258
Co	21	25	16
Y	30	42	39
La	9	5	13
Cr	4	5	6

REFERENCES CITED

Bauer, W., Walsh, G. J., de Waele, B., Thomas, R. J., Horstwood, M. S. A., Bracciali, L., Schofield, D. I., Wollenberg, U., Lidke, D. J., Rasaona, I. T., and Rabarimanana, M. H., 2011, Cover sequences at the northern margin of the Antongil Craton, NE Madagascar: Precambrian Research, v. 189, p. 292-312.

Bevins, R.E., Pharaoh, T.C., Cope, J.C.W., and Brewer, T.S., 1995, Geochemical character of Neoproterozoic rocks in southwest Wales. Geological Magazine, v. 132, p. 339-349.

Boynton, H.E., and Ford, T.D., 1995, Ediacaran fossils from the Precambrian (Charnian Supergroup) of Charnwood Forest, Leicestershire, England: Mercian Geologist, v. 13, p. 165-183.

Boynton, H.E., and Moseley, J., 1999, The geology of The Brand, Charnwood Forest, Leicestershire: Transactions of the Leicester Literary and Philosophical Society, v. 93, p. 32-38.

Bridge, D. M., Carney, J. N., Lawley, R. S., and Rushton, A. W. A., 1998, Geology of the country around Coventry and Nuneaton. Memoir for 1:50 000 Geological Sheet 169 (England and Wales), British Geological Survey, 185 p.

Carney, J. N., 1994, Geology of the Thringstone, Shepshed and Loughborough districts: 1:10000 sheets SK 41 NW, SK 41 NE and SK 51 NW. British Geological Survey Technical Report WA/94/08, 159 p.

Carney, J.N., 1999, Revisiting the Charnian Supergroup: new advances in understanding old rocks: Geology Today, Nov-Dec, p. 221-229.

Carney, J.N., 2000, Igneous processes within late Precambrian volcanic centres near Whitwick, north-western Charnwood Forest: Mercian Geologist, v. 15, p. 7-28.

Carney, J.N., 2000b, Beacon Hill, Geological Conservation Review Series No. 20, Joint Nature Conservation Committee, Peterborough, p. 30-42.

Carney, J.N., 2000c, Outwoods-Hangingstone Hills, Geological Conservation Review Series No. 20, Joint Nature Conservation Committee, Peterborough, p. 43-48.

Carney, J. N., and Pharaoh, T. C., 2000, Bardon Hill, In Carney, J.N., Horak, J.M., Pharaoh, T.C., Gibbons, W., Wilson, D., Barclay, W.J., and Bevins, R.E. Precambrian rocks of England and Wales, Geological Conservation Review Series No. 20, Joint Nature Conservation Committee, Peterborough, p. 40-43.

Carney, J. N., and Noble, S. R., 2007, Geological setting, environment and age of the Charnwood biota: Transactions of the Leicester Literary and Philosophical Society, v. 101, p. 49-51.

Compston, W., Wright, A. E., and Toghill, P., 2002, Dating the Late Precambrian volcanicity of England and Wales: Journal of the Geological Society [London], v. 159, p. 323-339.

Corfu, F., and Noble, S. R., 1992, Genesis of the southern Abitibi Greenstone-Belt, Superior Province, Canada - Evidence from zircon Hf isotope analyses using a single filament technique: Geochimica et Cosmochimica Acta, v. 56, p. 2081-2097.

Gerstenberger, H., and Haase, G., 1997, A highly effective emitter substance for mass spectrometric Pb isotope ratio determinations: Chemical Geology, v. 136, p. 309.

Hiess, J., Condon, D. J., McLean, N., and Noble, S. R., 2012, $^{238}U/^{235}U$ Systematics in Terrestrial Uranium-Bearing Minerals: Science, v. 335, no. 6076, p. 1610-1614.

Horstwood, M. S. A., Foster, G. L., Parrish, R. R., Noble, S. R., and Nowell, G. M., 2003, Common-Pb corrected in situ U-Pb accessory mineral geochronology by LA-MC-ICP-MS: Journal of Analytical Atomic Spectrometry, v. 18, p. 837-846.

Jaffey, A. H., Flynn, K. F., Glendenin, L. E., Bentley, W. C., and Essling, A. M., 1971, Precision measurement of half-lives and specific of ^{235}U and ^{238}U: Physics Reviews, v. C4, p. 1889-1906.

Jackson, S.E., Pearson, N.J., Griffin, W.L., and Belousova, E.A., 2004, The application of laser ablation-inductively coupled plasma-mass spectrometry to in situ U-Pb zircon geochronology: Chemical Geology, v. 211, p. 47-69.

Liu, A. G., McIlroy, D., Antcliffe, J. B., and Brasier, M. D., 2011, Effaced preservation in the Ediacara biota and its implications for the early macrofossil record: Palaeontology, v. 54, p. 607-630.

Ludwig, K. R., 2003, Isoplot 3.00. A geochronological toolkit for Microsoft Excel: Berkeley Geochronology Center Special Publication no. 4, 71p.

Ludwig, K. R., and Mundil, R., 2002, Extracting reliable U-Pb ages and errors from complex populations of zircons from Phanerozoic tuffs: Geochimica et Cosmochimica Acta, v. 66, no. Supplement 1. The Goldschmidt Conference Abstracts, p. A463.

Mattinson, J. M., 2005, Zircon U-Pb chemical abrasion ("CA-TIMS") method: Combined annealing and multi-step partial dissolution analysis for improved precision and accuracy of zircon ages: Chemical Geology, v. 220, p. 47-66.

Moseley, J.B., and Ford, T.D., 1985, A stratigraphic revision of the Late Precambrian rocks of the Charnwood Forest, Leicestershire: Mercian Geologist, v. 10, p. 1-18.

Murphy, J. B., Fernandez-Suarez, J., Jeffries, T. E., and Strachan, R. A., 2004, U-Pb (LA-ICP-MS) dating of detrital zircons from Cambrian clastic rocks in Avalonia: erosion of a Neoproterozoic arc along the northern Gondwanan margin: Journal of the Geological Society [London], v. 161, p. 243-254.

Noble, S. R., Tucker, R. D., and Pharaoh, T. C., 1993, Lower Paleozoic and Precambrian igneous rocks from Eastern England, and their bearing on late Ordovician closure of the Tornquist Sea - constraints from U-Pb and Nd isotopes: Geological Magazine, v. 130, p. 835-846.

Pharaoh, T.C., and Evans, C.J., 1987, Moreley Quarry No. 1 Borehole: Geological well completion report: Investigation of the geothermal potential of the UK, British Geological Survey Report.

Pharaoh, T.C., Webb, P.C., Thorpe, R.S., and Beckinsale, R.D., 1987, Geochemical evidence for the tectonic setting of late Proterozoic volcanic suites in central England: In Geochemistry and Mineralisation of Proterozoic volcanic suites (eds T.C. Pharaoh, R.D. Beckinsale and D. Rickard), Geological Society [London] Special Publication 33, p. 541-552.

Pharoah, T.C., Merriman, R.J., Evans, J.A., Brewer, T.S., Webb, P.C. and Smith, N.J.P., 1991, Early Palaeozoic arc-related volcanism in the concealed Caledonides of southern Britain. Annales de la Société Géologique de Belgique, T114, p. 63-91.

Pharaoh, T. C., and Carney, J. N., 2000, Introduction to the Precambrian rocks of England and Wales., Precambrian Rocks of England and Wales. Geological Conservation Review Series., v. 20, p. 3-17.

Sambridge, M. S., and Compston, W., 1994, Mixture modeling of multi-component data sets with application to ion-probe zircon ages: Earth And Planetary Science Letters, v. 128, p. 373-390.

Schmitz, M. D., and Schoene, B., 2007, Derivation of isotope ratios, errors, and error correlations for U-Pb geochronology using Pb-205-U-235-(U-233)-spiked isotope dilution thermal ionization mass spectrometric data: Geochemistry Geophysics Geosystems, v. 8, article no. Q08006, doi:10.1029/2006GC001492.

Schneider, J. L., Le Ruyet, A., Chanier, F., Buret, C., Ferriere, J., Proust, J. N., and Rosseel, J. B., 2001, Primary or secondary distal volcaniclastic turbidites: how to make the distinction? An example from the Miocene of New Zealand (Mahia Peninsula, North Island): Sedimentary Geology, v. 145, p. 1-22.

Simonetti, A., Heaman, L. M., Hartlaub, R. P., Creaser, R. A., MacHattie, T. G., and Bohm, C., 2005, U-Pb zircon dating by laser ablation-MC-ICP-MS using a new multiple ion counting Faraday collector array: Journal of Analytical Atomic Spectrometry, v. 20, p. 677-686.

Sláma, J., Kosler, J., Condon, D. J., Crowley, J. L., Gerdes, A., Hanchar, J. M., Horstwood, M. S. A., Morris, G. A., Nasdala, L., Norberg, N., Schaltegger, U., Schoene, B., Tubrett, M. N., and Whitehouse, M. J., 2008, Plesovice zircon -- A new natural reference material for U-Pb and Hf isotopic microanalysis: Chemical Geology, v. 249, p. 1-35.

Stix, J., 1991, Subaqueous, intermediate to silicic-composition explosive volcanism: a review: Earth-Science Reviews, v. 31, p. 21-53.

Tucker, R. D., and Pharaoh, T. C., 1991, U-Pb zircon ages for Late Precambrian igneous rocks in southern Britain: Journal of the Geological Society [London], v. 148, p. 435-443.

Wiedenbeck, M., Alle, P., Corfu, F., Griffin, W. L., Meier, M., Oberli, F., Vonquadt, A., Roddick, J. C., and Speigel, W., 1995, 3 Natural Zircon Standards for U-Th-Pb, Lu-Hf, Trace-Element and Ree Analyses: Geostandards Newsletter, v. 19, p. 1-23.

Wilby, P. R., Carney, J. N., and Howe, M. P. A., 2011, A rich Ediacaran assemblage from eastern Avalonia: Evidence of early widespread diversity in the deep ocean: Geology, v. 39, p. 655-658.

Worssam, B. C., and Old, R. A., 1988, Geology of the country around Coalville, Memoir of the British Geological Survey, Sheet 155 (England and Wales), 161 p.